

STATISTICAL THERMODYNAMICS OF ASSOCIATION COLLOIDS

The Equilibrium Structure of Micelles, Vesicles, and Bilayer Membranes

STATISTISCHE THERMODYNAMICA VAN ASSOCIATIEKOLLOIDEN

De Evenwichtsstructuur van Micellen, Vesikels en Bilaag Membranen

CENTRALE LANDBOUWCATALOGUS



0000 0212 9936

Promotor: dr. J. Lyklema, hoogleraar in de Fysische chemie, met bijzondere
aandacht voor de Grensvlak- en Kolloïdchemie

Co-promotor: dr. ir. J.M.H.M. Scheutjens, universitair hoofddocent

11111111111111111111

Frans A.M. Leermakers

Statistical Thermodynamics of Association Colloids
The Equilibrium Structure of Micelles, Vesicles, and Bilayer Membranes

Proefschrift
ter verkrijging van de graad van
doctor in de landbouwetenschappen,
op gezag van de rector magnificus,
dr. C.C. Oosterlee,
in het openbaar te verdedigen
op vrijdag 6 mei 1988
des namiddags te vier uur in de aula
van de Landbouwniversiteit te Wageningen

BIBLIOTHEEK
LANDBOUWUNIVERSITEIT
WAGENINGEN

ISBN = 268159

Tekstverwerkingsadviezen: Bert Bouman

Grafische medewerking: Gert Buurman

This work is part of the research programme of the Stichting Scheikundig Onderzoek Nederland (S.O.N.), which is financially supported by the Nederlandse Organisatie voor Wetenschappelijk Onderzoek (N.W.O.).

STELLINGEN

- I -

De poging van Baskir en medewerkers om de ketenstatistiek in een bolvormig rooster uit te voeren is mislukt. Eerst zondigen zij tegen de inversiesymmetrie regels en door opeenvolgende "correcties" neigt hun rooster vervolgens naar een vlakke geometrie.

J.N. Baskir, T.A. Hatton en U.W. Suter; *Macromolecules*, **20** (1987), 1300.

- II -

Het is mogelijk om de statistische thermodynamica van associatiekolloïden te ontwikkelen zonder bij voorbaat de posities van de kogroepen in het grensvlak vast te leggen.

Dit proefschrift.

- III -

Een gemiddeldveld theorie kan slechts dan de gel-vloeibaar faseovergang in bilaag membranen reproduceren indien een orientatieafhankelijke entropieterm in de statistische verwerking wordt meegenomen.

Dit proefschrift hoofdstuk 4.

- IV -

Het gedrag van ketenmoleculen in een grensvlak met laterale inhomogeniteiten kan bestudeerd worden met een tweedimensionale variant van het, door Scheutjens en Fleer geïntroduceerde, zelfconsistente veld model.

Dit proefschrift hoofdstuk 5.

J.M.H.M. Scheutjens en G.J. Fleer; *J. Phys. Chem.* **83** (1979), 1619.

- V -

Vloeistoffen laten zich het eenvoudigst modelleren met roostertheorieën, terwijl kristallen zich beter met continue theorieën laten beschrijven.

- VI -

De toenemende professionalisering in het ontwikkelingswerk is geen garantie voor een betere uitvoering van de professie.

- VII -

Het is afkeurenswaardig dat bij sporten zoals turnen, gymnastiek en ponyrijden zoveel militaristische trekjes terug te vinden zijn, vooral omdat er kinderen bij betrokken zijn.

- VIII -

Het maximale gewicht dat in een stelling gelegd kan worden wordt voornamelijk bepaald door het aantal steunpunten van de basis.

- IX -

Uitgerekend rekencentra kunnen er op rekenen dat ze over enkele jaren zijn uitgerekend.

- X -

Mozes was een kolloïdchemicus.

Exodus 34:20.

- XI -

In een proefschrift is een culinaire stelling op zijn plaats.

Proefschrift Frans A.M. Leermakers

STATISTICAL THERMODYNAMICS OF ASSOCIATION COLLOIDS

The Equilibrium Structure of Micelles, Vesicles, and Bilayer Membranes

Wageningen, 6 mei 1988

It is the author's wish that no agency should ever derive military benefit from the publication of this dissertation. Authors who cite this work in support of their own are requested to qualify similarly the availability of their results.

Contents

	Page
Introduction	1
Chapter 1 SURFACTANT MICELLES	7
Abstract	7
Introduction	7
Theory	8
Thermodynamics of small systems	11
Results	12
Conclusion	19
Literature	20
Chapter 2 LIPID BILAYER MEMBRANES	21
Abstracts	21
Introduction	21
First order Markov chains	23
Rotational isomeric state scheme	27
Computational aspects	32
Evaluation of the Markov chain and mean field approximations	33
Comparison with other theories	34
Results and discussion	35
Lipid molecules	35
Interaction parameters	35
Branch points	36
Membrane in a frame	36
Free floating membranes	38
First order Markov chains compared to Rotational isomeric state scheme	39
RIS membranes	40

	Page
Conclusions	45
Appendix A. RIS scheme in matrix vector notation	45
Appendix B. Numerical details	47
Literature	48
Chapter 3 LIPID VESICLES	51
Abstract	51
Introduction	51
The curved lattice	53
First order Markov approximation	56
Rotational isomeric state scheme in planar geometry	58
Rotational isomeric state scheme and curvature	60
Iteration	62
Excess free energy	62
Results	63
Lattice artefacts	64
Uni- and Bilamellar Vesicles	65
Multicomponent Vesicles	70
Addition of surfactants	71
Multicomponent lecithin vesicles	72
Vesicle Deformation	75
Discussion	77
Conclusions	78
Appendix A. Partition function	78
Literature	81
Chapter 4 THE GEL TO LIQUID PHASE TRANSITION	83
Abstract	83
Introduction	83
Self-Consistent Anisotropic Field theory	85
The partition function	86
Energy	86
Entropy	87
Segment density profiles	94
Order parameters	96

	Page
Computational aspects	96
Results and discussion	97
Some simplifications	97
Energy parameters	98
Non-interacting membranes	99
Interacting membranes	104
Conclusions	109
Appendix A. Modified Flory-Huggins theory	110
Literature	111
 Chapter 5 INHOMOGENEOUS MEMBRANE SYSTEMS	 113
Abstract	113
Introduction	113
Theory	114
Chain distributions in two dimensions	117
Boundary conditions	120
Results and discussion	120
Trans membrane configuration	121
One copolymer molecule in the bilayer	121
Cluster of four copolymer molecules in the bilayer	125
Lateral phase separation	127
Conclusions	130
Literature	130
 List of most important symbols	 131
 Summary	 135
 Samenvatting	 139
 Curriculum vitae	 147
 Nawoord	 149

Introduction

Oil and water don't mix. If we shake the two liquids vigorously, we can at best obtain an emulsion, that is a fine distribution of oil droplets in water or the other way around. However, such an emulsion is unstable, it separates into the two original liquids (phase separation).

In contrast to oil, there are other liquids, like alcohol, that mix very well with water. We refer to molecules that do dissolve in water as hydrophilic and as hydrophobic when they do not. Hydrocarbons belong to the latter category. Hydrocarbons with small molecules like methane, ethane and propane are inert gases at ordinary conditions and dissolve poorly in water. Higher hydrocarbons, like octane, nonane and decane are liquids which do not mix with water. Oil consists for a large fraction of hydrocarbons. In fact it is common usage to use the term "oil" as a collective noun for all liquids that do not significantly mix with water. Alcohol molecules are composed of ethane and a polar hydroxyl group. The influence of the polar group is so strong that the molecule as a whole is hydrophilic.

If, however, the hydrophobic hydrocarbon moiety is much longer than in ethane, one polar group at the end of the molecule is not strong enough to render the entire molecule so soluble that it can mix with water in all proportions. Let us modify decane by attaching a polar group at one end of the hydrophobic chain. The resulting molecule is pictured as having an apolar tail and a polar head and is referred to as amphipathic or amphiphilic. Experience has shown that large amounts of these amphipolar molecules can be dissolved in water, not as molecules but as associates of, usually several tens of molecules, called micelles.

Micelles can have various sizes and shapes. Irrespective of their morphology the heads are found at the interface between the apolar tails and water. The average sizes and shapes of these association colloids, the way the molecules arrange themselves in the structure, and whether or not any water is present in the micelles is determined by the energy and entropy balance, that is by a compromise between the tendency to organise itself due to intermolecular interactions and the tendency to randomise. At this point it is

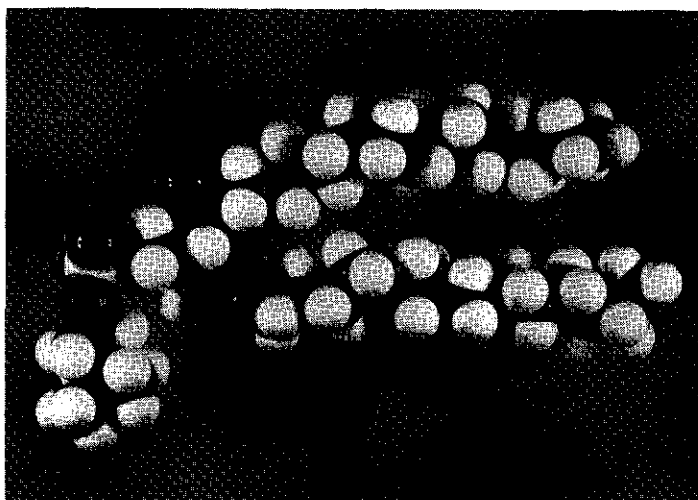


Figure 1.

A model of the lipid Dipalmitoylphosphatidylcholine.

worth while to realise that relatively small changes in conditions (increasing the concentration or the temperature, variations in polar/apolar ratio of the bipolar molecules) can dramatically effect the properties of the micelles. Spherical micelles are composed of 50 to 100 amphipathic molecules. Extremely high aggregation numbers are found in flat lamellar micelles called bilayer membranes. In biological systems membranes are formed by amphipathic molecules called lipids which commonly possess two apolar tails and one polar head group. Figure (1) gives an example of a (phospho)lipid.

Membranes are essential for life. Due to their structure membranes permit the compartmentalisation of living matter, that is: they prevent the mixing of the contents of cells with the surroundings. However, many membranes are semi-permeable, that is: some specific substances can pass it where all others are rejected. Membranes are not only part of the cell wall, but a large variety of membranes is found inside cells as well. The nucleus, mitochondria, liposomes, chloroplasts and many other cell organelles hold membranes and have a membrane-like envelope. Most membranes also contain proteins besides the constituent lipid molecules. These proteins can be loosely adsorbed on the membrane or they can have a strong interaction with it when they span the membrane in a trans-membrane configuration. The contact of the protein with

the membrane is in general essential for its biological activity. Further, and this illustrates the complexity of natural membrane systems, not only single membranes are observed, but double membranes or even multilayer membrane systems also occur. For example, the myelin sheath surrounding the axon of a nerve cell is several bilayers thick, in chloroplasts grana stacks (aggregated bilayers) are in equilibrium with stroma lamellae (non-aggregated bilayers) and in mitochondria two membranes are associated. In all these examples, the membrane-membrane interaction contributes significantly to the biological activity of the structures.

Membranes are not only found in cells. Certain viruses, like for example the retrovirus causing AIDS, possess a coat formed by a continuous bilayer in which viral coat proteins are embedded.

It is in the nature of man to use insights gained from the study of natural processes for his own benefit. We will illustrate this by mentioning a few examples of applications of membrane systems. Knowing membrane properties helps to develop drugs, anaesthetics, pesticides etc. Membrane-like vesicles are used to build artificial chloroplasts. These systems might help us to better understand photosynthesis. A very interesting application is the use of man-made liposomes to encapsulate drugs. These liposomes are designed to give a controlled release of the drug on the site of the human body where the drug is needed.

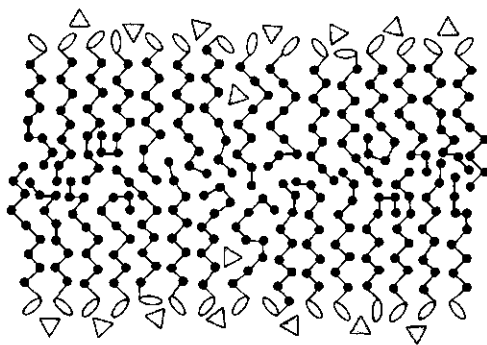


Figure 2.

Two-dimensional cross-section through a membrane composed of amphiphilic molecules with a head group segment and one tail of nine apolar segments each. The triangles indicate water. This membrane system has a high degree of order.

Several of these applications are still in an early stage of development. Research on these and several other applications will benefit from a better understanding of membrane structures and the factors that mould them, i.e., the very theme of this thesis.

Extensive experimental research on the lipid matrix showed, among other facts, that:

- the hydrophobic core of the membrane is virtually free of water.
- the membrane thickness is roughly twice the length of the extended apolar tails of the lipid molecules.
- there is a high degree of order along the bilayer.
- the lateral mobility in the membrane is high and fluid-like, while the transversal mobility (flip-flop) is slow and solid-like.
- membranes show a phase transition: they have a high-temperature fluid-like and a low-temperature gel-like phase. Biological membranes are always found to be in the fluid state.

A membrane is often pictured as in figure (2). The tails are ordered and the head groups are supposed to be all in the same plane. Although this is known to be an oversimplified representation, many experiments teach us that, in broad lines, figure (2) might not be too bad. Can we understand this membrane structure from a physical point of view? It is not straightforward why such a high degree of ordering should be expected in the bilayer. Why do lipid

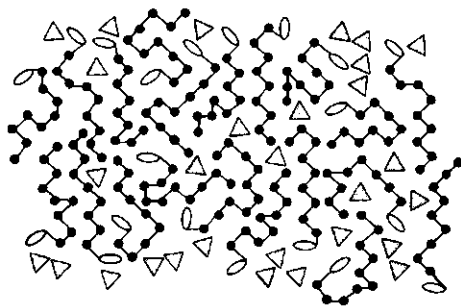


Figure 3.

A similar membrane as given in figure 2. In this case the membrane is more disordered.

molecules give up so much entropy in the membrane? We like to know why a significantly different membrane structure, as for example the one given in figure (3), is not found. One of the goals of the present thesis is to give answers to these questions.

Recently, considerable progress has been made on the statistical mechanics of interacting chain molecules in inhomogeneous systems. Especially the theoretical developments of Scheutjens and Fleer [1] have served as a starting point to elaborate a theory for association colloids [2]. The new theory, elaborated in much detail in this thesis can deal with many of the systems discussed above. The thesis contains five chapters which are written such that they can be read independently.

In chapter (1) we present some general aspects of the morphology of micelles. In agreement with experimental data, the theory predicts that small chain surfactants form spherical micelles whereas lipid molecules prefer membrane structures. This encouraged us to study in chapter (2) the structure of model membranes formed by model lecithin-like molecules. Realising that open membranes do not exist (in practice membranes are always closed) we treat lipid vesicles in chapter (3). The gel-liquid phase transition in lipid membranes is examined in chapter (4). Finally, in chapter (5) the theory is applied to study the interaction of copolymers with a model bilayer membrane.

[1] J.M.H.M. Scheutjens, and G.J. Fleer; "Statistical Theory of the Adsorption of Interacting Chain Molecules."

1. "Partition Function, Segment Density Distribution, and Adsorption Isotherms". *J.Phys.Chem.* **83** (1979) 1619.
2. "Train, Loop, and Tail Size Distribution", *J.Phys.Chem.* **84** (1980) 178.

[2] F.A.M. Leermakers, J.M.H.M. Scheutjens, and J. Lyklema; "On the Statistical Thermodynamics of Membrane Formation", *Biophys.Chem.* **18** (1983) 353.

CHAPTER 1

SURFACTANT MICELLES

Abstract

Recently we generalised the lattice theory for chain molecules in inhomogeneous systems of Scheutjens and Fleer [1] to amphipolar molecules in non-lamellar geometries [2,3,4]. This theory is used to study surfactant micelle systems.

In this paper it is shown that the critical micelle concentration for surfactant micelles is theoretically well defined. The fact that in most experimental systems the first order phase transition is not clearly observable is explained. The relation between chain architecture and overall surfactant concentration on the size and shape of surfactant micelles is discussed. Segment density profiles through a cross section of a spherical micelle are presented.

Introduction

Above the critical micelle concentration amphipolar molecules in aqueous solutions form association colloids. This phenomenon is of considerable theoretical and technological interest. In 1976 Hall and Pethica [5] published an extensive theoretical analysis of micellisation in solutions of nonionic surfactants, based on the thermodynamics of small systems developed by Hill [6]. This framework is used here to present a detailed analysis of surfactant systems over a wide concentration range. Statistical thermodynamics is used to give an interpretation on a molecular level. For example, the relation between the architecture of the amphiphiles and their aggregation structure is worked out in some detail. Segment density profiles for the association colloids are also obtained. Our approach is more general than other statistical mechanical theories [7-9], because no preassigned positions of the amphiphiles are required, i.e., the positions of the head groups are not a priori fixed onto certain lattice sites in the system. It is the first statistical approach which successfully applies the thermodynamics of small systems to it. Complementary to our approach, Molecular Dynamics [10] and Monte Carlo [11] simulations can also give detailed information on surfactant-water systems. In

these simulations methods the computation time is many orders of magnitude larger than for a statistical one. Typically, our statistical approach needs less than a minute CPU on a VAX 8700.

In the following part the theory is briefly reviewed. A more detailed discussion is given elsewhere [2]. See also ref. [3] for more results on surfactant micelles.

Theory

To facilitate the counting of conformations of chain molecules a lattice is introduced. The lattice is designed to have shells of $L(z)$ lattice sites of constant volume on which the segments of the chain molecules and the solvent molecules are placed. The lattice layers are numbered $z = 1, \dots, M$, where 1 is the centre of the lattice and M a layer in the bulk solution. In general the volume of the lattice from layer number 1 up to a layer z is (in units of lattice sites):

$$V(z) = 2 A_s z + \pi h z^2 + (4\pi/3) z^3 \quad (z > 0, h^2 > \pi A_s) \quad (1)$$

where the parameters A_s and h , determine the geometry of the lattice. For a spherical lattice, A_s and h are zero. For rods of length h , with a hemispherical cup at either end, A_s is zero. For planar parts we assume that an area A_s is surrounded by a curved half of a cylinder. A disk of radius R_d would have an area $A_s = \pi R_d^2$ and a contour length $2h = 2\pi R_d$; for all other structures $h^2 > \pi A_s$.

The number of lattice sites in layer z is given by the simple expression:

$$L(z) = V(z) - V(z-1) \quad (2)$$

The contact area $S(z)$ (in units of surface area of an unperturbed lattice site) between layer z and $z+1$ is given by:

$$S(z) = 2 A + 2 \pi h z + 4 \pi z^2 \quad (3)$$

Equation (2) and (3) determine $\lambda_{z'-z}(z)$ the fraction of contacts of a site in layer z with sites in layer z' where z' is $z-1$, z , and $z+1$, respectively:

$$\begin{aligned}
 \lambda_{-1}(z) &= \lambda_{-1} S(z-1)/L(z) \\
 \lambda_0(z) &= 1 - \lambda_{-1}(z) - \lambda_1(z) \\
 \lambda_1(z) &= \lambda_1 S(z)/L(z)
 \end{aligned}
 \tag{4}$$

Here $\lambda_{-1} = \lambda_{-1}$ are the fractions of contacts a site has in flat lattice with either of its neighbouring layers.

A spatial conformation of a chain molecule is specified by the lattice sites in which the consecutive segments, numbered $s = 1, \dots, r$, are situated. This definition implies that when one of the segments of conformation c is fixed on the lattice all other segments have a specified position. In a lamellar lattice the degeneration of a conformation c is $\omega^c = L$ because only the first segment can choose between L lattice sites. The degeneracy of a conformation c in a curved lattice is slightly more complicated while the degeneracy should not depend on which segment of a conformation is placed first. When segment number 1 of conformation c is free to choose its position in the lattice layer the degeneracy is given by:

$$\omega^c = L^c(z(1)) \prod_{s=2}^r \frac{\lambda_{z(s-1)-z(s)}^c(z(s))}{\lambda_{z(s-1)-z(s)}^c}
 \tag{5}$$

where $z(s)$ is the lattice number segment s is in. The superindex c indicates that the segment positions of conformation c are taken. Further, $\lambda_{z(s-1)-z(s)}^c$ is λ_{-1} , λ_0 , or λ_1 when segment $s-1$ is in a previous, same or following layer with respect to the position of segment s , respectively. Realising that the number of steps from z to $z+1$ must be equal to the number of steps from $z+1$ to z , i.e., $\lambda_1(z) L(z) = \lambda_{-1}(z+1) L(z+1)$, equation (5) can be transformed in order to assign an other segment than segment number 1 of conformation c to choose its position.

The conformations are generated by a Markov-type approximation [2]. In this procedure we accept chains which can intersect with themselves or with other molecules in the lattice. The structure of the molecules (branching, chain length etc.) determines the number of allowed conformations. The main advantage of accepting this possibility is, that the conformations can be generated using a recurrence relation. Very efficient computation schemes have been developed to generate all conformations [2]. Using them, the number of operations needed to generate all conformations is reduced from about 3^{r-1} to about r . We refer to reference [2] for more details of our computation method.

To calculate the statistical weight of each conformation, the potential of each conformation must be known. Three contributions are identified. First, the potential of a given conformation depends on the number of segment (x)-segment (y) and segment-solvent contacts. We will use a mean field approximation to calculate the average interaction each segment in the molecule has with the surrounding molecules. Second, differences between gauche and trans configurations are accounted for. To do this, a third order Markov process, the rotational isomeric state (RIS) scheme, is used to generate the various conformations of the chains. In the RIS scheme the "memory" of the random walk type of conformations is two bonds long. A third bond can only have three different directions. Two of them result in a gauche and a third one in a trans configuration. A third contribution to the potential of a conformation $u'(z)$ originates from hard core interactions. $u'(z)$ is chosen such that all lattice sites are filled, i.e., $\sum_x \phi_x(z) = 1$ for each layer z . The $u'(z)$ potentials are normalised with respect of the bulk. Thus this interaction is independent of the type of segment or solvent molecule.

The average segment density of segments of type x in layer z is given by $\phi_x(z) = n_x(z)/L(z)$, where $n_x(z)$ is the number of segments of type x in layer z . The potential u^c of conformation c is given by:

$$u^c = kT \sum_{s=1}^r \sum_x \chi_{xy}(s) \langle \phi_x(z_s^c) \rangle + n^{g^c} U^g + \sum_{s=1}^r u'(z_s^c) \quad (6)$$

n^{g^c} is the number of gauche bonds in conformation c and U^g the energy difference between a gauche and a trans configuration. The nature of segment number s is $y(s)$. In equation (6) the well known Flory-Huggins parameters χ_{xy} occurs. They are only non-zero when $x \neq y$, because the energetic effect of any xy contact is taken with respect to the pure phases x and y . The angular brackets in equation (6) indicate an averaging over three consecutive layers:

$$\langle \phi(z) \rangle = \lambda_{-1}(z) \phi(z-1) + \lambda_0(z) \phi(z) + \lambda_1(z) \phi(z+1) \quad (7)$$

The number of chains in conformation c is now given by:

$$n^c = C \omega^c e^{-u^c/kT} \quad (8)$$

Realising that a solvent molecule is a "chain" of only one segment, a similar

equation applies for solvent molecules. In equation (7) C is a normalisation constant which is either found from the number of molecules in the system, or from the bulk concentration.

Summation of all segments of each conformation result in the segment density distributions. With these segment density profiles, new statistical weights of each conformation can be calculated. In general a self-consistent set of conformations can only be found iteratively [2]. As soon as a self-consistent micelle profile is found the partition function can be evaluated.

Thermodynamics of small systems

For surfactant micelles, the excess free energy plays a key role in determining the stability of a given arrangement of molecules. We showed before [3] that for micelles with a fixed centre of mass the excess free energy A^σ is given by the following, rather forbidding equation:

$$A^\sigma/kT = - \sum_i n_i^\sigma + \sum_z L(z) \ln\left(\frac{\phi_w(z)}{\phi_w^b}\right) + \frac{1}{2} \sum_z \sum_x \sum_y (\chi_{xw} + \chi_{yw} - \chi_{xy}) L(z) [\phi_x(z) \langle \phi_y(z) \rangle - \phi_x^b \phi_y^b] \quad (9)$$

where i indicates the molecule type $i = 1$ (water), 2 (amphiphile),..., the superscript b indicates the bulk value and the superscript σ indicates that the quantity is counted as an excess value with respect to the bulk solution. Equation (9) contains an osmotic, an ideal mixing and an interaction term. The excess free energy given in equation (9) is identical to the subdivision potential for fixed centre of mass defined by Hill [6]. Hall and Pethica [5] showed that in equilibrium A^σ must be compensated for by terms not included in equation (9). The most important term of this kind is the translational entropy of the micelle, for the computation of which the volume fraction of micelles in the system must be known. Let V_s be the volume of the small system in which one micelle is present. Realising that $n_2^\sigma r_2$ is a good approximation for the volume of the micelle we find for the equilibrium condition of the micelle:

$$A^\sigma/kT \approx \ln \frac{V_s}{n_2^\sigma r_2} \quad (10)$$

From a mass balance we know that

$$\frac{n_2 r_2}{V_s} = \bar{\phi}_2 = \frac{n_2^\sigma r_2}{V_s} + \phi_2^b \quad (11)$$

where $\bar{\phi}_2$ is the overall surfactant concentration in the system. Combining equations (10) and (11) we find the useful formula:

$$\bar{\phi}_2 \approx \exp(-A^\sigma/kT) + \phi_2^b \quad (A^\sigma \gg 1) \quad (12)$$

Which gives us the overall surfactant concentration of the system at given $A^\sigma(\phi_2^b)$. We note that our present model is only valid for low micelle concentrations, i.e., as long as the micelles do not interact with each other.

Results

First, the behaviour of $A_{12}B_3$ is discussed, an unbranched surfactant with 12 tail segments and three head group segments. The interaction parameters are found by fitting known CMC values for a series of surfactants with different tail-lengths [3]. How to obtain CMC values with the present theory will be discussed below. The following set is used throughout this paper: $\chi_{AW} = 1.6$, $\chi_{BW} = -0.5$, $\chi_{AB} = 1.5$. The high value for the tail-water interaction is chosen to promote phase separation between tails and water. The

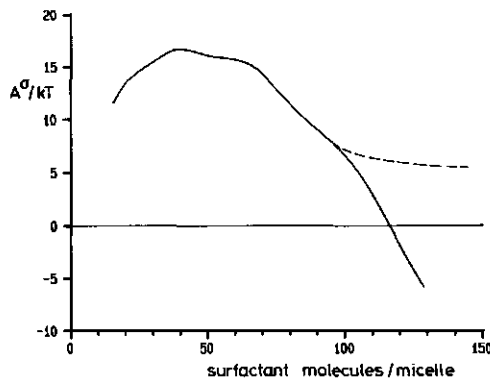


Figure 1.

The excess free energy A^σ as a function of n_2^σ for a surfactant $A_{12}B_3$ in a spherical aggregate. The dashed curve can be found when shape variations are taken into account.

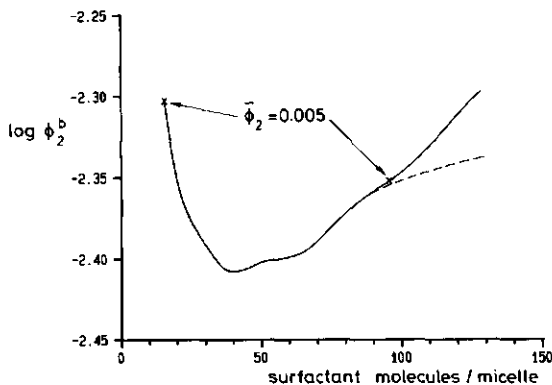


Figure 2.

$\log \phi_2^b$ as a function of the excess number of surfactants $A_{12}B_3$ aggregated in a globular geometry. Two arbitrary points of equal overall surfactant concentration are indicated.

negative head group-water interaction represents an attraction between these two species. Further, the tail-head interaction is chosen fairly repulsive, promoting the partitioning of head groups and tail segments. This increases the stability of the micelles. The flexibility of the acyl chain is reduced due to steric hindrance. This is modelled by an energy difference between a gauche and trans configuration of $U^g = 0.8 kT$ ($T = 300$ K).

Figure (1) gives the excess free energy A^g (with fixed centre of mass) as a function of the excess number of surfactants aggregated. The part with negative A^g is physically irrelevant. The part of the curve with a positive slope leads to micelles that are metastable because for a given composition another micelle system with a lower free energy can always be found (see figure 2). The very first thermodynamically stable micelles are found at the maximum in figure (1). From the equilibrium condition given in equation (10), we know that the translational entropy of the micelles also passes a maximum. We conclude that micelle concentration can not exist below a given concentration; in other words, the small system (which holds only one micelle) can not be arbitrarily large. At the CMC a micelle has the same average number of surfactant molecules in it and the concentration of micelles is finite (the size of the small system is limited). Thus, theoretically the CMC is well

defined. The same conclusion was reached by Ruckenstein and Nagarajan [12-14]. We note, that the slope $\partial A^\sigma / \partial n_2^\sigma$ contains information on the size fluctuations of micelles [5,15]. The steeper the curve the sharper the size distribution is. Near the maximum in A^σ large fluctuations in micellar size must be expected. Near the CMC the micelles change their aggregation number rather than that more micelles are formed. See also discussion of figure (4).

Figure (2) gives the relation between the equilibrium volume fraction on the number of aggregated surfactants. A^σ passes through a maximum when $\log \phi_2^b$ goes through a minimum in accordance with Gibbs' law; the pertaining value of ϕ_2^b is the CMC. At each overall concentration $\bar{\phi}_2$, beyond the CMC there are two possible equilibrium concentrations ϕ_2^b . In figure (2) one of such combinations is indicated. As can be easily seen, the molecules in the bigger micelle have always a lower chemical potential and these micelles are therefore thermodynamically more favourable. For very small micelles we require very high equilibrium concentrations, as would be characteristic for nucleation phenomena. In the physically realistic part of figure (2), beyond the CMC and for bigger micelles, the chemical potential rises with n_2^σ because gain in energy of the tails upon micellisation is counteracted by the loss in energy of the repulsive head groups. This repulsive force rises with increasing aggregation number, while this gives a larger number of head groups

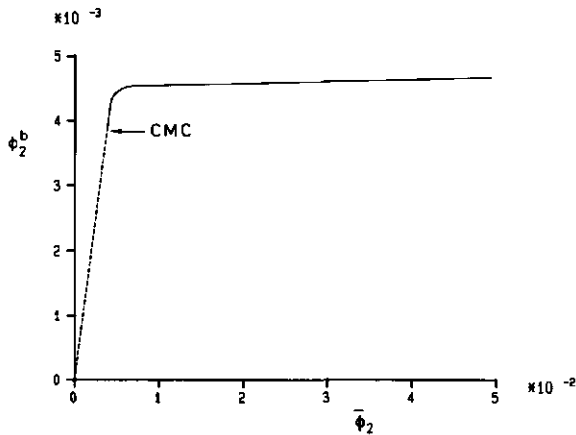


Figure 3.

The equilibrium bulk concentration as a function of the overall surfactant $A_{12}B_3$ volume fraction.

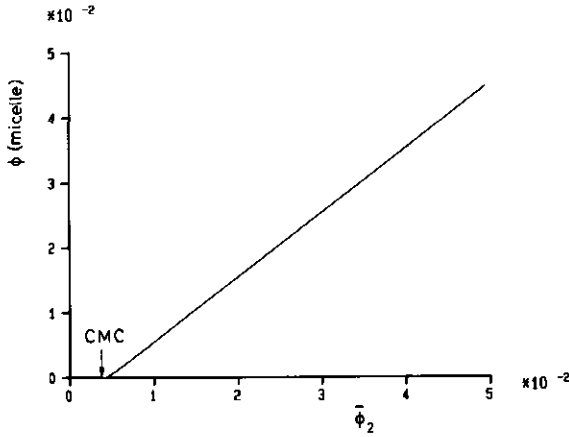


Figure 4.

The volume fraction of micelles as a function of the overall surfactant $A_{12}B_3$ volume fraction.

in the interface between the apolar tails and polar head groups. This mechanism is responsible for the finite dimensions of the micelles, i.e., it prevents the micelles from growing indefinitely towards macroscopic dimensions.

We note that especially when the maximum $A^\sigma(n_2^\sigma)$ is not high, the micelle concentration at the CMC is relatively high. Naturally, the first micelles can only be formed by a surplus of surfactants in the system. Thus there can be a difference between the theoretically defined CMC at the maximum in $A^\sigma(n_2^\sigma)$ and the lowest possible equilibrium volume fraction of the system.

In many experimental systems the overall concentration is fixed. In figure (3) the equilibrium bulk concentration ϕ_2^b is related to the overall concentration $\bar{\phi}_2$. Obviously, below the CMC $\bar{\phi}_2 = \phi_2^b$, as there are no micelles. Surprisingly, the difference between ϕ_2^b and $\bar{\phi}_2$ remains undetectable over a considerable concentration range just beyond the CMC. Only at higher concentrations becomes ϕ_2^b essentially independent of the overall concentration. As given in equation (12), as long as A^σ is large no big difference between $\bar{\phi}_2$ and ϕ_2^b can be expected. The behaviour changes dramatically when $\exp(-A^\sigma/kT)$ becomes of the order of ϕ_2^b . As a consequence, the theoretical CMC is difficult to determine experimentally. In the last case a more convenient definition of the CMC is useful, for example, the point where the ϕ_2^b and $\bar{\phi}_2$ start to deviate can be identified as the experimental CMC.

The concentration of micelles as a function of composition is given in

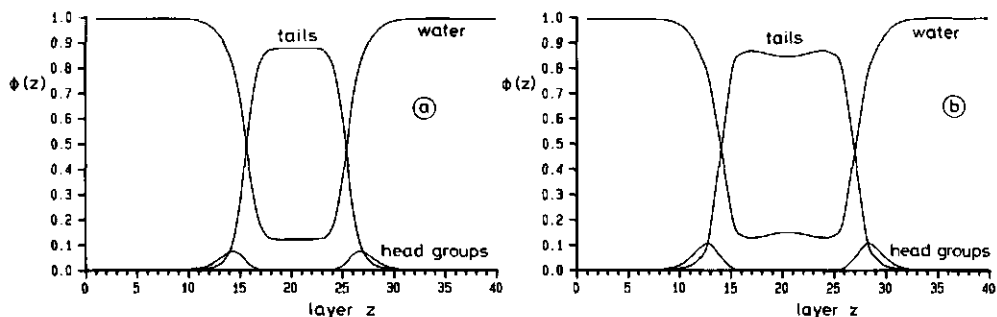


Figure 5.

Segment density distribution through a cross section of a globular micelle composed of: a) 45 molecules $A_{12}B_3$ (the equilibrium bulk volume fraction is $3.92 \cdot 10^{-3}$ (CMC), and $A^\sigma = 16.51$ kT per micelle), b) 97 molecules $A_{12}B_3$ (the equilibrium bulk volume fraction is $4.46 \cdot 10^{-3}$, and $A^\sigma = 7.5$ kT per micelle).

figure (4). As anticipated in figure (1), the micelle concentration is not detectable initially, although the concentration of micelles is finite at the CMC. The presence of micelles often defies experimental observation at the thermodynamic criterion for the CMC. Only when the micelles are larger does their concentration become linear with the overall surfactant concentration.

In figure (5a) the segment density distribution through a cross section of a micelle is given at the CMC. The micelle consists of 45 $A_{12}B_3$ molecules. The layers are numbered arbitrarily, so the origin of the lattice and the centre of the micelle is between layers 20 and 21. As can be seen from the segment distributions, the head groups are not confined to one layer but spread out over several layers. The local concentration of head groups is low. This gives plenty of room for many tail-water contacts. The distribution of segments of a given rank in the surfactant molecule (not presented) is also wide. This indicates that the entropy of the chain molecules in the aggregates is rather large, and that a dynamic picture of the micelles is more correct than a static one. The profiles show that some solvent is found in the core of the micelle. Indeed, this must be expected for a liquid consisting of simple unassociated isotropic monomers. For water this is not a good model. Therefore, we believe that the amount of solvent in the micelle is

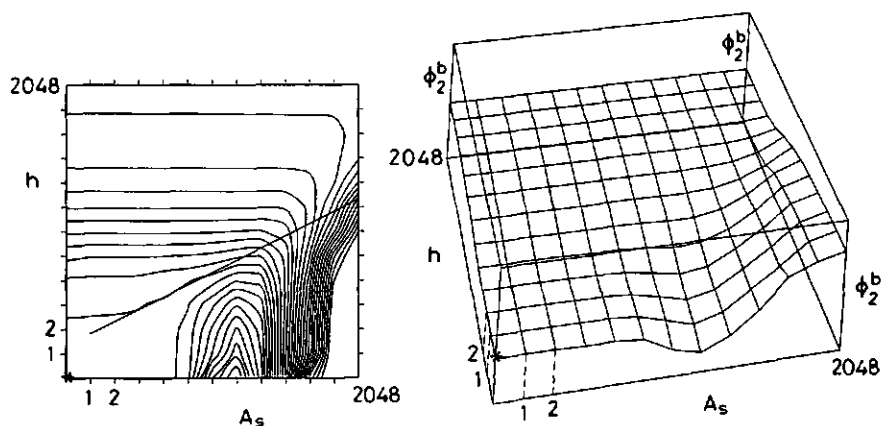


Figure 6.

Stability domains for micelles of varying shapes. Given is the relative change in equilibrium concentration ϕ_2^b for $A_{11}B_3$ micelles of different shapes, characterised by the parameters A_s and h . The overall surfactant volume fraction is near its CMC. In the graph with iso- ϕ_2^b lines the fault line gives the limit of the physically significant area.

overestimated. In figure (5b) the segment distributions of a cross section through a globular micelle in which 97 surfactant molecules are aggregated is given. These micelles are found at an overall surfactant volume fraction of $\bar{\phi}_2 = 0.005$. The unfavourable inhomogeneities observed in the centre of this micelle originate from the fact that the radius of the micelle is too big. This indicates that other micellar shapes might be more favourable at this surfactant concentration.

We showed that in more concentrated systems the micelles are larger, the corresponding chemical potential of the surfactants is higher and the excess free energy of the micelles are lower. In general, when A^σ approaches zero, the system can change its surface area without change in Gibbs energy. Thus we can expect shape fluctuations in the concentrated regime. In order to investigate this phenomenon, the equilibrium bulk concentration at given composition has been calculated for micelles of other geometries by changing h and A in equations (1) and (3). Figure (6) shows how, for the surfactant $A_{11}B_3$ near the CMC, the shape variations are related to the equilibrium bulk

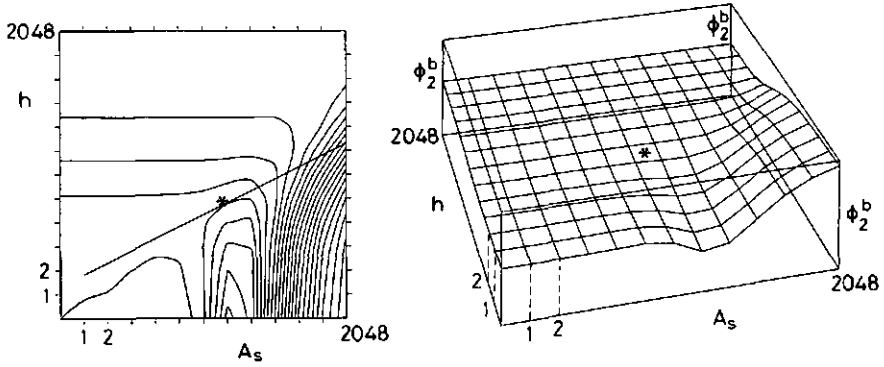


Figure 7.

Stability domains for micelles of varying shapes. See also figure (6). The overall surfactant concentration is very high so that the micelles do not have any translational entropy ($A^\sigma = 0$).

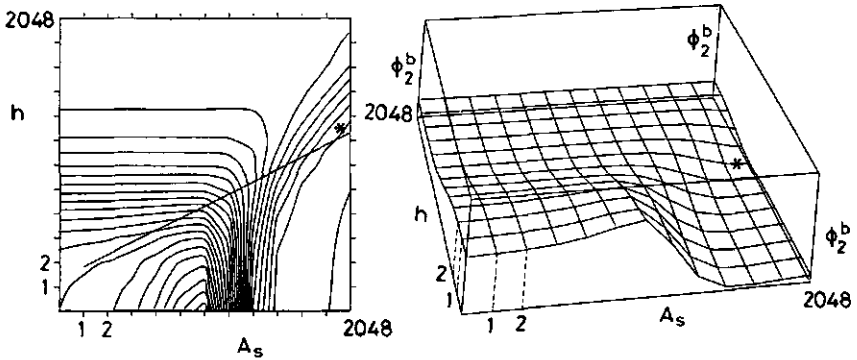
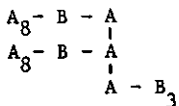


Figure 8.

Stability domains for micelles of varying shapes for the lipid molecule with a lecithin-like structure:



for moderate overall volume fractions. See also figure (6).

concentration. As can be seen, the globular micelle has the lowest free energy. (In figure (6) the most favourable micelle shape is indicated by an asterisk.) Therefore it is concluded that the very first micelles are globular.

At very high overall concentration (micelles with $A^{\sigma} = 0$; translational entropy is neglected) we see in figure (7) that for the same molecules disk-like structures have the lowest free energy. However, the variation in chemical potential as a function of micellar shape is small, so that a homodisperse micelle system is very unlikely. Consequently, the curve shown in figure (1) is modified for small A^{σ} when we allow shape variations. In this case a dashed curve as sketched in figure (1) will more likely be followed.

Similar analysis for a lipid lecithin-like molecule with two apolar tails of 8 (A) segments, a glycerol backbone, and three head group (of type B) segments, shows that the very first association colloids are again globular micelles. Increasing the concentration of the lipids has the effect that the aggregates grow in to flat membrane-like structures. This is illustrated in figure (8). This tendency is more pronounced when the tails are longer. Therefore, lecithin molecules are likely to prefer flat membranes over small micelles. Additional details of the cross over from a given association structure into another as a function of molecular architecture are given elsewhere [3].

Conclusions

The thermodynamics of small systems is combined with a statistical thermodynamical Self-Consistent Field theory and applied to amphiphilic molecules in aqueous solutions. Micelle formation is found to be a first order phase transition, but because of the low concentration of the micelles at the CMC, the theoretical critical point is not easily found experimentally. We showed that the very first micelles to form are globular and have fluctuations in size. At higher surfactant concentration the micelles can change their shapes. Then larger fluctuations with respect to their shapes are predicted. This behaviour strongly depends on the architecture of the molecules. Lecithin-like molecules are shown to prefer membrane-like structures, whereas short chain surfactants will form relatively small aggregates even at high surfactant concentration.

Literature

1. J.M.H.M. Scheutjens, and G.J. Fleer; *J. Phys. Chem.* **83** (1979) 1619.
2. F.A.M. Leermakers; PhD thesis, Wageningen (1988) Chapter 3.
3. F.A.M. Leermakers, P.P.A.M. van der Schoot, J.M.H.M. Scheutjens, and J. Lyklema; in: "Surfactants in Solution. Modern Applications" (K.L. Mittal, Ed.), in press.
4. P.P.A.M. van der Schoot, and F.A.M. Leermakers; submitted to *Macromolecules*.
5. D.G. Hall, and B.A. Pethica; in: "Nonionic surfactants", (M.J. Schick, Ed.), Marcel Dekker, N.Y. (1976), Ch. 16.
6. T.L. Hill; "Thermodynamics of small systems", Vols 1 and 2, Benjamin, N.Y. (1963, 1964).
7. D.W.R. Gruen; *J. Coll. Interf. Sci.* **89** (1985) 153.
8. K.A. Dill, and P.J. Flory; *Proc. Natl. Acad. Sci. USA* **78** (1981) 676.
9. A. Ben-Shaul, I. Szleifer, and W.M. Gelbart; *Proc. Natl. Acad. Sci. USA* **81** (1984) 4601.
10. P. van der Ploeg, and H.J.C. Berendsen; *J. Chem. Phys.* **76** (1982) 3271.
11. B. Owenson, and L.R. Pratt; *J. Phys. Chem.* **88** (1984) 2965.
12. E. Ruckenstein, and R. Nagarajan; *J. Phys. Chem.* **79** (1975) 2622.
13. R. Nagarajan, and E. Ruckenstein; *J. Coll. Interf. Sci.* **60** (1977) 221.
14. E. Ruckenstein, and R. Nagarajan; *J. Phys. Chem.* **85** (1981) 3010.
15. D.G. Hall; in "Nonionic Surfactants", (M.J. Schick, Ed.), Marcel Dekker, N.Y. (1987), Ch. 5.

CHAPTER 2

LIPID BILAYER MEMBRANES

Abstract

Step-weighted random walks (modified Markov chain statistics) combined with a self-consistent field approximation form the basic concepts of a Flory-Huggins type of theory to describe the lipid bilayer [1]. The purpose of the present paper is to extend this model by incorporating the rotational isomeric state scheme, both for linear and branched chain molecules. Only three measurable interaction energy parameters of a Flory-Huggins type are required, namely for the head group tail, the head group water, and the tail water contacts. In addition, the theory needs one energy parameter for the internal trans/gauche transition energy of the chain. Results of this self-consistent field (SCF) theory are given for membranes formed by lecithin-like molecules. With respect to earlier work, more detailed insight is obtained in the behaviour of the lipid bilayer above the gel to liquid phase transition temperature. Equilibrium conditions are formulated. Segment density profiles and solvent distributions are calculated. It is shown that the two apolar tails of the lecithin do not behave identically. The tail next to the head group is lifted slightly more out of the membrane than the other tail. The well-known balance of forces, responsible for membrane formation is analysed. We found that the repulsive tail head interaction, often ignored in theories, is essential for the stability of association colloids.

Introduction

Lipid bilayer membranes provide the living cell with a surface on which protein molecules have interaction. Membranes also are the interfaces between cell compartments. The recognition that these properties serve vital functions in living material has stimulated the research on lipid bilayers. There is a need for a general theory which describes equilibrium properties of lipid bilayers, explains the polymorphism of lipid aggregates, gives insight into the molecular behaviour of the lipids in an aggregate, and eventually shows the gel to liquid phase transition behaviour. These topics have been the

subject of many studies and several theories deal with various aspects of this problem. In a series of papers we will show that it is possible to design a comprehensive statistical thermodynamical theory which is able to deal with all of these aspects simultaneously.

Molecular dynamics (MD) is an alternative method to obtain detailed information on aggregates of amphipolar molecules. One of the first MD studies on the bilayer membrane is performed by Van der Ploeg and Berendsen [2]. The excluded volume of the molecules is treated rigorously and all interactions are taken into account with high accuracy. Indeed, modern simulations do not fix the head groups positions to a certain plane and the few results obtained so far seem realistic [3]. Unfortunately, MD needs many parameters. It has been shown recently that results depend on the model which is used to simulate the solvent phase [4]. Further, the method is limited by the small number of molecules, and the relatively short tail lengths, which can be taken into account. Because of the time scale of the simulations (in the order of 100 pico seconds) a slow process like the exchange of lipids between a membrane and the bulk solution cannot yet be simulated by molecular dynamics.

In principle, Monte Carlo (MC) simulations may also be useful to gain insight into the behaviour of amphipolar molecules in aqueous media. Results for small surfactant molecules have recently been obtained by Owenson and Pratt [5]. They did not restrict the positions of the head groups, and therefore their results should compare well with ours. However, for computational reasons, detailed information on lipid membranes formed by lecithins is not yet available.

Statistical mechanical calculations based on a self-consistent field do not rely as much on the computer capacity as MD or MC techniques do. The quality of the outcome of such calculations depend on the rigour of the partition function derived. Several groups studied the conformations of hydrocarbon tails anchored to a given plane [6,7] or have used (arbitrary) head group positions [8]. The main result of these theories is the order profile along the hydrocarbon chain. Very critical for this profile is the effective head group area or, in other words, the number of chains per surface area. This parameter can be estimated from experimental values of the membrane thickness. The question why a given membrane thickness is found remains to be solved.

Our theory has a more ab initio character. It allows all molecules to

distribute freely throughout the system. In this way, equilibrium with the bulk solution is automatically guaranteed. In other words, the membrane structure can no longer be dictated. The membrane thickness and the average surface area per molecule are results of the calculations. The composition of the molecules and the values for the interaction parameters determine the properties of the aggregates. The morphology of the association colloids can also be studied if one allows for non-planar aggregates as well.

This article explains the statistical and computational aspects of the rotational isomeric state scheme in a Markov approximation, applied to branched molecules in a lamellar geometry. All conformations of a chain are generated in the mean field due to all of the other chains. During this generating process the different conformations are properly weighted. Our method of generating chain conformations shows similarities with the theory of Dill and coworkers [8]. After some manipulations the segment density profile is found. The statistical weight of each individual conformation can be calculated when this profile is known. Therefore, the theory can also be formulated in terms of a set of conformations defining the equilibrium properties of the system [9]. When doing so, the relation between our theory and MC simulations [5], or with theories in which the individual (tail) conformations are generated, as in the work of Gruen [7], is more clear. From this set of chain conformations, the partition function of the system can be calculated from which all necessary thermodynamic quantities follow. For more details of the derivation of the partition function, we refer to other papers [1,10].

First order Markov chains

A polymer chain is built up of r segments (e.g. CH_2 groups), with ranking numbers $s = 1, \dots, r$. Each segment may be connected to one or more other segments in the chain, but we assume that no ring structures are present, so that each chemical bond connects two independent parts of the chain. One of the main goals of a many-chain problem is to calculate the whole set of conformations of all molecules in a give volume. To deal with this, it is convenient to design a lattice composed of lattice sites to which polymer segments or solvent molecules are confined. Scheutjens and Fleer modified a matrix method first introduced by Di Marzio and Rubin [11] to generate all conformations of the polymer chains in this lattice. In the absence of a

potential field, this matrix formalism can be shown to be equivalent with random walk statistics. It is characteristic for the random walk on the lattice that each step has Z options, irrespective of previous steps, where Z is the co-ordination number of the lattice, i.e., the number of neighbouring lattice sites. In the present elaboration the lattice consists of parallel layers of L lattice sites each. They are numbered $z = 1, \dots, M$, where layer numbers 1 and M form the boundaries of the system. A fraction λ_{-1} of these Z sites is situated in a previous layer, a fraction λ_1 in the next layer and a fraction λ_0 in the same layer. We are interested in the density distribution of each segment for a given potential profile $u(z)$ (a free energy per segment). This profile is usually different for each type of segment or solvent molecule and includes hard core interactions and specific contact energies. In this way we can use simple Boltzmann statistics to obtain the distribution functions. For example, the density distribution of solvent, denoted by subscript W , is given by

$$\phi_W(z) = \phi_W^b G_W(z) \quad (1)$$

where $\phi_W(z)$ is the volume fraction of solvent in layer z , ϕ_W^b that in the bulk solution and $G_W(z) = \exp(-u_W(z)/kT)$ gives the distribution function of solvent molecules. Similarly, $G_A(z) = \exp(-u_A(z)/kT)$ gives the distribution function of monomers of type A in a potential field $u_A(z)$, whereas $G_A(z) \lambda_{z,-z} G_B(z')$ gives the distribution function of AB dimers, where segment A is in layer z and segment B in layer z' . The distribution of A segments of these dimers is thus given by $G(z, AB) = G_A(z) \sum_{z', z'-z} \lambda_{z', -z} G_B(z')$.

Generally, each segment s contributes a factor $G_1(z, s)$ to the distribution function of a chain i and the distribution function of the last segment of a chain of s segments can be expressed in a Markov approximation

$$G(z, s_1) = G(z, s) \sum_{z', z'-z} \lambda_{z', -z} G(z', s'_1) \quad (2)$$

The subscript 1 refers to the bond 1 with which the rest of the chain is connected. Note that the subindex i is dropped to indicate that the equation is general applicable. $G(z', s'_1)$ is the distribution function of segment s' when the bond between s and s' is disconnected. In shorthand notation equation (2) is written as

$$G(z, s_1) = G(z, s) \langle G(z, s_1') \rangle \quad (3)$$

The angular brackets denote a weighted averaging of $G(z, s_1')$ over layers $z-1$, z , and $z+1$. Equation (3) is a recurrence relation that expresses the end segment distribution into that of a chain that is one segment shorter. A segment with chain parts at two of its bonds (1 and 2) has a distribution function $G(z, s_{12}) = \langle G(z, s_1') \rangle G(z, s) \langle G(z, s_2'') \rangle$ or

$$G(z, s_{12}) = G(z, s_1) G(z, s_2) / G(z, s) \quad (4)$$

We have assumed that segment s' and s'' may overlap each other occasionally (Markov-type behaviour). The volume fraction of segment s in layer z is now calculated as

$$\phi(z, s_{12}) = C G(z, s_{12}) \quad (5)$$

where C is a normalisation constant, obtained from the volume fraction ϕ^b

$$C = \frac{\phi^b}{r} \quad (6)$$

or from the total amount of segments $\theta = \sum_z \sum_s \phi(z, s)$ in the system. Since $\sum_z G(z, s_{12})$ is independent of s , $\sum_s \sum_z G(z, s_{12}) = r \sum_z G(z, r_1) = r G(r_1)$, the normalisation constant is

$$C = \frac{\theta}{r G(r_1)} \quad (7)$$

Starting at either chain end, equation (3) generates all end segment distribution functions needed in equation (4) from the monomer distribution function $G(z, s)$ (substituted by $G_A(z)$, $G_B(z)$, etc., depending on the type of segment s), so that the volume fraction distributions can be obtained from equation (5). This procedure is repeated for each type of molecule (1) in the system. For monomers equation (5) reduces to the simple form of equation (1).

The segment density distributions should obey the volume restriction requirement (constant density) in each layer z :

$$\sum_x \phi_x(z) = 1 \quad (8)$$

Here, x denotes segment or solvent type ($x = A, B, W, \dots$). In the simplest case there are only hard core interactions in the system, so that $G_x(z) = \exp(-u'(z)/kT)$ for all segment types x . In this case $u'(z)$ is the hard core potential and is chosen such that equation (8) is satisfied. More generally, the potential profile of segment x includes energetic contributions from nearest neighbour interactions, which can be expressed in terms of Flory-Huggins parameters χ_{xy} :

$$u_x(z) = u'(z) + kT \sum_y \chi_{xy} \{ \langle \phi_y(z) \rangle - \phi_y^b \} \quad (9)$$

The summation y runs over all segment types. The angular brackets again indicate a weighted average over three consecutive layers ($z' = z-1, z, z+1$):

$$\langle \phi(z) \rangle = \sum_{z'} \lambda_{z'-z} \phi(z') \quad (10)$$

The number of equations ((8) and (9)) always equals the number of unknowns ($u'(z)$ and $u_x(z)$), so that the set of simultaneous equations can be solved numerically.

Branched molecules are treated very similarly. If segment s (connected with bonds 1 and 2 in the chain) has a branch at bond 3, we apply equation (4) to connect the chain parts at bonds 1 and 2 and an equivalent equation (11) to connect the branch at bond 3

$$G(z, s_{123}) = G(z, s_{12}) G(z, s_3) / G(z, s) \quad (11)$$

$G(z, s_3)$ is generated using equation (3) and starting at the end of the branch chain. The density distribution of the branching segment follows from $\phi(z, s_{123}) = C G(z, s_{123})$. Equations (4) and (5) remain valid for all other segments, because these segments have only two bonds each. However, $G(z, s_1)$ or $G(z, s_2)$ should include the contribution of the branch. If the branch is in the chain part that is connected to bond 1 of segment s and the branch point is s' , we can obtain $G(z, s_1)$ using equation (3) starting at $G(z, s_{13})$: $G(z, s_1) = G(z, s'') \langle G(z, s_{13}) \rangle$, where s'' is the segment directly connected to s' .

Rotational isomeric state scheme

Due to steric hindrance, a sequence of three C-C bonds has three favourable, one trans (t) and two gauche (g^+ , g^-), configurations (see figure 1). The two gauche configurations have an energy $U^g \approx 1$ kT higher than the trans configuration. Each additional C-C bond has again three possible orientations which form trans or gauche configurations with its two predecessors. The whole chain will fit on a tetrahedral (diamond) lattice, where each bond is in one of four orientations e'' , f'' , g'' , or h'' . In each of these orientations we distinguish two opposite directions: e and e' , f and f' , g and g' , h and h' , respectively (see figure 2). We orient the lattice in such a way that bonds in orientations f'' and g'' connect segments within the same lattice layer and bonds in orientations e'' and h'' connect segments in neighbouring lattice layers. If we rotate this lattice around its z axis over

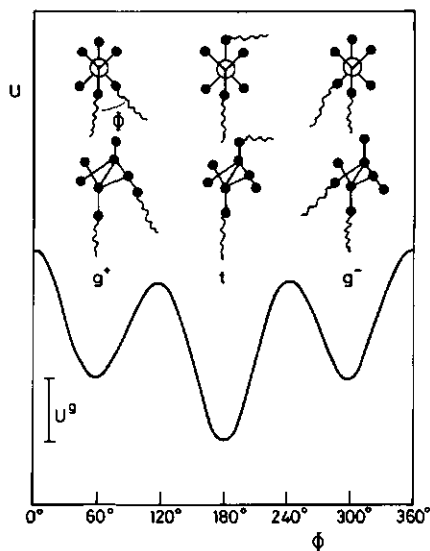


Figure 1.

Schematic drawing of gauche and trans configurations in a chain and the energy as a function of the angle ϕ between two consecutive bonds in the chain. The three minima in the energy curve correspond with a g^+ , t , and g^- configuration, respectively. The trans configuration is energetically most favourable.

angles of 120 degrees we get a superposition of 3 tetrahedral lattices which is very similar to a hexagonal lattice: each lattice site gets 12 instead of 4 neighbours, but the 6 of them in the same layer do not form a hexagon. As we will apply a mean field approximation within each layer, this difference will not affect the results. Hence it will suffice to consider only the tetrahedral lattice with the four bond orientations defined above.

There are two types of sites in the lattice which are mirror images of each other. Sites of type I have neighbours (all of type II) in directions e, f, g, and h, whereas sites of type II are surrounded by sites of type I in directions e', f', g' and h' (see figure 2b). We will assume that a segment can at the most have four possible bonds. These bonds give a segment an orientation, irrespective whether the bonds are free or not. A segment on a site in a tetrahedral lattice may assume one out of 12 orientations: one bond

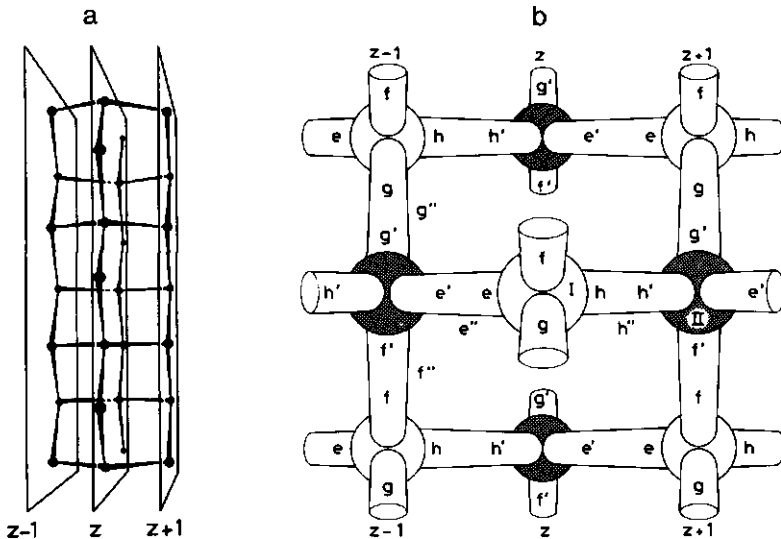


Figure 2.

- a. Identification of lamellae in a tetrahedral lattice. All segments are on one of the parallel planes.
- b. Alternative representation of the same lattice. The eight bond directions, four bond orientations and the two types of sites are indicated.

Table 1. Compilation of segment orientations in a tetrahedral lattice.

segment	isomer I				isomer II			
	I		II		I		II	
site	I	II	I	II	I	II	I	II
bond number	1234	1 2 3 4	1234	1 2 3 4	1234	1 2 3 4	1234	1 2 3 4
orientation	ehfg	h'e'f'g'	hefg	e'h'f'g'	efgh	h'f'g'e'	hfge	e'f'g'h'
	efgh	h'f'g'e'	hfge	e'f'g'h'	eghf	h'g'e'f'f'	hgfe	e'g'h'f'f'
	eghf	h'g'e'f'f'	hgfe	e'g'h'f'f'	fhge	f'e'g'h'h'	fegh	f'h'g'e'h'
	fhge	f'e'g'h'h'	fegh	f'h'g'e'h'	fgeh	f'g'h'e'	fghe	f'g'e'h'h'
	fgeh	f'g'h'e'	fghe	f'g'e'h'h'	feh'g	f'h'e'g'	fheg	f'e'h'g'h'
	feh'g	f'h'e'g'	fheg	f'e'h'g'h'	gef'h	g'h'f'e'	ghfe	g'e'f'h'h'
	gef'h	g'h'f'e'	ghfe	g'e'f'h'h'	gfhe	g'f'e'h'	gfeh	g'f'h'e'h'
	gfhe	g'f'e'h'	gfeh	g'f'h'e'h'	gh'ef	g'e'h'f'f'	geh'f	g'h'e'f'f'
	gh'ef	g'e'h'f'f'	geh'f	g'h'e'f'f'	hg'fe	e'g'f'f'h'	eg'fh	h'g'f'e'h'
	hg'fe	e'g'f'f'h'	eg'fh	h'g'f'e'h'	hf'eg	e'f'h'g'	ef'hg	h'f'e'g'h'
	hf'eg	e'f'h'g'	ef'hg	h'f'e'g'h'	he'gf	e'h'g'f'f'	eh'gf	h'e'g'f'f'
	he'gf	e'h'g'f'f'	eh'gf	h'e'g'f'f'				

can choose between four directions and a second bond between three. The directions of any other bonds are then fixed because of its stereo specificity. The first column of table (1) lists all these orientations for a site of type I. Each orientation can be obtained from another one by rotation around one of the bonds (keep any one bond in position and exchange the three others). The stereo isomer is obtained by exchanging any two bond orientations. The third column of table (1) lists all orientations of the isomer on a site of type I (exchanging h and e). As a mirror image of a segment on a site I is equivalent to its stereo isomer on a site II, we obtain a complete list of bond direction combinations on sites II by reversing all directions in the first and third column in table (1), giving columns four and two, respectively.

A segment orientation is defined by specifying the directions of two of its bonds. We will use the symbol s^{ef} when the first bond of segment s is in direction e and the second bond in direction f . Equivalently, $s^{g'h'}$ signifies that bond one is in direction g' and bond three is in direction h' . To indicate the fact that the segment is part of a chain we write $s_{14}^{h'..e'}$ if bond 1 in direction h' and bond 4 in direction e' are connected to other chain

parts.

In this paper we assume that the potential profile (equation (9)) is independent of the orientation of a segment, so that

$$G(z, s^{\alpha\beta}) = \begin{cases} 0 & \text{if } \alpha = \beta \\ G(z, s) & \text{otherwise} \end{cases} \quad (12)$$

where α and β stand for the bond directions e, f, g, and h (or e', f', g', and h' for sites of type II). There are 24 non-zero independent values $G(z, s^{\alpha\beta})$. Equation (2), describing elongation of the chain at s' by one segment s , becomes:

$$G(z, s_1^{\alpha\beta}) = G(z, s^{\alpha\beta}) \sum_{\gamma'} \lambda^{\beta''-\alpha''-\gamma''} G(z', s_1^{\gamma'\alpha'}) \quad (2a)$$

In this case bond 1 of segment s (in direction α) is connected to bond 2 of segment s' (in direction α'). Layer z' is either $z-1$, z , or $z+1$, depending on the direction of α' . There are only three non-zero contributions to $G(z, s_1^{\alpha\beta})$, because all combinations with $\alpha = \beta$ are excluded by equation (12). The superscript $\beta''-\alpha''-\gamma''$ refers to a sequence of three bonds, in orientation β'' , α'' , and γ'' , respectively (a superscript $\beta''\alpha''\gamma''$ would refer to three bond orientations of the same segment), forming a gauche or trans configuration. The three configurations are properly weighted by λ^t or λ^g :

$$\lambda^{\alpha''-\beta''-\gamma''} = \begin{cases} \lambda^t & \text{if } \alpha'' = \gamma'' \\ \lambda^g & \text{otherwise} \end{cases} \quad (13)$$

where $\lambda^g = 1/(2+\exp(U^g/kT))$ and $\lambda^t = 1 - 2\lambda^g$. Equation (2a) applies even to dimers and end segments, because the difference between t and g affects only the orientation of the next bond, which is a free bond in these cases. Therefore, the recurrence equation (2a) can be started at $G(z, s_1^{\alpha\beta}) = G(z, s^{\alpha\beta})$. The equivalent of equation (2a), starting at the other chain end reads:

$$G(z, s_2^{\alpha\beta}) = G(z, s^{\alpha\beta}) \sum_{\gamma'} \lambda^{\alpha''-\beta''-\gamma''} G(z', s_2^{\beta'\gamma'})$$

where bond 2 of segment s in direction β is attached to bond 1 of segment s' in direction β' .

The end to end connection of two chains at segment s in orientation $\alpha\beta$ is

now just a variation of equation (4), because all gauche and trans energies are already accounted for.

$$G(z, s_{12}^{\alpha\beta}) = G(z, s_1^{\alpha\beta}) G(z, s_2^{\alpha\beta}) / G(z, s^{\alpha\beta}) \quad (4a)$$

and $G(z, s_{12})$ in equation (5) becomes the average value of $G(z, s_{12}^{\alpha\beta})$

$$G(z, s_{12}) = \sum_{\alpha} \sum_{\beta} \lambda^{\alpha\beta} G(z, s_{12}^{\alpha\beta}) \quad (14)$$

Here, $\lambda^{\alpha\beta} = 1/24$ is the inverse of the number of segment orientations on sites of type I and II. The number of segments on sites of type I must be equal to those on type II, i.e., $\sum_I \phi_I(z_I) = \sum_{II} \phi_{II}(z_{II}) = 0.5$. In the present treatment there is no numerical difference between $G(z, s^{\alpha\beta})$ and $G(z, s^{\alpha'\beta'})$, so that this constraint is automatically obeyed. Moreover, the consecutive segments in a chain are placed on alternate type of sites. Only the chain as a whole may in certain systems prefer to start always on the same type of site. For example, in a crystal the chains would be all in the same orientation.

A branch in the chain presents some extra difficulties. Instead of equation (11) we have

$$G(z, s_{123}^{\alpha\beta\gamma}) = G(z, s_1^{\alpha\beta\gamma}) G(z, s_2^{\alpha\beta\gamma}) G(z, s_3^{\alpha\beta\gamma}) / G(z, s^{\alpha\beta\gamma})^2 \quad (11a)$$

Although the orientation of a segment is fixed by the direction of two of its bonds, all three bond directions are indicated in equation (11a) for the sake of clearness. Obviously, $G(z, s^{\alpha\beta\gamma}) = G(z, s^{\alpha\beta})$. The chain end distribution function $G(z, s_1^{\alpha\beta\gamma})$ indicates that the rest of the chain is connected to bond 1 of s , which is in the α direction. This quantity is found by a modification of equation (2a). When s' is the segment adjacent to the branching segment s then

$$G(z, s_1^{\alpha\beta\delta}) = G(z, s^{\alpha\beta\delta}) \sum_{\gamma'} \lambda^{\gamma''-\alpha''-\beta''\delta''} G(z', s_1^{\gamma'\alpha'}) \quad (2b)$$

where bond 2 of segment s' in direction α' is connected to bond bond 1 of s in direction α . To segment s also the directions β and δ are assigned to which bond 2 and 3 will be connected, respectively. The parameter $\lambda^{\gamma''-\alpha''-\beta''\delta''}$ weights their contributions:

$$\lambda^{\alpha''-\beta''-\gamma''\delta''} = \begin{cases} \lambda^{tg} & \text{if } \alpha'' = \gamma'' \text{ or } \alpha'' = \delta'' \\ \lambda^{gg} & \text{otherwise} \end{cases} \quad (15)$$

where $\lambda^{tg} = \lambda^t \lambda^g / (2 \lambda^t \lambda^g + \lambda^g \lambda^g)$ and $\lambda^{gg} = 1 - 2 \lambda^{tg}$. It is illustrative to give the equivalent expression (2b) for the case that bond 3 of s' in direction β' is connected to bond 2 of segment s , while bond 1 and 3 of segment s are in directions α and δ , respectively:

$$G(z, s_2^{\alpha\beta\delta}) = G(z, s^{\alpha\beta\delta}) \sum_{\gamma'} \lambda^{\gamma''-\beta''-\alpha''\delta''} G(z', s_2^{\gamma'\beta'})$$

Obviously, by the following equation a segment s'' in orientation $\alpha\beta$ is connected with bond 1 to bond 2 of segment s which has other chain parts at bonds 1 and 3:

$$G(z, s_1^{\alpha\beta}) = G(z, s^{\alpha\beta}) \sum_{\gamma'} \lambda^{\beta''-\alpha''-\gamma''\delta''} G(z', s_{13}^{\gamma'\alpha'\delta'}) \quad (2c)$$

where $G(z, s_{13}^{\alpha\beta\gamma}) = G(z, s_1^{\alpha\beta\gamma}) G(z, s_3^{\alpha\beta\gamma}) / G(z, s^{\alpha\beta\gamma})$. The summation over γ' represents the three directions of bond 1 of segment s with bond 2 in direction α' . These orientations can be obtained from table 1 and determine the directions δ' simultaneously. This formalism is easily extendible for a branch point with four groups. For example, a segment s'' in orientation $\alpha\beta$ is connected through bond 1 to bond 2 of segment s' to other chain parts at bonds 1, 3, and 4 by:

$$G(z, s_1^{\alpha\beta}) = G(z, s^{\alpha\beta}) \sum_{\gamma'} \lambda^{\beta''-\alpha''-\gamma''\delta''\epsilon''} G(z', s_{134}^{\gamma'\alpha'\delta'\epsilon'}) \quad (2d)$$

where $\lambda^{\beta''-\alpha''-\gamma''\delta''\epsilon''} = \lambda^{gggt} / (3 \lambda^{gggt}) = 1/3$.

Computational aspects

Due to the symmetry of the lattice and the mean field approximation, many of the quantities G are numerically equal. We have already mentioned the equivalence of sites of type I and II. Moreover, there will be an equal number of bonds in orientations e'' and h'' (between two layers) and similarly in orientations f'' and g'' (within a layer). Generally, for a segment with two bonds there are only 7 numerically different segment orientations $\alpha\beta$, instead of 24. These are listed in table (2). In appendix A the resulting equations ((2a) and (4a)) are given in matrix notation.

Table 2. Degenerate segment orientations

$eh \equiv h'e'$
$ef \equiv eg \equiv h'g' \equiv h'f'$
$fh \equiv gh \equiv g'e' \equiv f'e'$
$fg \equiv gf \equiv g'f' \equiv f'g'$
$fe \equiv ge \equiv g'h' \equiv f'h'$
$hf \equiv hg \equiv e'g' \equiv e'f'$
$he \equiv e'h'$

For a segment with three or four bonds each orientation on a site of type I has only one numerically equivalent orientation on a site of type II, e.g., $ehfg \equiv h'e'f'g'$, $efgh \equiv h'f'g'e'$, etc., so that 12 different numbers remain. (The corresponding pairs are listed in table 1 next to each other.)

To fix the membrane on the lattice we place a reflecting boundary in the centre of the the bilayer [1] (there is no reason why the bilayer would be asymmetric), between layers 0 and 1. This is accomplished by setting all (image) quantities in layer $1-z$ equal to those in layer z . Thus $G(1-z, s_{efgh}^{12}) = G(z, s_{hgfe}^{12})$, $\phi(1-z, s) = \phi(z, s)$, etc. In fact, the molecules are rotated over 180 degrees, rather than reflected, because a reflection would produce the stereo isomer. The rule to find the rotated bond directions is to replace e, f, g, h, e', f', g' , by h' for h, g, f, e, h', g', f' , and e' , respectively.

Obviously, the reflecting boundary could also be placed in layer 0 so that quantities in layer $-z$ equal those in layer z . A similar reflecting boundary can be placed in the bulk solution, between layers M and $M+1$ or in layer M . Hence, calculations for only M or $M+1$ layers are to be performed. Membranes are initiated in the first few layers by a suitable initial guess (see appendix B).

Evaluation of the Markov chain and mean field approximations

It is appropriate to summarise the shortcomings and advantages of the Markov chain approximation and, consequently, the local mean field approximation coupled to it. Strictly spoken, our chain statistics has pure Markov behaviour only if all steps are weighted with a constant factor, i.e., for a homogeneous system. In a concentration gradient the steps are weighted

according to the local potential and therefore our method may also be characterised as "a step weighted random walk". Since in a Markov approximation only short range correlations (along the chain) are taken care of, we were able to use a recurrent relation which guarantees (within certain limits) the generation of all allowed conformations of a chain in the average field of all other chains. By incorporation of some memory along the chain path (RIS scheme), direct backfolding can be forbidden. With this method we cannot prevent a chain segment to enter a lattice site which is already occupied by a segment of one of the other chains. We also allow the chain to enter a lattice site which is already occupied by a segment of the same chain if it is more than four bonds apart. We compensate for any multiple occupancy of sites by allowing only L segments in each lattice layer.

The consequence of using the average segment density in each layer is that inhomogeneities in each layer parallel to the membrane are neglected. When a lamellar lattice is used, the membrane is forced to be flat and spontaneous undulations along the bilayer are not taken into account.

There are a few impressive achievements in the present treatment. One can generate all conformations of chains of up to 10,000 segments without too much computational effort. The segment density profiles of each conformation can be calculated so that very detailed information on the segment positions is available. Any number of different types of molecules (for example polydisperse polymers, additives etc.) can be introduced without undue complications. If necessary, other interactions (for example electrostatic) or external potentials (for example long range Van der Waals interactions) can be taken into account as well.

Comparison with other theories

Dill and coworkers use a different but similar recurrence relation to generate all possible conformations of chains on a lattice [8]. However, they fix the head groups in particular layers and allow all segments only to be in the same layer or in the layers closer to the centre of the aggregates.

Gruen either samples the set of conformations, or generates the whole set [7]. His approach does not make use of a lattice and consequently his set of conformations for the lipid molecules is in this respect more realistic than ours. For computational reasons, a predetermined number of head groups were confined to a given layer so that equilibrium with the bulk solution was lost.

A more severe drawback of his approach is that one cannot be sure to find the set of conformations which minimises the free energy. Gruen generated several solutions obeying the space filling requirement. The chain packing corresponding to the lowest free energy found was accepted as the physical realistic solution.

Both Gruen and Dill et al. did not allow solvent molecules or head groups in the tail region, and therefore they did not need to take energetic interactions into account. For the space filling requirement both theories need a kind of osmotic potential like our $u'(z)$.

In our theory all essential energetic interactions are accounted for. Our segment density profiles are self-consistent, and equilibrium with the bulk solution is always guaranteed. Standard thermodynamics are used to find the equilibrium properties of the system.

Results and discussion

Lipid molecules

We will concentrate on lecithin-like molecules modelled by a glycerol backbone, two identical tails of p (CH_2) apolar (A) segments each and a head group of q polar (B) segments:



We disregard volume differences between a terminal CH_3 group and a CH_2 group, nor do we specify more details in the head group. Henceforth the solvent simply is indicated as "water" and is modelled as a monomer of segment type W. The solvent molecules are denoted by $i = 1$ and the lipids by $i = 2$.

Interaction parameters

In the most simple case there are three χ parameters for the various contacts in the system. Roughly, χ_{AW} (tail segment/water interaction) is 1.6, χ_{BW} (head group segment/water interaction) is 0 or slightly negative, and χ_{AB} (tail segment/head group segment interaction) is around 1.5. This set of χ values implies that head groups are soluble in water, but the tails avoid

head groups and water molecules (high χ values). It mimics the well-known opposing forces stabilising the lipid aggregates. Phase separation between tails and water is the driving force for association. Head groups repel tails and therefore they are forced to be on the outside of the aggregate. As they like water, micelle or membrane growth is limited and the aggregate stabilises at a certain size. In literature the interaction between tails and heads is often neglected. The choice $\chi_{AB} = 1.5$ mimics a repulsion between these types of segments. If this interaction is too weak, the head groups mix too easily with tail segments and consequently too many tail segments would be exposed to the water phase. In this case no stable associates are formed. In the RIS scheme one extra parameter is needed namely the energy difference between a gauche and a trans configuration. We used a value of 1 kT at $T = 275$. This resembles a literature value of around 0.8 kT at room temperature [12].

Branch points

We have allowed minor simplifications with respect to the computations at the branch point. We will only account for non-overlapping chain parts. In other words, a second order Markov approximation is used instead of a third order (RIS) Markov approximation. Typically, a second order Markov approximation has a chain end distribution function $G(z, s_1^\alpha)$ which states that the free bond 2 will be connected with a segment in direction α , while bond 1 is connected with a chain in any of the three remaining directions. In this case all $\lambda^{\alpha-\beta-\gamma-\delta}$ equal 1/3 for all possible combinations of the three meeting chain parts. Further, we did not distinguish between the two enantiomers. Consequently, the number of ways to connect the three subchains in the branch point is doubled. Therefore, in this case the normalisation given in equation (14) for the branch segment $\lambda^{\alpha\beta\gamma} = \frac{1}{2} \lambda^{\alpha\beta}$ is used. In this way the number of operations for the branch point is reduced from 12 to 3.

Membrane in a frame

Membranes in a frame are known as black lipid films. Since they are restricted from translation, they are relatively easy examined experimentally. The membrane thickness and, more generally, the membrane composition can be modified by a suitable experimental conditions. In our theory the membrane composition is changed by changing the lipid concentration in the system. In doing so, thermodynamic data can be calculated. Figure (3a) shows how the

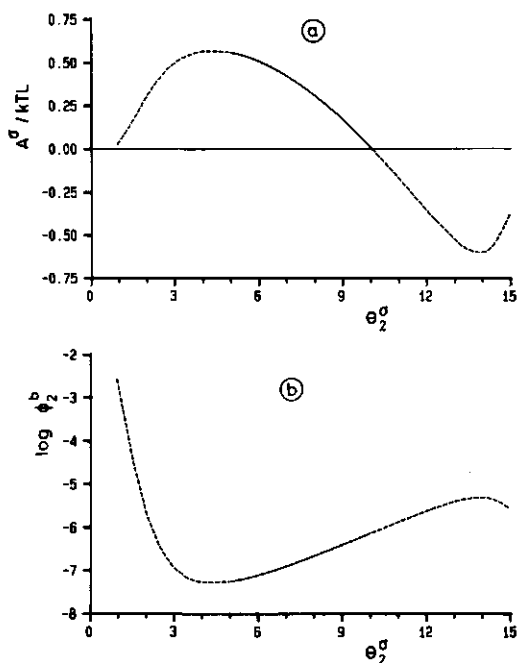


Figure 3.

a. Excess surface free energy per lattice site as a function of θ_2^σ ("membrane thickness").

b. Equilibrium volume fraction of lipids in the bulk as a function of θ_2^σ . The lipid membrane is composed of lecithin-like molecules of tail length 14 and head group size 3, see text. The solid parts of the curves represent stable membranes. Energy parameters: $\chi_{AW} = 1.6$; $\chi_{BW} = -0.3$; $\chi_{AB} = 1.5$; $U^B = 275/300$ kT. Temperature: 300 K.

excess free energy A^σ expressed as

$$A^\sigma / kTL = - \sum_i \frac{\theta_i^\sigma}{r_i} + \sum_z \ln \frac{\phi_w(z)}{\phi_w} + \frac{1}{2} \sum_x \sum_y (\chi_{xw} + \chi_{yw} - \chi_{xy}) [\phi_x(z) \langle \phi_y(z) \rangle - \phi_x^b \phi_y^b] \quad (17)$$

depends, among other quantities, on the excess amount of lipids, θ_2^σ , which is a measure of the membrane thickness:

$$\theta_2^\sigma = \sum_{z=1}^M (\phi_2(z) - \phi_2^b) \quad (18)$$

Figure (3b) gives the equilibrium concentration of lipids in solution as a function of θ_2^σ . For very thin membranes the equilibrium concentration of lipids in the bulk (and hence their chemical potential) is high, but passes a minimum when the membranes grow thicker. A second minimum is present at high θ_2^σ , when on the membrane a second bilayer is formed (only present if the bilayers attract each other). In figure (3a), the excess free energy of the film is behaving oppositely: when the chemical potential decreases, the excess free energy increases. This is in accordance with Gibbs' law.

Only the middle parts of the curves (solid lines) in figure (3) are operational. If A^σ is negative the membrane will spontaneously increase its surface area and thin membranes are unstable because $\partial A^\sigma / \partial \theta_2^\sigma > 0$ (see below).

Free membranes

In contrast with a membrane in a frame, a free membrane does not feel the constraint of the frame and therefore it will adjust its surface area A_s until the surface tension vanishes. From thermodynamics the change in Gibbs energy A at constant pressure p and temperature T , surface tension γ and chemical potential μ_i .

$$dA = \gamma dA_s + \sum_i \mu_i dn_i \quad (19)$$

Indeed, equilibrium is established when $(\partial A / \partial A_s)_{p, T, n_i} = 0$, thus $\gamma = 0$. For stable equilibrium the free energy A as a function of the area must be convex at this point: $(\partial^2 A / \partial A_s^2)_{p, T, n_i} > 0$, thus $(\partial \gamma / \partial A_s)_{p, T, n_i} > 0$. Since

$$\frac{\partial \theta_2^\sigma}{\partial A_s} < 0 \quad (20)$$

stable equilibrium is found when $(\partial \gamma / \partial \theta_2^\sigma) < 0$, or equivalently,

$$\frac{\partial (A^\sigma / L)}{\partial \theta_2^\sigma} < 0 \quad (21)$$

The stable points for the free membranes and the stability range for membranes in a frame are found with the help of figure (3a).

The conclusion that free membranes have no surface tension is also reached by applying the thermodynamics of small systems [13,14], assuming that

the membrane has no translational entropy. Indeed, the translational entropy of the membrane is relatively small, but there are contributions due to undulations. The number of undulations and their distribution depend on the free energy of curvature of the bilayer. Curved bilayers (vesicles) will be examined in a following publication [15]. The wave length of the undulations, is large compared to the membrane thickness, so that only a very small excess free energy per surface site is present. Therefore, all membrane systems discussed below are assumed to have a zero excess free energy.

First order Markov chains compared to rotational isomeric state scheme

Figure (4) shows the overall segment density profiles through a cross section of membranes consisting of lecithin molecules with tails of 14 segments. In figure (4a) the first order Markov approximation is used, whereas in figure (4b) the result for the RIS scheme is shown. The difference between the two graphs is obvious. As expected, the RIS scheme leads to considerably thicker membranes. As the chain density in the membranes is the same for both approximations, the head group density for the RIS membrane is higher. Nevertheless, the head group density is still rather low and therefore many tail segments are in contact with the water phase.

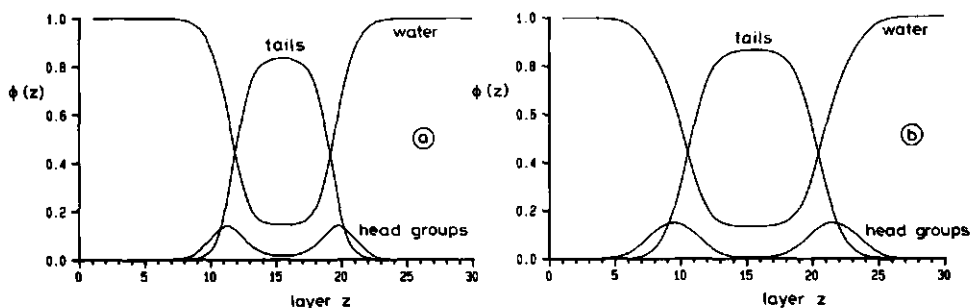


Figure 4.

Segment density profiles through cross sections of a membrane composed of lecithin-like molecules. Parameters as in figure(3). The layers are numbered arbitrarily.

a) First order Markov approximation. b) RIS approximation.

Figures (4a) and (4b) suggest that a large amount of water is present in the membrane, which is certainly an overestimation. The water concentration in the membrane reaches the binodal concentrations predicted by the Flory-Huggins (FH) theory [16]. It is well-known that the FH theory (and hence also our theory) successfully predicts phase separation qualitatively, but that the compositions of the phases are wrong. Corrections for this defect are rather involved. One very successful method to improve the membrane picture will be discussed in a future publication where an orientation-dependent molecular field is introduced in the theory [17]. The model also needs to be improved with respect to the water phase (water molecules are treated as unpolarisable monomers). Further, a more advanced description of the membrane system must include the compressibility of the system. A full analysis of these last two factors are also left for future work.

RIS membranes

Figure (5) shows the segment density profiles of the lipids from figure (4b) on a logarithmic scale for the volume fractions. In this figure we see that the segment density profiles outside the membrane fall off more or less exponentially until the bulk volume fraction is reached. This takes place over a distance comparable with the tail length of the lipids and with the membrane thickness. Apparently, very few dangling tails stick out of the membrane.

Our membranes are symmetrical with respect to the midplane, but the

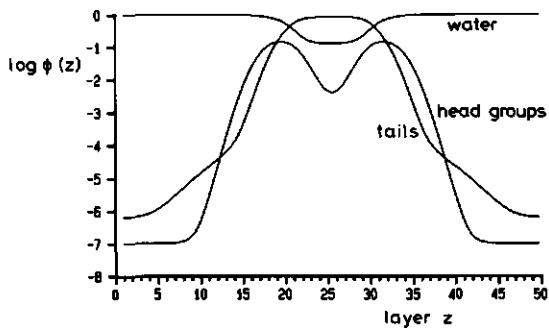


Figure 5.

Density profiles of the lipids of the membrane of figure (4b) on a logarithmic scale for the volume fractions.

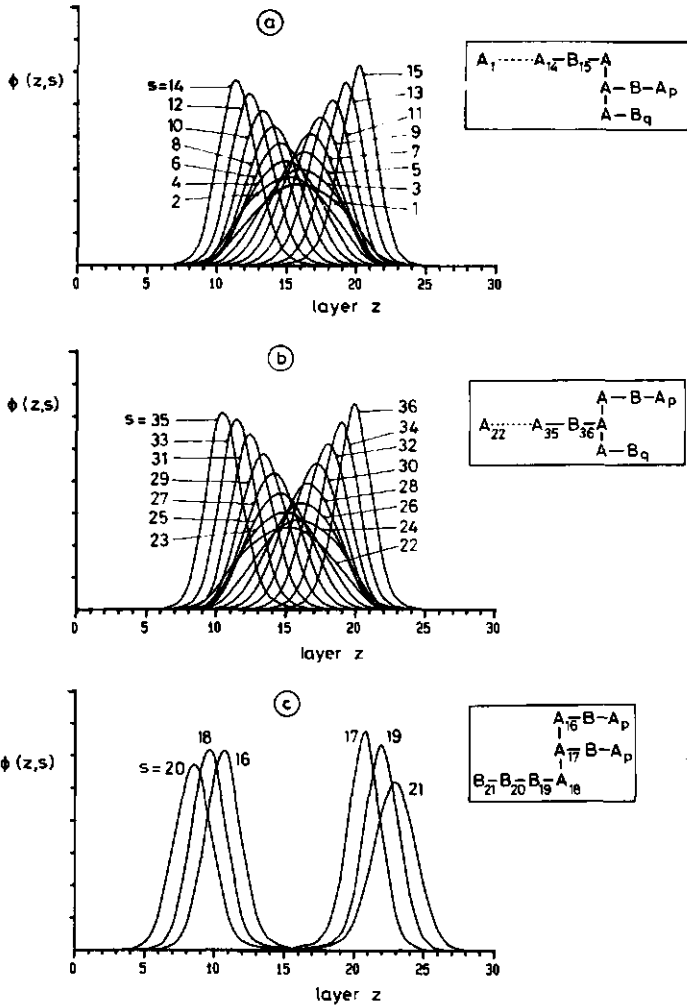


Figure 6.

Individual segment density profiles (in arbitrary units) for the membrane given in figure (4b). The segment numbers are indicated (see (16)). Only one side of each distribution is given. Details are given in the text.

overall symmetrical segment density profile is composed of two asymmetrical contributions: one from each side of the membrane. We define a molecule to belong to that side of the membrane where the branching segment is found. Figure (6) shows the individual segment distributions in the membrane of

figure (4b). For every segment either the left or the right hand side profile is shown. Figure (6a) represents tail number 1, figure (6b) tail number 2 (closest to the head group) and figure (6c) the glycerol backbone and the head group (see (16)). All segments have a wide distribution, although segments in the glycerol backbone are confined to less layers than those in the molecular extremities (the two tail ends and the end of the head group). These results suggest that the glycerol backbone is the most rigid part of the molecule. Note that this rigidity is not due to intrinsic sterical hindrances inside the molecule itself but to interactions with the environment. Interestingly, the first tail (the one further away from the head group) is buried about half a layer deeper in the membrane than the tail next to the head group, and its segments have slightly wider distributions (compare figures (6a) and (6b)). Clearly, the head group pulls the molecule towards the water phase and the tail closest to this head group is affected most. Similar trends are observed experimentally [18].

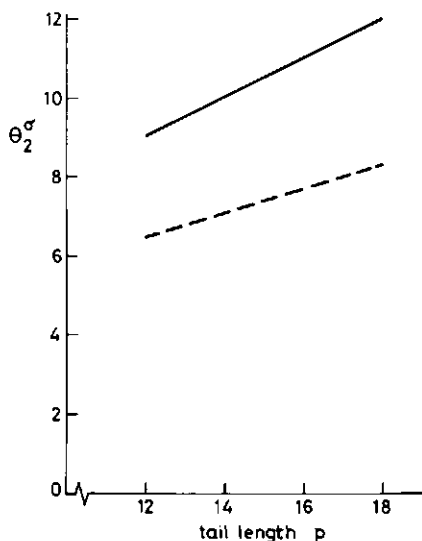


Figure 7.

Membrane thickness as a function of tail length of the lecithin molecules. Dashed line: first order Markov approximation, solid line: RIS Markov approximation. Energy parameters as in figure (3). Short molecules do not form membranes.

Figure (7) gives θ_2^σ as a function of the tail length p , for both first order Markov and RIS scheme calculations. Clearly, the RIS scheme produces thicker membranes and a larger increase in thickness per added tail segment. The membrane thickness is actually larger than θ_2^σ , because the volume fraction of segments in the membrane is less than 1. The membranes found by our theory are about 50% too thin compared to experimental values [19]. (Other definitions of the membrane thickness can be given, which give up to 20% larger values.) One of the main reasons for this discrepancy is that in our approach the excluded volume of neighbouring chains is only weakly incorporated. The tails bend too easily. In a future publication we will correct for this [17]. Other theories, which fix the head group density in a given plane, actually force the chains to do steps towards the centre of the membrane, and therefore do not suffer from this problem, though at the expense of other (severe) simplifications.

Qualitatively, the results of figure (7) correspond with measurements reported by Cornell et al. [19]. Their conclusion, that a change in length of the acyl chain gives a smaller change in membrane thickness, is fully supported by our calculations. Their measurements indicate also, in accordance with our predictions, that in the centre of the membrane the segments must have a more isotropic distribution. Quantitatively, our results overestimate this behaviour, as explained above.

Table 3. Dependence of $\log \phi_2^b = u p + v$ on the energy parameters.

X_{AW}	X_{BW}	X_{AB}	U^g/kT	u	v
1.7	-0.3	1.5	275/300	-0.3186	1.745
1.6	-0.3	1.5	275/300	-0.2803	1.711
1.5	-0.3	1.5	275/300	-0.2426	1.656
1.6	-0.2	1.5	275/300	-0.2802	1.622
1.6	-0.4	1.5	275/300	-0.2804	1.799
1.6	-0.3	1.4	275/300	-0.2803	1.646
1.6	-0.3	1.6	275/300	-0.2803	1.775
1.6	-0.3	1.5	250/300	-0.2800	1.715
1.6	-0.3	1.5	300/300	-0.2806	1.708

For surfactants (amphiphilic molecules with one apolar tail and a polar

head group) often a linear relation between $\log(\phi_2^b)$ ($\approx \log \text{CMC}$) and the number of apolar tail segments is found: $\log(\phi_2^b) = u p + v$, where p is the number of tail segments, u the slope and v the intercept [20]. Our calculations also show this linearity. Data for u and v are collected in table (3) for various values of the four parameters in the model. The calculations are performed with the RIS scheme, but the first order Markov approximation gives similar trends. Inspection of table (3) reveals that for the slope u only the interaction χ_{AW} between tails and solvent is important. The intercept is influenced by all parameters, but the head solvent interaction is most effective.

Table 4. Dependence of the membrane thickness on the energy parameters.

χ_{AW}	χ_{BW}	χ_{AB}	U^g/kT	θ_2^σ
1.5	-0.3	1.5	275/300	10.31
1.6	-0.3	1.5	275/300	11.01
1.7	-0.3	1.5	275/300	11.66
1.6	-0.2	1.5	275/300	11.18
1.6	-0.4	1.5	275/300	10.86
1.6	-0.3	1.4	275/300	11.12
1.6	-0.3	1.6	275/300	10.92
1.6	-0.3	1.5	250/300	10.87
1.6	-0.3	1.5	300/300	11.16

Table (4) collects data for the dependence of θ_2^σ , a measure for the membrane thickness, on the energy parameters for a lecithin molecule with tail lengths of 16 segments. As can be seen in table (4), the thickness increases when the interaction between tails and water becomes less favourable (χ_{AW} higher), when the head groups and water attraction is less (χ_{BW} less negative) and when the interaction between tails and head groups becomes smaller (χ_{AB} lower). The membrane thickness also increases if the stiffness of the chains increases. The energy parameters can only be chosen between certain limits: if, e.g., the head tail repulsion is too weak, no membranes exist for which the excess free energy is vanishing. Fitting the calculations with experimental values, especially critical micellisation concentration data, will give an indication of the values for the energy parameters.

Conclusions

The elegance of the present theory is that only four measurable energy parameters are needed to model the association behaviour of lipid molecules to form membrane-like structures, without the need to restrict the head groups to given layers. Real equilibrium with a bulk solution is maintained. The Markov chain approximation allows for a very efficient generation of the set of conformations which can be calculated with standard numerical techniques in about 60 CPU seconds on a VAX 8600 computer. The extension of the Markov statistics to the rotational isomeric state scheme improves the model considerably, as direct backfolding is excluded. The theory gives good insight into the force balance of the membrane. Some membrane properties found are not yet in full agreement with experiments, but the theory is easily improved and can be readily adopted to a wide range of complicated systems.

Appendix A

Referring to table (2) equation (2a) is written in the form:

$$\underline{G}(z, s_1) = \underline{G}(z, s) \sum_{z', -z} \lambda_{z', -z} \underline{G}(z', s'_1) \tag{A1}$$

where

$$\underline{G}(z, s) = \begin{pmatrix} G(z, s^{eh}) & 0 & 0 & 0 & 0 & 0 & 0 \\ 0 & G(z, s^{ef}) & 0 & 0 & 0 & 0 & 0 \\ 0 & 0 & G(z, s^{fh}) & 0 & 0 & 0 & 0 \\ 0 & 0 & 0 & G(z, s^{fg}) & 0 & 0 & 0 \\ 0 & 0 & 0 & 0 & G(z, s^{fe}) & 0 & 0 \\ 0 & 0 & 0 & 0 & 0 & G(z, s^{hf}) & 0 \\ 0 & 0 & 0 & 0 & 0 & 0 & G(z, s^{he}) \end{pmatrix}, \tag{A2}$$

$$\lambda_{-1} = \begin{pmatrix} \lambda^t & 0 & 2\lambda^g & 0 & 0 & 0 & 0 \\ \lambda^g & 0 & \lambda^t + \lambda^g & 0 & 0 & 0 & 0 \\ 0 & 0 & 0 & 0 & 0 & 0 & 0 \\ 0 & 0 & 0 & 0 & 0 & 0 & 0 \\ 0 & 0 & 0 & 0 & 0 & 0 & 0 \\ 0 & 0 & 0 & 0 & 0 & 0 & 0 \\ 0 & 0 & 0 & 0 & 0 & 0 & 0 \end{pmatrix} \lambda_1 = \begin{pmatrix} 0 & 0 & 0 & 0 & 0 & 0 & 0 \\ 0 & 0 & 0 & 0 & 0 & 0 & 0 \\ 0 & 0 & 0 & 0 & 0 & 0 & 0 \\ 0 & 0 & 0 & 0 & 0 & 0 & 0 \\ 0 & 0 & 0 & 0 & 0 & 0 & 0 \\ 0 & 0 & 0 & 0 & \lambda^t + \lambda^g & 0 & \lambda^g \\ 0 & 0 & 0 & 0 & 2\lambda^g & 0 & \lambda^t \end{pmatrix}$$

$$\underline{\lambda}_0 = \begin{pmatrix} 0 & 0 & 0 & 0 & 0 & 0 & 0 & 0 \\ 0 & 0 & 0 & 0 & 0 & 0 & 0 & 0 \\ 0 & \lambda^t & 0 & \lambda^g & 0 & \lambda^g & 0 & 0 \\ 0 & \lambda^g & 0 & \lambda^t & 0 & \lambda^g & 0 & 0 \\ 0 & \lambda^g & 0 & \lambda^g & 0 & \lambda^t & 0 & 0 \\ 0 & 0 & 0 & 0 & 0 & 0 & 0 & 0 \\ 0 & 0 & 0 & 0 & 0 & 0 & 0 & 0 \end{pmatrix} \quad \underline{G}(z, s_1) = \begin{pmatrix} G(z, s_1^{eh}) \\ G(z, s_1^{ef}) \\ G(z, s_1^{fh}) \\ G(z, s_1^{fg}) \\ G(z, s_1^{fe}) \\ G(z, s_1^{hf}) \\ G(z, s_1^{he}) \end{pmatrix} \quad (A3)$$

The equivalent equation (A1) for evaluating the chain end distribution functions from the opposite chain end reads

$$\underline{G}(z, s_2) = \underline{G}(z, s) \sum_z \underline{X} \underline{\lambda}_{z, -z} \underline{X} \underline{G}(z', s_2') \quad (A4)$$

where the product $\underline{X} \underline{\lambda} \underline{X}$ is a $\underline{\lambda}$ matrix that operates on bond 1 of segment s' , instead of bond 2. The matrix \underline{X} rearranges the segment orientations, so that orientation $\alpha\beta$ replaces $\beta\alpha$, and is given by:

$$\underline{X} = \begin{pmatrix} 0 & 0 & 0 & 0 & 0 & 0 & 0 & 1 \\ 0 & 0 & 0 & 0 & 1 & 0 & 0 & 0 \\ 0 & 0 & 0 & 0 & 0 & 0 & 1 & 0 \\ 0 & 0 & 0 & 1 & 0 & 0 & 0 & 0 \\ 0 & 1 & 0 & 0 & 0 & 0 & 0 & 0 \\ 0 & 0 & 1 & 0 & 0 & 0 & 0 & 0 \\ 1 & 0 & 0 & 0 & 0 & 0 & 0 & 0 \end{pmatrix} \quad (A5)$$

The volume fractions are calculated with (see equations (4a) and (14)):

$$\underline{G}(z, s_{12}) = \underline{G}^T(z, s_1) \underline{G}^{-1}(z, s) \underline{W} \underline{G}(z, s_2) \quad (A6)$$

after suitable normalisation. In equation (A6)

$$\underline{W} = 1/12 \begin{pmatrix} 1 & 0 & 0 & 0 & 0 & 0 & 0 \\ 0 & 2 & 0 & 0 & 0 & 0 & 0 \\ 0 & 0 & 2 & 0 & 0 & 0 & 0 \\ 0 & 0 & 0 & 2 & 0 & 0 & 0 \\ 0 & 0 & 0 & 0 & 2 & 0 & 0 \\ 0 & 0 & 0 & 0 & 0 & 2 & 0 \\ 0 & 0 & 0 & 0 & 0 & 0 & 1 \end{pmatrix} \quad (A7)$$

Alternatively, one can use the same $\underline{\lambda}$ matrices as given in equation (A3), but then the vectors \underline{G} are replaced by vectors $\underline{X} \underline{G}$ and the matrix \underline{G} by $\underline{X} \underline{G} \underline{X}$. The equivalent equation (A4) reads:

$$\underline{X} \underline{G}(z, s_2) = (\underline{X} \underline{G}(z, s) \underline{X}) \sum_{z', z''} \lambda_{z', z''} (\underline{X} \underline{G}(z, s_1')) \quad (A4a)$$

When there is no preferential orientation of a monomer then $\underline{X} \underline{G} \underline{X} = \underline{G}$. Equation (A6) becomes:

$$\underline{G}(z, s_{12}) = \underline{G}^T(z, s_1) \underline{G}^{-1}(z, s) \underline{W} \underline{X} (\underline{X} \underline{G}(z, s_2)) \quad (A6a)$$

Equations (A6) and (A6a) are identical because the product $\underline{X} \underline{X}$ gives the identity matrix.

Appendix B

The volume fraction profiles cannot be found analytically. We have an implicit set of equations which can be solved, for instance, with the FORTRAN program of Powell [21]. If we formulate the k^{th} guess for the free segment weighting factors as $G_x^{(k)}(z)$, then:

$$-u_x'(z)/kT = \ln(G_x^{(k)}(z)) - \sum_y \chi_{xy} \left(\frac{\langle \phi_y(z) \rangle}{\sum_{y'} \phi_{y'}(z)} - \phi_y^b \right) \quad (B1)$$

The volume fractions $\phi_x(z)$ are obtained from $G_x^{(k)}(z)$ and normalised by $\theta_i / (r_i G_i(r_1))$ except for the solvent profile, for which we use $\phi_1^b = 1 - \sum_{i \neq 1} \phi_i^b = 1 - \sum_{i \neq 1} \theta_i / (G_i(r_1))$. The denominator $\sum_{y'} \phi_{y'}(z)$ is the sum of volume fractions in layer z and is introduced to avoid too strong fluctuations of $u_x'(z)$ during the iterations. It will be 1 when the final solution is attained. Further, we define:

$$u'(z) = \frac{1}{\sum_y} \sum_y u'_y(z) \quad (\text{B2})$$

as the average $u'(z)$. The boundary conditions are

$$\sum_y \phi_y(z) = 1 \quad (\text{B3})$$

and

$$u'_x(z) = u'(z) \quad (\text{for all segment types } x) \quad (\text{B4})$$

The following function can be formulated which combines all requirements

$$f_x(z) = 1 - \frac{1}{\sum_y \phi_y(z)} + u'(z) - u'_x(z) \quad (\text{B5})$$

This function is reasonably linear in $G_x^{(k)}(z)$ and only zero for all x and z when equations (B3) and (B4) are obeyed.

The iteration is started by a small (step) profile in the free segment weighting factors to initiate inhomogeneities near the reflecting boundary. The tolerance $\sqrt{(\sum_x f_x(z)^2)}$ was typically less than 10^{-8} .

Literature

- 1) F.A.M. Leermakers, J.M.H.M. Scheutjens, and J. Lyklema; *Biophys. Chem.* **19** (1983) 352.
- 2) P. van der Ploeg, and H.J.C. Berendsen; *J. Chem. Phys.* **76** (1982) 3271.
- 3) H.J.C. Berendsen, and Egberts, B.; In press.
- 4) B. Jönsson, O. Edholm, and O. Teleman; *J. Chem. Phys.* **85** (1986) 2259.
- 5) B. Owenson, and L.R. Pratt; *J. Phys. Chem.* **88** (1984) 2965.
- 6) I. Szleifer, A. Ben-Shaul, and W.M. Gelbart; *J. Chem. Phys.* **85** (1986) 5345.
- 7) D.W.R. Gruen; *J. Coll. Interf. Sci.* **89** (1985) 153.
- 8) K.A. Dill, and R.S. Cantor; *Macromolecules* **17** (1983) 380.
- 9) F.A.M. Leermakers, P.P.A.M. van der Schoot, J.M.H.M. Scheutjens, and J. Lyklema; in: "Surfactants in Solution. Modern Applications.", (K.L. Mittal, Ed.) (in press).
- 10) J.M.H.M. Scheutjens, and G.J. Fleer; *J. Phys. Chem.* **83** (1979) 1619.

- 11) E.A. Di Marzio, and R.J. Rubin; *J. Chem. Phys.*, **55** (1971) 4318.
- 12) N.K. Adan, and G. Jessop; *Proc. Roy. Soc. London, Ser A* **112** (1926) 362.
- 13) D.G. Hall, and B.A. Pethica; in: "Nonionic Surfactants", (M.J. Schick, Ed.), Marcel Dekker, N.Y. (1976), Ch. 16.
- 14) T.L. Hill; "Thermodynamics of small systems" Vols 1 and 2, Benjamin, N.Y. (1963, 1964).
- 15) F.A.M. Leermakers; PhD thesis, Wageningen (1988) chapter 3.
- 16) P.J. Flory; "Principles of polymer chemistry", Cornell University Press, Ithaca, NY (1953).
- 17) F.A.M. Leermakers; PhD thesis, Wageningen (1988) chapter 4.
- 18) G. Büldt, H.U. Gally, A. Seelig, and J. Seelig; *Nature* **271** (1978) 183.
- 19) B.A. Cornell, and F. Separovic; *Biochem. Biophys. Acta* **733** (1983) 189.
- 20) C. Tanford; "The Hydrophobic Effect: Formation of Micelles and Biological Membranes", J. Wiley & Sons, Inc., NY (1973).
- 21) M.J.D. Powell; in: "Numerical methods for nonlinear algebraic equations", (P. Rabinowitz, Ed.), Gordon and Breach, London (1970) 115.

CHAPTER 3

LIPID VESICLES

Abstract

We present a statistical thermodynamical theory to study lipid vesicles in aqueous media. All conformations of the amphiphilic molecules are generated in a rotational isomeric state scheme. The statistical weight of each conformation is calculated using standard Boltzmann statistics for which self-consistent equipotential layers of variable curvature are introduced in a way that parallel planes give flat membranes, whereas lattice layers with spherical geometry give globular micelles or vesicles.

Unilamellar, multilamellar and multicomponent vesicles are examined. Segment density profiles through cross sections of the vesicle membranes are found to be asymmetric: the inner shell is compressed, while the outer one is slightly expanded.

The free energy of curvature per vesicle composed of one type of lipid molecules is of the order of 200 kT and is independent of its radius. Therefore, these vesicles are considered thermodynamically unstable and are expected to grow. The small amount of curvature energy of the lecithin vesicles implies that they are easily deformed. This is confirmed by calculations on vesicles with a cylindrical geometry.

In multicomponent vesicles the amphipolar molecules distribute themselves between the inner and outer shell to optimise energetic interactions and packing constraints. This enhances the asymmetry of the vesicle membrane. Adding surfactants can lead to degradation of the vesicle system into composite micelles. On the other hand, vesicles composed of two types of lecithin-like molecules with a repulsive interaction between them can be extremely asymmetric and tend to be thermodynamically stable at a given vesicle radius.

Introduction

Lipid vesicles are found in a large variety of sizes and composition. Unilamellar, bilamellar or even multilamellar vesicles have been encountered experimentally. Recent experimental research concentrates on various

applications of the spherical membrane particles. They can be used as capsules for drug delivery [1], as artificial chloroplasts for the conversion of solar energy [2,3], and as model systems for the study of biological membranes.

The self-assembly of lipid molecules into membranes or vesicles has much in common with the formation of micelles from small surfactant molecules. Pioneering theoretical work has been done by Israelachvili et al., who combined the thermodynamics of the self-assembly of association colloids with the architecture of the amphiphilic molecules [4,5]. Their analysis of lipid vesicles is focused on the packing phenomena of the outer monolayer, assuming that the inner monolayer has always an optimal packing. Based on this assumption, they predict that vesicles are thermodynamically stable. In contrast to this, Helfrich argues that vesicles are distorted membranes, and therefore are inherently unstable [6]. We will contribute to the solution of this discussion.

Both the approaches of Israelachvili et al. and that of Helfrich are semi phenomenological models which give only limited information on a molecular level. More detailed insight into the structure and organisation of lipid vesicles can be obtained from so called computational physics. For the case of lipid bilayers, recent Monte Carlo [7] and Molecular Dynamic [8] simulations have given promising results, but up to now no results for lipid vesicles have been generated with these techniques. This is due to computational problems.

One way to overcome these problems is to make use of statistical methods based on a self-consistent field principle. The state of the art of statistical thermodynamics of association colloids is that the "effective" head group area (or, equivalently, the number of chains per surface area) are input parameters [9,10,11]. Since for the vesicles the inner and outer sheaths are expected to have a different packing, the exact head group areas at both sides of the asymmetric membrane are uncertain. There was to the authors knowledge, no statistical thermodynamical analysis for the entire lipid vesicles available.

Recently, we introduced a theory for the lipid bilayer [12], which is an extension of the theory of Scheutjens and Fleer, originally developed for the study of polymers in inhomogeneous systems [13,14]. In contrast with older statistical approaches, in this bilayer theory the condition of spatial restrictions of the molecules is relaxed. The head groups of the amphiphilic molecules are not confined to any pre-assigned position. A mean field argument

is used to project the 3D space on a concentration gradient in one dimension. This mean field approximation was previously used for a lamellar geometry. In this paper we will generalise the theory for various curvatures of the associates. See reference [15] for results of the theory applied to surfactant micelles.

The curved lattice

Because of the complexity of the system, statistical mechanics of a system which contains chain molecules is bound to demand with approximations. In order to restrict the number of configurations, frequently one uses a lattice on which the conformations of the molecules are generated. However, even on a lattice the number of different conformations is very large. Often more assumptions must be introduced. A Markov approximation is commonly used, which assumes that the position of a segment depends only on that of the

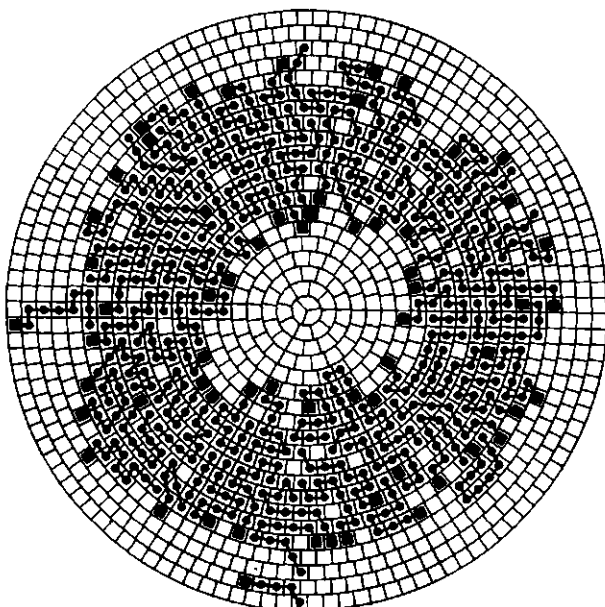


Figure 1.

A schematic two dimensional representation of a curved lattice with spherical geometry. The amphiphatic molecules in various conformations form a spherical vesicle.

preceding segment along the chain, as if the consecutive segments would form the path of a random walker. One of the best known theories along this line is the Flory-Huggins theory for polymer solutions [16] which, in addition to the Markov approximation, introduces a mean field assumption to account for the interactions of segments with the other molecules. Although inhomogeneities in the system are neglected, thermodynamic properties of polymer solutions are qualitatively well described.

The Scheutjens-Fleer theory is an extension of this theory. Here, in this approach the mean field approximation is restricted to only two dimensions, i.e., within parallel lattice layers, and a modified Markov process (a step-weighted random walk) is applied to account for the inhomogeneities normal to these layers. In this way several interfacial studies were performed [13,14,15,17].

Originally, a lattice composed of M flat parallel layers of L lattice sites each was used. Since the mean field assumption forces the association structure to have the same symmetry as the lattice, only flat membranes could be considered [12,17]. To study variations in shape one needs to design lattices with other geometries [15]. Figure (1) gives a two dimensional representation of a spherical lattice in which amphiphilic molecules are arranged (arbitrarily drawn) in a vesicle-type association structure. The layers are numbered starting from the centre: $z = 1, \dots, M$, where $z = 1$ is the centre of the vesicle and $z = M$ is a layer in the bulk solution. We require that all lattice sites have equal volumes and that all lattice layers are equidistant. As a consequence, the number of lattice sites $L(z)$ varies from layer to layer and is not necessarily an integer. We assume that the coordination number Z , that is the number of lattice sites in direct contact with a given site, is independent of the curvature of the lattice layer.

Most frequently, association colloids are either spherical, (finite) cylindrical, or lamellar. The volume $V(z)$ (in number of lattice sites) of a lattice with any of these geometries up to layer z is given by:

$$V(z) = 2 A_s z + \pi h z^2 + \frac{4}{3} \pi z^3 \quad (z > 0, h^2 > \pi A_s) \quad (1)$$

where $2 A_s z$ is the number of sites in planar and $\pi h z^2$ the number of sites in cylindrical geometry. A spherical geometry results if both A_s and h are zero. The situation with $A_s = 0$ and h finite represents a rod of length h with a half sphere at each end, whereas other cases apply for disk-like structures.

The restriction $h^2 > \pi A_s$ is necessary, because the contour around the planar area is formed by half a cylinder. The number of lattice sites in layer z is easily found:

$$L(z) = V(z) - V(z-1) \quad (2)$$

The contact area $S(z)$ between layers z and $z+1$ is obtained by differentiation of equation (1) with respect to z

$$S(z) = 2 A_s + 2 \pi h z + 4 \pi z^2 \quad (3)$$

We define $\lambda_{z,-z}(z)$ as the fraction of contacts that a given lattice site in layer z has with layer z' . Obviously,

$$\lambda_{-1}(z) + \lambda_0(z) + \lambda_1(z) = 1 \quad (4)$$

The total number of possible steps from lattice sites in layer z to say, layer $z+1$, must be equal to those from layer $z+1$ to z . Mathematically:

$$Z L(z) \lambda_1(z) = Z L(z+1) \lambda_{-1}(z+1) \quad (5)$$

for every layer z . We expect $\lambda_1(z)$ to be proportional to the contact area $S(z)$ between layer z and $z+1$, and $\lambda_{-1}(z)$ to be proportional to $S(z-1)$, the surface area between the layers z and $z-1$. Therefore,

$$\begin{aligned} \lambda_{-1}(z) &= \lambda_{-1} S(z-1)/L(z) \\ \lambda_0(z) &= 1 - \lambda_{-1}(z) - \lambda_1(z) \\ \lambda_1(z) &= \lambda_1 S(z)/L(z) \end{aligned} \quad (6)$$

where $\lambda_{-1} = \lambda_1$ are the corresponding transition probabilities for a planar lattice in the bulk solution.

The total volume of the system is $V = \sum_z L(z)$ lattice sites. Each of these sites must contain either a segment of a lipid molecule or a solvent molecule. We will refer to apolar segments in the system as segments A, to polar segments as segments B, and to solvent molecules as segments W. Index x is used to denote any of these segment types. Thus, $L(z) = \sum_x n_x(z)$ where $n_x(z)$ is the number of segments x in layer z . We will not consider free

unoccupied lattice sites here. (If necessary, compressibility can be incorporated by introducing artificial monomers representing empty lattice sites.)

The volume fraction $\phi_x(z)$ of segments x in layer z is obviously

$$\phi_x(z) = \frac{n_x(z)}{L(z)} \quad (7)$$

When all segments along the polymer chain of type i are numbered, $s = 1, \dots, r_i$, we can specify the volume fraction $\phi_i(z, s)$ of segment s of molecule i in layer z .

First order Markov approximation

We force the system to have a constant density, i.e., $\sum_i \phi_i(z) = 1$ for all layers z . If no energetic interactions are present, the molecules only experience a hard core potential $u'(z)$. We normalise $u'(z)$ such so that for large z (in the bulk solution) $u'(z) = 0$. In general, every segment x , has in addition to this, energetic interactions originating from the contacts with its neighbouring molecules and feels a total potential $u_x(z)$. In the mean field approximation, the exact positions of the neighbouring molecules in each layer is not known. Instead, we make use of volume fractions to calculate the composition-dependent potential:

$$u_x(z) = u'(z) + kT \sum_y \chi_{xy} \{ \langle \phi_y(z) \rangle - \phi_y^b \} \quad (8)$$

The bulk solution is again taken as the reference state where $u_x^b \equiv 0$. In equation (8) the angular brackets indicate an averaging over three consecutive layers:

$$\langle \phi_x(z) \rangle = \sum_{z'} \lambda_{z'-z} \phi_x(z') \quad (9)$$

Further, in equation (8) the well-known Flory-Huggins interaction parameters are used. These χ_{xy} are exchange parameters and therefore they are zero by definition when $x = y$. If we do not account for the chain connectivity, the weighting factor $G_x(z)$ to find a segment x in layer z is given by the Boltzmann factor containing the local potential experienced by segment x :

$$G_x(z) = \exp(-u_x(z)/kT) \quad (10)$$

The volume fraction of a loose segment x in layer z would be given by:

$$\phi_x(z) = \phi_x^b G_x(z).$$

We now will take the chain connectivity into account. In a Markov approximation the chain generation can be expressed in a recurrence relation, one for each layer z . These relations can be expressed in a matrix-vector type operation. This method has been used by Scheutjens and Flerer to study polymers near flat interfaces. Modifications to allow for curvature effects of the lattice will be discussed below. More details of the chain generation method are discussed at length elsewhere [18].

For unbranched chains, a segment along the polymer chain has two bonds. Let us refer to them by subscript 1 and 2. From the point of view of a segment s' , the chain part connected at bond 1 may contain a string of segments attached at, for example, segment number 1. Then the other bond (2) is connected with the tail that ends at segment number r . Let us define a weighting factor $G(z, s_1)$ which accounts for the probability that the end of an s mer is in layer z and that only bond 1 of this s -mer is connected with a string of in this case $(s-1)$, segments. The position of segment $s' = (s-1)$, is confined to three layers, namely $z' = z+1$, $z' = z$, and $z' = z-1$. The weighting factor $G(z, s_1)$ is built up from the weighting factor $G(z, s)$ of segment s and that of the rest of the chain, $G(z', s_1)$, averaged over all viable positions of s' :

$$G(z, s_1) = G(z, s) \sum_{z'} \lambda_{z', z} G(z', s_1) \quad (11)$$

As equation (11) is recurrent, and $G(z, 1_1) = G(z, 1)$, only the λ 's and the free segment weighting factors (given in equation (10)) are needed to generate the end segment distribution functions $G(z, s_1)$ in layers z .

The properties for the boundary layers $z = M$ and $z = 1$ must be chosen so as to avoid influences of the boundary of the system on the segment density profiles. In most cases reflecting boundary conditions are used to minimise the unwanted influence.

As compared with a naive way of calculating the segment density profiles, namely by generating each conformation one by one, the advantage of this recurrence relation is that it adds, and properly weights, many conformations together. After $(r-1)$ step operations, all possible conformations are generated. The cost for adding together the individual conformations is that the segment density distribution can only be found after additional

calculation of the complementary chain end distribution functions $G(z, s_2)$. The values for $G(z, s_2)$ are found by starting the chain generation procedure from the other end of the chain, that is at segment r , using equation (11) and replacing bond 1 by bond 2. The segment density distributions are found by a composition formula which connects the two chain ends together:

$$\phi_i(z, s) = C_i G_i(z, s_1) G_i(z, s_2) / G_i(z, s) \quad (12)$$

The division by $G_i(z, s)$ is a correction for double counting of the overlapping segment s and C_i is a normalisation constant. The total volume fraction molecules of type i contribute in layer z is found after summation over all its segments: $\phi_i(z) = \sum_s \phi_i(z, s)$.

If the number of molecules n_i is known ($= \sum_z \phi_i(z) L(z) / r_i$), the normalisation constant in equation (12) is given by $C_i = n_i / G_i(r_1)$, where $G_i(r_1) = \sum_z G_i(z, r_1) L(z)$. For given bulk volume fraction ϕ_i^b the normalisation constant is $C_i = \phi_i^b / r_i$. These two cases represent a canonical (closed) and grand canonical (open) system, respectively.

Rotational isomeric state scheme in planar geometry

The chain statistics discussed above exploits a first order Markov-type approximation. Direct backfolding of a chain to a previously occupied lattice site is not forbidden. For long polymer molecules one can consider each set to 4-8 bonds as one statistical chain element that can be treated as an ideally flexible, i.e., independent segment. For small lipid molecules, we would lose too much detail if the number of segments would be reduced by, say a factor of 6. Therefore we prefer to improve on the conformational statistics. Details of the RIS scheme for planar symmetry have already been described elsewhere [18]. Here we summarise the significant parts and in the next section we will give details of the RIS scheme in arbitrary lattice geometries.

Our goal is to keep track of three successive bond directions of the molecules in a tetrahedral (diamond) lattice. In this lattice, four bond orientations denoted by e'' , f'' , g'' , and h'' , are present per site. We distinguish two opposite directions in each orientation. For example, e and e' are the directions in orientation e'' . Bonds in orientations e'' and h'' connect segments in different layers. The two other orientations, i.e., f'' and g'' are parallel to the lattice layers. Each site on the tetrahedral lattice has four neighbours. There are two types of sites. For a given site of type I the four

directions are e, f, g, and h. The neighbouring sites are of type II and have bond directions e', f', g' and h'. The consecutive segments in a chain molecule are alternately on sites of type I and II. The rotational isomeric state scheme is a three choice propagation scheme. This means that a step in, e.g., orientation e" can only be followed by a step in one of the three other orientations, in his case f", g", or h". We define the chain end distribution function $G(z, s_1^{\alpha\beta})$ as the weighting factor for conformations with the end of a chain of s segments in layer z, while the string of (s-1) segments is connected to segment s at bond 1 in direction α and the next segment (s+1) will be attached to bond 2 in direction β . Directions α and β are two out of e, f, g, and h, or two out of e', f', g', and h', depending on the type of site where the orientation of a segment s is on. The spatial orientation of a segment is fully determined by specifying the directions of two of its bonds. We assume that there is no preferent orientation for a segment when it is not connected in a chain. Therefore, we can set $G(z, s^{\alpha\beta}) = G(z, s)$ for all $\alpha \neq \beta$ and $G(z, s^{\alpha\beta}) = 0$ in other cases. For each of the 24 possible $\alpha\beta$ segment orientations the recurrence relation is given by:

$$G(z, s_1^{\alpha\beta}) = G(z, s^{\alpha\beta}) \sum_{\gamma'} \lambda^{\beta''-\alpha''-\gamma''} G(z', s_1^{\gamma'\alpha'}) \quad (13)$$

In this case bond 2 of segment s' (in direction α') is connected to bond 1 of segment s (in direction α). Layer z' is either z-1, z, z+1, depending on the direction α' . The summation over γ' will only have 3 nonzero contributions, for which $\gamma' \neq \alpha'$. Each step is weighted by either trans or gauche probabilities:

$$\lambda^{\alpha''-\beta''-\gamma''} = \begin{cases} \lambda^t & \text{if } \alpha'' = \gamma'' \\ \lambda^g & \text{otherwise} \end{cases} \quad (14)$$

If U^g is the energy difference between a gauche and a trans configuration (due to steric hindrance) then $\lambda^g = 1/(2 + \exp(U^g/kT))$ and $\lambda^t = 1 - 2\lambda^g$. The equivalent equation (13) for the case that a string of segments is attached to bond number 2 is:

$$G(z, s_2^{\alpha\beta}) = G(z, s^{\alpha\beta}) \sum_{\gamma'} \lambda^{\alpha''-\beta''-\gamma''} G(z', s_2^{\beta'\gamma'})$$

The volume fraction of a segment in a given orientation is again given by a composition formula:

$$\phi(z, s^{\alpha\beta}) = C \lambda^{\alpha\beta} G(z, s_1^{\alpha\beta}) G(z, s_2^{\alpha\beta}) / G(z, s^{\alpha\beta}) \quad (15)$$

In equation (15) the volume fractions for each segment orientation $s^{\alpha\beta}$ are weighted according to the a priori probability $\lambda^{\alpha\beta} = 1/24$ for each orientation. The volume fraction of segment s in layer z is found by summation over all its orientations:

$$\phi(z, s) = \sum_{\alpha} \sum_{\beta} \phi(z, s^{\alpha\beta}) \quad (16)$$

Rotational isomeric state scheme and curvature

A molecule with chain length r in an all-trans configuration is not likely to have all its segments in the same layer z of a spherical lattice when $r > L(z)/2$. Following an all-trans molecule in a direction towards the centre of the lattice, starting from one end, we would probably pass the centre at either side and move away from it. Although we have continually moved in essentially the same direction, we have changed our orientation with respect to the centre by almost 180 degrees.

In order to keep track of the bond orientations in a spherical lattice, it is convenient to define bond directions in spherical co-ordinates. Hence for each site of type I we will call e directions those most closely pointing towards the centre and h directions those most closely pointing outwards. The remaining directions, f and g , are the most tangential ones. For sites of type II these directions are h' , e' , g' , and f' , respectively. Far from the centre, sites of type I and type II alternate and the lattice layers are essentially planar. A segment on a site of type I has a neighbour on a site of type II in the layer z in direction f and is seen by that neighbour in direction f' . However, there are anomalies because of the curvature. Its neighbour in the (planar) direction f could well be in layer $z+1$, i.e., in spherical co-ordinates this neighbour is in direction h . Apparently sites are occasionally rotated with respect to each other. This occurs at regular intervals, but we will only account for average probabilities of such transitions. Let us examine the neighbours of a site of type I in layer z more closely. As there are four bond directions per site and $\frac{1}{2} L(z)$ sites of type I in layer z , we have $\frac{1}{2} L(z)$ bonds emanating in direction e (toward the centre). However, there are only $\frac{1}{2} L(z-1)$ sites of type II in layer $z-1$, so that only $\frac{1}{2} L(z-1)$ bonds in direction e' are available to connect with. We know, from the first order

Markov statistics above, that we can expect a total of $S(z-1)$ ($\approx L(z-\frac{1}{2})$) possible bonds between layers z and $z-1$, hence there are $\frac{1}{2} S(z-1)$ bonds with sites of type I in layer z . We must conclude that $\frac{1}{2} (S(z-1) - L(z-1))$ of them are bonds from layer $z-1$ into directions f' and g' (same number of each), pointing to layer z because of the curvature. The remaining $\frac{1}{2} (L(z-1) - S(z-1))$ possible bonds in direction e must be connected with bonds of segments in the same layer z , in directions f' and g' . A similar reasoning applies to the bonds between layer z and $z+1$ and for sites of type II. Normalising by $\frac{1}{2} L(z)$ gives the average distribution of connections per site in layer z .

Equation (13) can now be written as:

$$G(z, s_1^{\alpha\beta}) = G(z, s^{\alpha\beta}) \sum_{\gamma'} \lambda^{\beta''-\alpha''-\gamma''} G'(z', s_1^{\gamma'\alpha'}) \quad (13a)$$

where $G'(z', s_1^{\alpha\beta})$ is composed of contributions from segments s' in layer z' , connected to bond 1 of segment s in direction α . Bond 2 of segment s' is supposed to be in direction α' , but may differ in spherical co-ordinates. The analysis above leads to the following relations

$$G'(z-1, s_1^{\alpha'e'}) = \frac{L(z-1)}{L(z)} G(z-1, s_1^{\alpha'e'}) + \frac{1}{2} \left(1 - \frac{S(z-1)}{L(z)}\right) \{G(z, s_1^{\beta'f'}) + G(z, s_1^{\gamma'g'})\} + \frac{1}{2} \frac{S(z-1) - L(z-1)}{L(z)} \{G(z-1, s_1^{\beta'f'}) + G(z-1, s_1^{\gamma'g'})\} \quad (17a)$$

$$G'(z, s_1^{\alpha'f'}) = \left[1 - \frac{1}{2} \left(\frac{S(z) - S(z-1)}{L(z)}\right)\right] G(z, s_1^{\alpha'f'}) + \frac{1}{2} \left(1 - \frac{S(z-1)}{L(z)}\right) G(z, s_1^{\gamma'e'}) + \frac{1}{2} \left(\frac{S(z)}{L(z)} - 1\right) G(z+1, s_1^{\gamma'e'}) \quad (17b)$$

$$G'(z, s_1^{\alpha'g'}) = \left[1 - \frac{1}{2} \left(\frac{S(z) - S(z-1)}{L(z)}\right)\right] G(z, s_1^{\alpha'g'}) + \frac{1}{2} \left(1 - \frac{S(z-1)}{L(z)}\right) G(z, s_1^{\beta'e'}) + \frac{1}{2} \left(\frac{S(z)}{L(z)} - 1\right) G(z+1, s_1^{\beta'e'}) \quad (17c)$$

$$G'(z+1, s_1^{\alpha'h'}) = G(z+1, s_1^{\alpha'h'}) \quad (17d)$$

Obviously, in planar geometry all corrections are zero and equations (13) and (13a) are identical. Another limiting case is the homogeneous solution where all equations G and G' are equal.

Directions α' in equation (17) refer to either appropriate directions e' , f' , g' , and h' . Directions β' and γ' are related to α' according to table (1), because fixed segment orientations are rotated by 90 degrees.

Table 1. Relation between α' , β' , and γ' in equation (17).

α'	β'	γ'
e'	f'	g'
f'	h'	e'
g'	e'	h'
h'	g'	f'

It may for some sites be difficult to recognise the bond which is pointing most outwards (direction e') that which is pointing most inwards (direction h'), but there will be no candidates for both directions. Consequently, there are no transitions between e' and h' directions. Also, a segment in, e.g., orientation e'f' is easily distinguished from a segment in orientation f'e', which is rotated over 180 degrees. Excluding these obviously impossible transitions table (1) can be constructed.

Equation (17) and table (1) apply to sites of type II, but similar results are obtained for sites of type I, by exchanging e', f', g', and h' with h, g, f, and e, respectively.

In the first layer of the lattice ($z = 1$) there are about 4 sites ($L(1) = 4\pi/3$), two of type I and two of type II. They form two pairs, connecting bonds in (planar) directions e - e' and h - h', respectively. This requirement is met by placing a reflecting boundary at $z = 0$, i.e., set $L(0) = S(0) = L(1)$ and rotate orientations $\alpha\beta$ over 180 degrees (replace e, f, g, h, e', f', g', and h' by h, g, f, e, h', g', f', and e', respectively).

Iteration

For a given set of segment potential profiles $\{u_x^{\alpha\beta}(z)\}$ the segment density distributions can be evaluated for any segment type x. These distribution functions are used to check equation (8) and the boundary constraint $\sum_x \phi_x(z) = 1$. The potential profiles are changed until these conditions are met. Mathematically this problem can only be solved iteratively. Details on the computational aspects of the problem have been published before [12].

Excess free energy

For association colloids, the excess free energy of the aggregates with respect to the free energy in the bulk solution is of great importance. An elegant study of the equilibrium conditions of micellar solutions, by Hall and

Pethica [19], shows that the small system thermodynamics developed by Hill [20] is very useful in this respect. In the present calculations the grand canonical partition function (Ξ) for one association colloid with fixed centre of mass is available (see appendix A). From this partition function the excess free energy A^σ of this colloid can be derived in a similar way as done before [13]:

$$A^\sigma/kT = -\ln \Xi = -\sum_i n_i^\sigma + \sum_z L(z) \ln \frac{\phi_w(z)}{\phi_w^b} + \frac{1}{2} \sum_z \sum_x \sum_y (\chi_{xw} + \chi_{yw} - \chi_{xy}) L(z) [\phi_x(z) \langle \phi_y(z) \rangle - \phi_x^b \phi_y^b] \quad (18)$$

where:

$$n_i^\sigma = n_i - V_s \phi_i^b / r_i \quad (19)$$

is the excess number of molecules with respect to the bulk solution, and V_s is the small system volume, i.e., the volume available per aggregate. For big vesicles the excess free energy as given in equation (18) is the main contribution to the "subdivision potential" as defined by Hill [20]. Small entropical contributions (e.g. due to the translational entropy of the vesicle) can in first approximation be neglected.

Results

In this section we will describe the association of lecithin-like molecules (type $i = 2$) in vesicles in aqueous solution. The water molecules (type $i = 1$) are modelled as amorphous monomers. This is not a very good model for water but, as we will see, good first order results are obtained. The lecithin molecules are composed of a glycerol backbone with two apolar tails of p segments each and a head group of q segments:



We have chosen a somewhat schematic architecture of the molecules. It is assumed that all head group segments are of the same polarity, and we ignore the difference in volume between a CH_3 and CH_2 groups. The overall shape of

the molecule can be modified by changing the tail length p and head group size q . Extensions of the theory to incorporate branched molecules have been published elsewhere [18]. Surfactant molecules are modelled as linear amphiphilic molecules $A'_p B'_q$. In most elaborations we will choose the apolar (A') and polar (B') segments to be identical to the apolar (A) and polar (B) segments of the lecithin molecules and drop the prime. Usually, the interaction between the apolar tail segments and the water molecules is chosen as $\chi_{AW} = 1.6$. The interaction between head groups and tail segments is set to χ_{AB} mimicking rather strong repulsion between these types of segments. The interaction between head group segments and water is chosen slightly attractive: $\chi_{BW} = -0.3$. We do not include electrostatic interactions. If necessary, the interaction between the water molecules and the head groups can be varied to simulate changes in ionic strength. A more rigorous treatment of electrostatic contributions is possible, but only at the cost of a large number of new parameters. The chain stiffness is a property of the chemical nature of the chains and refers to the difference in intramolecular energy between the rotational isomers of the chain sections. We selected an energetic difference between a gauche and a trans orientation of 1 kT at $T = 275$, which corresponds to the 2100 kJ/mole at room temperature often quoted in literature [21].

Lattice artifacts

The calculated thickness and chemical potential of the lipid associates vary slightly when the membrane is "moved" gradually over the lattice. Consequently, the excess free energy also changes upon this process. For very big vesicles, A^σ variations can become very large because of $L(z)$ in equation (18). The variation is periodical with a "wavelength" of one lattice layer. This problem is solved in most cases by "growing" the vesicle stepwise, by adding more lipids to the system, until the radius of the vesicle is increased by one layer. The average of the A^σ values is essentially free from lattice artefacts.

All calculations are performed canonically. The mathematical routes that we have followed to generate vesicles during the iteration procedure is not necessarily identical to the mechanisms by which they evolve in practice. Mathematically two approaches are available. The first one is to start with a spherical micelle ($h = A_g = 0$ in equation (1)) and increase the amount of lipids to force the micelle to grow until, after some rearrangements of the lipid molecules, water is found in the centre of the micelle and a closed

lipid bilayer is formed. This method is useful to study small vesicles. A second method is to start with a flat membrane and curve it until a vesicle with given radius is formed. Changing the curvature of the lattice is mathematically realised by modifying $L(z)$ and $\lambda_{z,-z}(z)$. This last method is used to generate big vesicles, composed of over 50,000 aggregated molecules.

We start with discussing a two-component system composed of lecithin molecules in water. Both uni- and bilamellar vesicles will be analysed. In the subsequent part we will discuss some aspects of multicomponent systems. We will return to the two-component system in a final section where the deformation of the vesicles is studied.

Uni- and Bilamellar Vesicles

Figure (2a) shows the excess free energy of a spherical association colloid as a function of n_2^σ , the number of molecules aggregated, and figure (2b) gives the corresponding equilibrium volume fraction of lipids in solution, again as a function of n_2^σ . For very small aggregation numbers, a

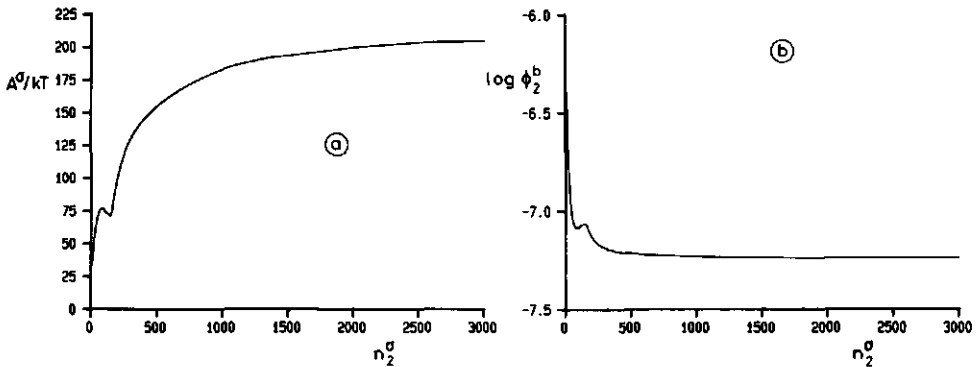


Figure 2.

Free energy of curvature of a vesicle (a) and corresponding equilibrium volume fraction of lipids in the bulk solution (b) as a function of the number of lecithin molecules aggregated in the vesicle. The lecithin molecules have two apolar tails, each 16 segments long and three head group segments. The energy parameters are $\chi_{AW} = 1.6$, $\chi_{BW} = -0.3$, $\chi_{AB} = 1.5$ where A = tail segment, B = head group segment, W = water molecule. The stiffness parameter $U^S = 275/300$ kT (T = 300 K).

globular micelle is found, then some intermediate structures are observed before a spherical unilamellar vesicle is found. The intermediate structures causes the dip in figure (2a). Above the point where the excess free energy per vesicle levels off and the equilibrium volume fraction stabilises, bulk solution is found in the heart of the vesicle. As we know from the thermodynamic analysis, a free flat membrane has a vanishing excess free energy per unit surface area when boundary effects are neglected. Therefore, the excess free energy of the aggregate in figure (2a) can be interpreted as a free energy of curvature. Helfrich [6] predicted that this free energy is independent of the radius of the vesicle. His estimation for this quantity is about 300 kT per aggregate, which is of the same order of magnitude as our result.

As can be seen from figure (2b), the equilibrium concentration of lipids in solution stabilises at a lower value as found for the globular micelle. This indicates that micelles formed from those molecules are not very stable. Such micelles develop spontaneously into lamellar membranes, or vesicles. Note that the total number of aggregates decreases when they grow, since the total amount of lipids in the system is fixed.

We have not accounted for the translational freedom of the vesicles, which is dependent on the average lipid concentration (or equivalently the vesicle concentration) of the system. This effect would change the excess free energy by only a few kT, and can be neglected in most cases.

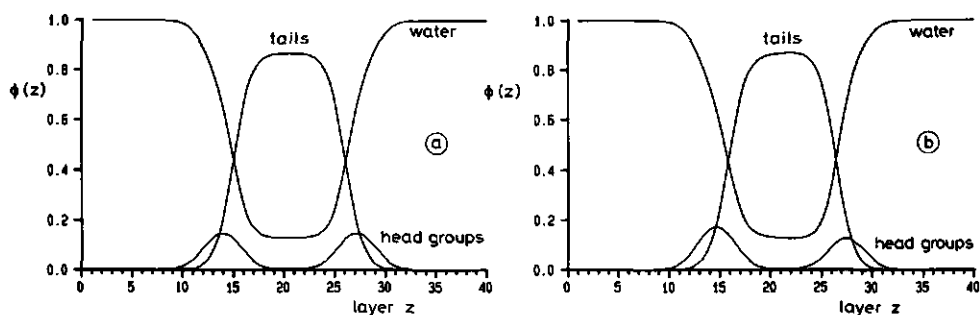


Figure 3.

Segment density profile of a cross section through a flat membrane (a) and curved vesicle (b) composed of the same lecithin molecules as in figure (2). In the vesicle 2220 molecules are aggregated.

Figure (3a) gives the overall segment density distribution across a flat membrane composed of the same molecules as in figure (2). This situation corresponds to an infinitely big vesicle. (The lattice layers in figure (3a) are numbered arbitrarily.) Figure (3b) gives the corresponding profiles for a globular vesicle composed of 2220 molecules. Here, layer 1 is towards the centre of the vesicle. The membrane thicknesses of the curved and non-curved membranes are the same, but the differences in segment density profiles are obvious. Apparently, the free energy of curvature is stored into the segment density profiles. With respect to the flat membrane, the head group density is higher on the inside of the vesicle and slightly lower on the outside. The tail segment distributions are also affected by curvature as can be seen from the slight increase of the tail density in the outer half of the bilayer with respect to the inner half. These findings are in perfect agreement with NMR data for small unilamellar vesicles [22-26].

Since the excess free energy per vesicles is independent of the radius, the curvature energies can be tabulated.

Table 2. The effect of the energy parameters on the free energy of curvature and n_2^σ/L , (a measure for the membrane thickness), for a small unilamellar vesicle composed of lecithin molecules ($p = 16$, $q = 3$).

χ_{AW}	χ_{BW}	χ_{AB}	$U\mathcal{E}(kT)$	n_2^σ/L	$A^\sigma(kT)$
1.6	-0.3	1.5	275/300	11.01	207
1.3	-0.3	1.5	275/300	8.69	101
1.6	0	1.5	275/300	11.55	230
1.6	-0.3	1.2	275/300	11.40	219
1.6	-0.3	1.5	300/300	11.16	215

Table (2) shows that the free energy of curvature increases with increasing tail water or head-group water repulsion and with decreasing head-group tail repulsion. Also the stiffness of the molecules increases the free energy of curvature. As we will see below, the free energy of curvature increases with increasing tail length as well.

In table (2) n_2^σ/L , the excess number of molecules per unit area (lattice site) which are aggregated in the corresponding flat lattice, i.e., for infinitely big vesicles, is also given. There is a correlation between the free energy of curvature and n_2^σ/L . Clearly, the energy needed to bend a

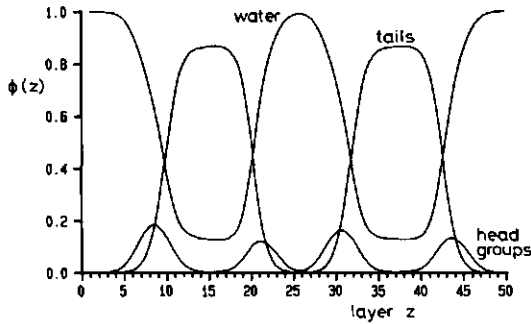


Figure 4.

A vesicle composed of two membranes. The lecithin molecules are identical to the ones used in figure (2). This double membrane is in equilibrium with an equilibrium lipid volume fraction of $\phi_2^b = 5.72 \cdot 10^{-8}$ in the bulk. There are 7200 molecules aggregated.

membrane is highest for the thickest membrane. This is not very surprising since deviations in positions of the lipids upon curving are more significant in thick membranes than in thin ones.

Figure (4) shows density profiles through a cross section of a bilamellar vesicle composed of the same molecules as in figure (2). In this complex structure 7200 molecules are aggregated. Obviously, the inner membrane is more affected by the curvature than the outer one. The excess free energy of this aggregate is 404 kT, which is twice the amount of the corresponding unilamellar counterpart. By the given choice of parameters, the membranes do not attract each other. The equilibrium concentration of lipids in the bulk, and consequently also the chemical potential of the lipids in the bilamellar vesicles, is close to that of the unilamellar vesicle. As in the unilamellar case, the free energy of curvature of this bilamellar vesicle independent of the radius of the vesicle. This indicates that the two membranes forming the vesicle can be considered as virtually independent. Since the two membranes which form the bilamellar vesicle are forced to be between the two boundary layers $z = 1$ and $z = 50$, the observed membrane separation is not likely the equilibrium one.

The equilibrium distance between two flat membranes is found by minimising the chemical potential as a function of this distance, because at all times the excess free energy of the lipid membranes is essentially zero,

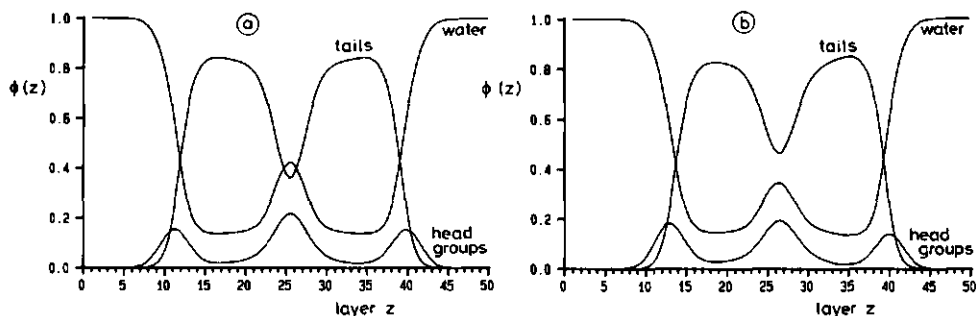


Figure 5.

Bilamellar planar membrane (a) and vesicle (b) composed of the same lecithin as in figure (2). The membranes attract each other. This is realised by increasing χ_{BW} from -0.3 to 0 and decreasing χ_{AB} from 1.5 to 1.2.

as argued above. When approaching each other, the membranes are allowed to change their composition (thickness) in order to relax any induced surface free energy, so that equilibrium is continually ensured.

Figure (5a) shows two strongly attracting flat membranes. Attraction between the membranes could be realised by lowering the interaction between tail and head group segments to $\chi_{AB} = 1.2$ and zeroing the repulsion between head-groups: $\chi_{BW} = 0$. Because of this attraction the two membranes become asymmetrical. The number of lipids aggregated per membrane per unit surface area is reduced from $n_2^\sigma/L = 12.2$ for an isolated membrane to $n_2^\sigma/L = 11.6$ for the mutually adsorbed bilayers. Figure (5b) shows the corresponding bilamellar vesicle. As is shown in figures (5a) and (5b) the head group area between the two tail regions overlap considerably. As compared to the segment density profiles in figure (5a), those in figure (5b) show some distortion originating from the strong curvature. The bilamellar vesicle has a total free energy of curvature of 440 kT, which is significantly smaller than twice the free energy of curvature for the corresponding unilamellar vesicle (250 kT). This is related to the fact that the mutually interacting bilayers are slightly thinner than the isolated ones. Both for the unilamellar and bilamellar vesicle the free energy of curvature is independent of its radius. In this case, the chemical potential of the lipids in the unilamellar membrane (not shown) is slightly higher than that in the bilamellar membrane. The

equilibrium volume fractions are $1.84 \cdot 10^{-8}$ and $1.76 \cdot 10^{-8}$, respectively.

In conclusion, for attracting membranes multilamellar vesicles are energetically more favourable than unilamellar ones. Not only multilamellar vesicles will be formed, but they will attract each other mutually: a phase separation is observed.

In the case of repulsive bilayers we showed that uni- and bilamellar, and undoubtedly also multilamellar, lecithin vesicles are thermodynamically unstable. If two of such identical vesicles fuse, half of their curvature energy is gained. Volume restrictions prevent eventually the growth of the vesicles except if they form more multilayers.

Multicomponent Vesicles

Experimentally vesicles composed of one type of lipid are not very interesting. Frequently multicomponent systems are found. In the following we will discuss the physical behaviour of vesicles composed of two types of amphiphiles. First we study the addition of small chain surfactants, leading to degradation of the vesicle system at high surfactant concentration. Secondly we consider vesicles composed of two kinds of lipid molecules.

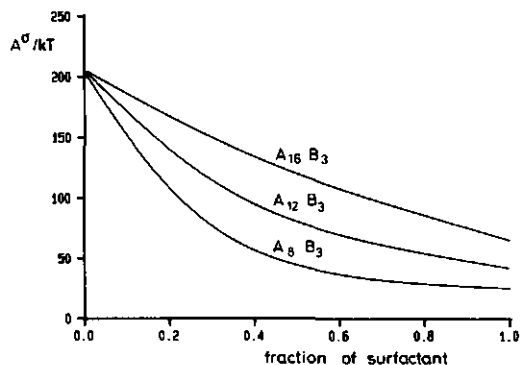


Figure 6.

Free energy of curvature of a unilamellar vesicle composed of a mixture of lecithin and surfactant molecules as a function of the relative (volume) fraction of surfactant in the system. The lecithin molecules are identical to the ones considered in figure (2). The surfactant is of an $A_p B_3$ type, for which the A and the B segments are energetically identical to the A and B segments in the lecithin molecules. Curves for $p = 8, 12,$ and 16 are plotted.

Addition of surfactants

To isolate proteins from (bio)membranes, the latter must be broken up in order to free the protein. Surfactants are frequently used for this purpose. The physics of this process is analysed below.

In the previous section, we have shown that a vesicle has a (low) free energy of curvature. Surfactant molecules are expected to accommodate well in a vesicle. If this is the case, the free energy of curvature must be affected. Figure (6) shows the effect on the free energy of curvature as a function of the fraction of surfactants in a unilamellar vesicle, for a series of surfactants (A_9B_3 up to $A_{16}B_3$). Fraction zero represents a vesicle composed of only lipids, whereas fraction 1 represents a surfactant vesicle. The lecithin molecules are the same as in figure (2). As can be seen from figure (6), elongation of the acyl tail length with one apolar segment, gives rise to an increment of the free energy of curvature of the surfactant vesicles of about 5 kT. Further, figure (6) shows that the free energy of curvature can be rather small (~ 50 kT) at high surfactant lipid ratio. There are at least two reasons to expect that in this regime a real vesicle membrane will break up into parts.

- Since the excess free energy is very low, it does not cost much energy to increase the total surface area. Because subdivision will increase the entropy of the system, free energy is gained. (In the calculation this subdivision was disregarded.)

- At these high surfactant concentrations the critical micelle concentration of the surfactants is passed. For example, for the ratio lecithin:surfactant $A_{12}B_3$ of 2:8 the equilibrium bulk volume fraction of the surfactant is $3.75 \cdot 10^{-3}$, while the CMC is $3.45 \cdot 10^{-3}$. Thus, micelles composed of surfactants accommodating a few lipids are formed. Although interesting by itself we will not deal with the structure of these micelles here. Increasing the fraction of surfactants will eventually transform the whole system into a micellar one.

Figure (7) gives the segment density profiles of a cross section through a vesicle composed of lecithin and surfactant $A_{12}B_3$ molecules (volume fraction ratio 6:4). As can be seen in figure (7), these surfactants prefer the outer side of the vesicle. The preference is not very large. The tail profile is particularly affected and has a clear maximum at the outer half of the vesicle. The head group densities of the surfactant and the lipid molecules are about equal on the inside, but on the outside more surfactant head groups are observed than lipid head groups.

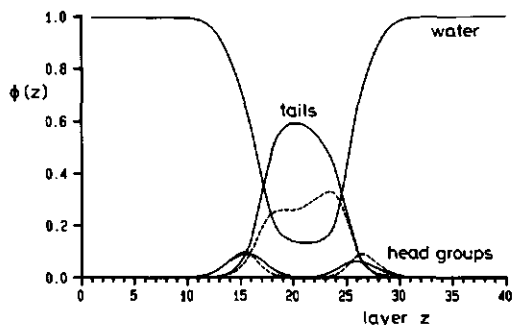


Figure 7.

Segment density profiles through a cross section of a unilamellar vesicle composed of a mixture of lecithin molecules as in figure (2) and $A_{12}B_3$ molecule (dashed curves). The relative (volume) fraction of surfactants in the mixture is 0.4. Parameters as in figure (2).

Multicomponent lecithin vesicles

In multicomponent vesicles the various constituents can distribute themselves differently over inner and outer layer of the curved membrane. In figure (8), the excess free energy of a vesicle composed of two slightly different lipid molecules is shown as a function of their relative proportion in the mixture. The lipids in the mixture differ only with respect to their tail lengths. Molecules as in figure (2) with $p = 16$ are mixed with molecules with $p' = 12, 14, 16,$ and 18 . It appears that the excess free energy is essentially a linear function of the composition in the mixture or, in this case, the average tail length. This linear behaviour is found when the fractionation of lipids between the inner and outer layer is weak, i.e., when the two lipids mix readily. Each segment that the tails are longer increases the free energy of curvature by about 12 kT per vesicle. As lecithins have two tails, this increment is on a molecular basis about the same as for a simple surfactant, see figure (6).

When the head group size increases, the free energy of curvature decreases. This is shown in Figure (9), where the excess free energy of a vesicle is plotted as a function of the fraction of lipids that differ only in head group size, $q' = 6$ compared to $q = 3$ (uppermost curve). A linear behaviour is again apparent, but this can no longer be expected when the

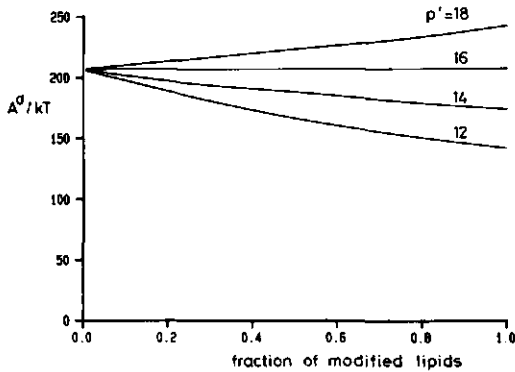


Figure 8.

Free energy of curvature of a unilamellar vesicle composed of two types of lecithin molecules as a function of the (volume) fraction of lipid molecules for which the tail lengths are modified. One lipid molecule is as in figure (2), the modified tail length p' is indicated. Parameters as in figure (2).

difference between the lipids in the mixture becomes much larger. To verify this, we have increased the attraction between water and head groups of the bigger molecule, by changing $\chi_{B,W}$ from -0.3 to -0.5 . As long as there is no repulsion between the two types of molecules, there is again an almost linear dependence of the free energy of curvature on the fraction of modified lipid in the system (see second curve from top). In the two lower curves of figure (9) additional repulsive interactions between the head-groups (third curve from top) or between the tails (bottom curve) are introduced. Although the repulsion between the head groups ($\chi_{BB'} = 1$) was chosen much stronger than between the different tails ($\chi_{AA'} = 0.2$), the latter interaction is much more effective. There are two reasons for this. Firstly, the head group density is much lower than the tail density, so that head groups have less unfavourable contacts than the tail segments in the densely packed inner part of the membrane. Secondly, per molecule the number of tail segments is much larger than the number of head group segments, so that a more co-operative behaviour can be expected for the tails.

As can be seen in figure (9), the free energy of curvature goes through a minimum for $\chi_{AA'} = 0.2$ at a modified lipid fraction of about 0.68. As expected, studying the segment density profiles at this minimum, given in

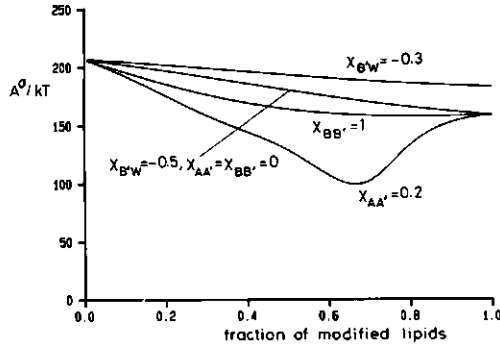


Figure 9.

Free energy of curvature of a unilamellar vesicle composed of two types of lecithin molecules (one of them is as in figure (2)) as a function of the (volume) fraction of the lipid molecules for which the head group size is increases from $q' = 3$ to $q' = 6$. The interaction parameters are the same as in figure (2) (upper curve). The three lower curves are for molecules which after modification differ also in interaction parameters: $\chi_{B'W} = -0.5$ in stead of -0.3 . In addition, for one curve a repulsive force between polar segments, $\chi_{BB'} = 1$, and for another curve a repulsive force between apolar segments, $\chi_{AA'} = 0.2$ is introduced. The primes indicate segments of modified molecules.

figure (10), reveals that the two lipid species fractionate themselves between the outer and inner layer. The bigger head groups prefer the outer layer and the corresponding molecules are necessarily present in higher numbers.

Figure (11) shows the free energy of curvature as a function of the radius of the vesicle in figure (10) at a fixed composition of the mixture. Here, the radius of the vesicle is defined as the number of layers from the centre of the vesicle up to the centre of the bilayer membrane. The optimal vesicle size for the given mixture composition is found at the minimum in figure (11). The deeper this minimum the more narrow the vesicle size distribution. In example the optimal vesicle radius is about 25 lattice units. Because the minimum in figure (11) is not very deep, the size distribution is probably not very sharp. The chemical potentials of the two lipids are also functions of the vesicle radius. For the smaller lipid, which is situated on the inside of the vesicle, the chemical potential passes through a weak

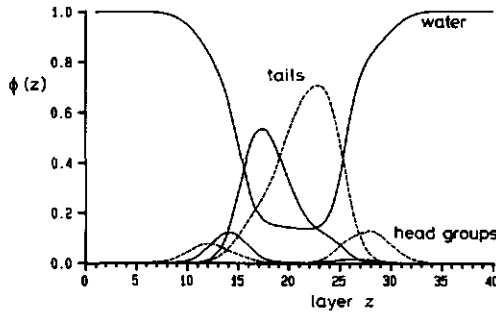


Figure 10.

Segment density profiles through a cross section of the vesicles given at the minimum in figure (9) ($\chi_{B,W} = -0.5$, $\chi_{AA} = 0.2$, and $\chi_{BB} = 0$). The dashed curves are the profiles for the fraction (0.68) of modified lipids.

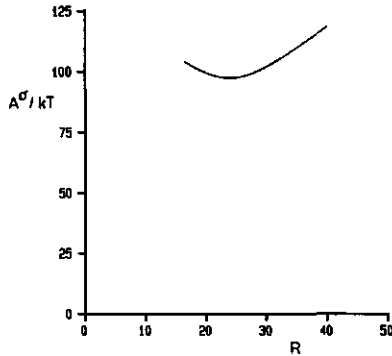


Figure 11.

Free energy of curvature of the vesicle in figure (10) as a function of its radius.

minimum near the optimal vesicle radius. In this region the chemical potential of the bigger lipid goes through a weak maximum. These two trends compensate each other.

Vesicle Deformation

In this part we will discuss the free energy expenditure for deforming a globular vesicle into a rod-like vesicle. To this end we could use a finite h

and $A_s = 0$ in equation (1). The difference in excess free energy of this structure with respect to the perfectly globular one could then be identified as to the deformation energy. However, in this approach the mean field approximation would mix the sphere and cylinder geometry. Since the two cups of a hollow rod are essentially half spheres with known curvature energy, we only have to add the curvature energy of a part of an infinitely long hollow cylinder with the same radius. In this case equation (1) reduces to $V(z) = \pi h z^2$. This last method is also preferred, because it gives more information and more accurate data. Strictly, the combination of a sphere with a cylinder can be done done when the chemical potentials of the lipids of both structures are identical. In this approach this is not necessarily the case. However, the deviations are small. Figure (12) gives the curvature energy per unit length (the thickness of a lattice layer) of the cylinder as a function of the number of lecithin molecules aggregated per unit length, which is a measure of the radius of the cylinder. Similar to the curve found for globular vesicles in figure (2), some irregularities at very small cylinder radius are found. For these intermediate structures between filled cylinders and hollow cylinders are responsible. As can be seen in figure (12), the free energy of curvature of a hollow cylinder decreases with increasing radius. Thus, the amount of free energy needed for curving a flat membrane into a cylinder depends on the radius of the cylinder in contrast to the constancy of the free

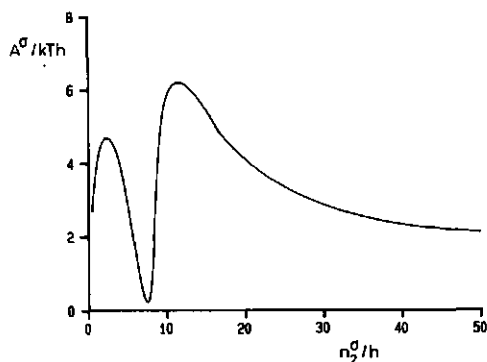


Figure 12.

Dependence of the free energy of curvature per unit length of a cylinder composed of lecithin molecules as in figure (2) on the number of lecithin molecules aggregated per unit length.

energy of curvature of a sphere.

Applying this to the deformation of a globular vesicle into a rod, we conclude that the excess free energy increases with deformation. When a globular vesicle is deformed into a very long rod, the energy required is not only high because of the small radius of curvature, but also because the energy is proportional to the length of the rod.

Discussion

Although the present theory underestimates the membrane thickness and overestimates the amount of water in the membranes, some general observations of the segment density profiles do give interesting insights. Our theory shows that the entropy of the tails in the aggregates is quite high. All segments have many options regarding their spread in positions, i.e., they are not confined to one layer, but have a distribution over several layers. The segments near the tail ends have the highest entropy, while the segments close to the branch point are more confined. Physically, the interfaces between the solvent and the apolar phase extend over several layers. There are many tail-water contacts, notwithstanding the repulsive energy between them. The overlap between the head group profile and the tail profile is so strong that the head groups are in rather apolar medium. This supports the observation that substantial repulsion between tails and head groups, as expressed in the positive χ_{AB} parameter, is important for the membrane stability.

Our results for single component unilamellar and multilamellar vesicles show that the vesicles are thermodynamically unstable because they lose free energy when fusing. Vesicles can grow either by fusion or by diffusion of single lipids from other vesicles (via the solution). By our theory we do not get mechanistic information on how the vesicles grow. Eventually, when vesicles fill up the whole solution, the growth of the vesicles is expected to stop.

Most vesicles analysed in this paper have a free energy of curvature of the order of 200 kT. Small artefacts inherent in lattice calculations are responsible for uncertainties in this parameter of about 5 to 10 kT. Other vesicles, composed of surfactants or mixtures appear to have a very low free energy of curvature. In these systems, the energy cost for enlarging the surface area is very small, and therefore the lattice artefacts will manifest themselves more strongly. Obviously, when the excess free energy per surface area is very small, large curvature fluctuations may occur.

In many biological systems, the membrane surface area is essentially constant. The vesicle and liposome sizes are controlled. In nature, the various lipids are not likely to repel each other as effectively as we assumed in figure (10). However, like the lipids in this figure, many proteins adsorb preferentially on one side of the vesicle. In the presence of a low molecular weight additive, the free energy of curvature might be very low at a certain curvature. Thus, the complex multicomponent vesicles found in nature may be close to real thermodynamical equilibrium.

Conclusions

For the first time a detailed a priori statistical thermodynamical analysis of the lipid vesicle system is possible. We showed that non-interacting unilamellar as well as multilamellar vesicles are thermodynamically unstable. Both for uni- and multilamellar vesicles the free energy of curvature per associate is basically independent of the radius of the vesicle. A correlation between the thickness of the membrane and the free energy of curvature is observed. Although the segment density profiles predict more solvent in the thin membranes than is usually observed for water, several details of the organisation of the lipid molecules in the vesicles correspond well with experimental data. As expected, in multicomponent vesicles the various lipids distribute differently between the inner and outer layer of a curved membrane. This fractionation is never complete. Repulsion between the different amphipolar molecules promotes the partition. If the partitioning is strong the vesicles may show a narrow size distribution. Addition of small surfactants is found to destabilise the vesicles at a high surfactant-lipid ratio. From comparison between curvature energy of spheres and cylinders it can be concluded that the excess free energy of vesicles increases very with the degree of deformation.

Appendix A. Partition function

The grand canonical partition function Ξ of a system of n_i molecules of various type i of which n_i^c in conformation c in equilibrium with a bulk solution with chemical potential μ_i , can be expressed by:

$$\Xi(V, T, \{\mu_i\}) = \Xi^* \sum_{\{n_i^c\}} \frac{\Omega \exp\{-U(\text{int})/kT\} \exp(\sum_i n_i \mu_i / kT)}{\Omega^* \exp\{-U^*(\text{int})/kT\} \exp(\sum_i n_i \mu_i^* / kT)} \quad (\text{A1})$$

The * indicates the pure component reference state. The summation is over all

possible sets $\{n_i^c\}$ in volume V at temperature T . In a first order Markov approximation a conformation is defined by the layer numbers in which each of the successive chain elements finds itself. $U(\text{int})$ is the interaction energy between all molecules in the system, $U^*(\text{int})$ the same in the reference system. The quantity $U(\text{int}) - U^*(\text{int})$ contains all possible segment-segment and segment-solvent nearest neighbour contact energies in the volume V in excess to those in the reference state. For this excess energy we have

$$(U(\text{int}) - U^*(\text{int}))/kT = \frac{1}{2} \sum_i \sum_z \sum_x \sum_y n_{xi}(z) \chi_{xy} (\langle \phi_y(z) \rangle - \frac{r_{yi}}{r_i}) \quad (\text{A2})$$

where the division by 2 corrects for double countings. In equation (A3) r_{yi} indicates the number of segments y of molecule i . Thus, the quotient r_{yi}/r_i gives the fraction of y segments in the chain i and hence in the reference state. $n_{xi}(z)$ is the number of segments x of molecule type i in layer z .

The total degeneracy Ω^* in the reference state is composed of the individual degeneracies Ω_i^* of the reference systems of various molecules. These degeneracies have been derived by Flory [16]:

$$\Omega^* = \prod_i \Omega_i^* = \prod_i \left[\frac{(r_i n_i)!}{n_i!} \left(\frac{z}{r_i n_i} \right)^{(r_i - 1)n_i} \right] \quad (\text{A3})$$

The degeneracy of the system can be derived following the same line of arguments as in reference [13]. Now some extra attention must be paid to the fact that not each lattice layer has the same number of lattice sites. The result is:

$$\Omega(\{n_i^c\}, V) = \prod_z \frac{L(z)!}{L(z)^{L(z)}} \prod_i \prod_c \left[\frac{\binom{\omega_i^c}{n_i^c}}{n_i^c!} \right] \quad (\text{A4})$$

where the degeneracy of a chain in conformation c in the curved lattice is given by:

$$\omega_i^c = L_i^c(1) \prod_{s=2}^{r_i} z \lambda^{z(s-1)-z(s)} \quad (\text{A5})$$

Here $L_i^c(1)$ gives the number of lattice sites of the layer z where conformation starts. For a flat lattice $L(z)$ is independent of z . For this case the present partition function reduces to the one derived in reference [13].

The chemical potential for a mixture of polymers in solution can be expressed as [28]:

$$(\mu_i - \mu_i^*)/kT = \ln \phi_i^b + 1 - r_i \sum_j \phi_j^b / r_j + \frac{1}{2} r_i \sum_x \sum_y \chi_{xy} (\phi_{xi}^* - \phi_x^b) (\phi_y^b - \phi_{yi}^*) \quad (A6)$$

In a rotational isomeric state scheme all spatial configurations are kept apart so that the degeneracy of a chain in conformation c in the curved lattice (originating from translation) is given by:

$$\omega^c = L^c(z(1)) \prod_{s=2}^{r_i} \frac{\lambda_{z(s-1)-z(s)}^c(z(s))}{\lambda_{z(s-1)-z(s)}^c} \quad (A7)$$

Further, in equation (A1) a term Q^g/Q^{g*} must be included, which is the canonical partition function accounting for the various gauche (or trans) configurations in the system compared to the reference state:

$$\frac{Q^g}{Q^{g*}} = \frac{\exp(-\sum_i n_i^g U_i^g / kT)}{\prod_i 4^3 (2 \exp(-U^g/kT) + 1)^{n_i} (r_i^{-3})} \quad (A8)$$

where U^g is the energy difference between a gauche and a trans configuration. n_i^g is the number of gauche bonds in molecules of type i. Finally due to the modified definition of a conformation, equation (A4) is simplified to:

$$\Omega^* = \prod_i \frac{(r_i n_i)!}{n_i!} \quad (A9)$$

It is possible to write the partition function in terms of segment density profiles. See reference [13].

Literature

1. G. Poste, and D. Papahadjopoulos; in: "Uses of liposomes in biology and medicine", (G. Gregoriadis and A. Allison Eds.), Wiley, NY (1979) 101.
2. M. Calvin; *Accounts Chem. Res.* **11** (1978) 369.
3. C. Laanen, W.E. Ford, J.W. Otvos, and M. Calvin; *Proc. Natl. Acad. Sci. USA* **78** (1981) 2017.
4. J.N. Israelachvilli, D.J. Mitchell, and B.W. Ninham; *J. Chem. Soc. Faraday Trans. II* **72** (1976) 1525.
5. J. N. Israelachvilli, D.J. Mitchell, and B.W. Ninham; *Biochem. Biophys. Acta* **470** (1977) 185.
6. W. Helfrich; *Z. Naturforsch.* **28c** (1973) 693.
7. B. Owenson, and L.R. Pratt; *J. Phys. Chem.* **88** (1984) 6049.
8. P. v.d. Ploeg, and H.J.C. Berendsen; *J. Chem. Phys.* **76** (1982) 3271.
9. A. Ben-Shaul, I. Szleifer, and W.M. Gelbart; *Proc. Natl. Acad. Sci. USA* **81** (1984) 4601.
10. K.A. Dill, and P.J. Flory; *Proc. Natl. Acad. Sci. USA* **78** (1981) 676.
11. D.W.R. Gruen; *J. Colloid Interface Sci.* **89** (1985) 153.
12. F.A.M. Leermakers, J.M.H.M. Scheutjens, and J. Lyklema; *Biophys. Chem.* **19** (1983) 353.
13. J.M.H.M. Scheutjens, and G.J. Fleer; *J. Phys. Chem.* **83** (1979) 1619.
14. J.M.H.M. Scheutjens, and G.J. Fleer; *J. Phys. Chem.* **84** (1980) 178.
15. F.A.M. Leermakers, P.P.A.M. v.d. Schoot, J.M.H.M. Scheutjens, and J. Lyklema; in: "Surfactants in Solution. Modern Applications", (K.L. Mittal Ed.) in press.
16. P.J. Flory; "Principles of Polymer Chemistry", Cornell University Press, Ithaca, NY (1953).
17. J.M.H.M. Scheutjens, F.A.M. Leermakers, N.A.M. Besseling, and J. Lyklema; in: "Surfactants in Solution. Modern Application", (K.L. Mittal Ed.), in press.
18. F.A.M. Leermakers; PhD thesis, Wageningen (1988) chapter 2.
19. D.G. Hall, and B.A. Pethica; in: "Nonionic surfactants", (M.J. Schick, Ed.), Marcel Dekker, NY (1976), Ch. 16.
20. T.L. Hill; "Thermodynamics of small systems", Vols 1 and 2, Benjamin, NY (1963,1964).
21. N.K. Adan, and G. Jessop; *Proc. Roy. Soc. London, Ser A*, **112** (1926) 362.
22. B.A. Cornell, J. Middlehurst, and F. Separovic; *Faraday Discuss. Chem. Soc.* **81** (1986) (in press).

23. B.C. Cornell, J. Middlehurst, and F. Separovic; *Biochem. Biophys. Acta* **598** (1980) 405.
24. D.G. Brouillette, J.P. Segrest, D.Ng. Thian, and J.L. Jones; *Biochemistry* **21** (1982) 4569.
25. C. Huang, J.T. Mason; *Proc. Natl. Acad. Sci. USA* **75** (1978) 308.
26. A. Chrzesczyk, A. Wishnia, and C.S. Springer, Jnr.; *Biochem. Biophys. Acta* **470** (1977) 161.
27. O.A. Evers; PhD thesis, Wageningen (1988).

CHAPTER 4

THE GEL TO LIQUID PHASE TRANSITION

Abstract

A new theory is introduced to model the lipid membrane structure and stability both above and below the gel to liquid phase transition temperature. Recently, we elaborated a Self-Consistent Field (SCF) theory, in which the full set of conformations was generated in a Rotational Isomeric State scheme and Boltzmann statistics was used to determine the statistical weight per conformation. In the new theory we take into account that the anisotropic distribution of the molecules on the lattice induce a self-consistent anisotropic molecular field. This field, which is a function of the bond orientations, is an extra factor which influences the statistical weight of each conformation and is based on a generalisation of Di Marzio's analysis of systems with rigid rods. This elegant refinement follows from elementary statistics, is free of new adjustable parameters and significantly improves details of the structure of the model membranes.

To examine the properties of this SCAF (Self-Consistent Anisotropic Field) theory we use a model membrane built up by lecithin-like molecules composed of apolar and polar segments. The model has three nearest neighbour interaction parameters of the Flory-Huggins type, namely: for the interaction between apolar segments and water, that between polar segments and water, and that between polar and apolar segments. A fourth parameter is the dihedral trans/gauche energy difference.

The theory predicts a first order gel to liquid phase transition for the model membranes. Depending on the membrane concentration both an intercalated (in the dilute regime) and a non-intercalated (in the concentrated regime) gel phase are observed. Detailed information on the various membrane phases is obtained. Order parameter and segment density profiles are given.

Introduction.

Many biological processes depend on the physical properties of the bilayer membranes. One of the best known aspects of the bilayer membrane is that at a characteristic temperature an order to disorder phase change takes

place. Many experimental and theoretical studies have been performed in order to understand this critical behaviour. During the main phase transition, the membrane changes dramatically from a high temperature fluid-like nature, in which the apolar tails have considerable flexibility and disorder, to a low temperature gel-like nature, in which the apolar tails are aligned [2-6]. Recently, also intercalated gel phases have been found experimentally in which the tails of many lipids cross the centre of the membrane and the CH₃ groups are found near the glycerol backbone of the lipids on the other side of the membrane [7-9]. Simultaneously with the main gel to liquid phase transition, the membrane system changes from a high-temperature state where interaction between the membranes is repulsive so that the system is very soluble, to a low-temperature attractive state. The transition temperature or rather, very narrow temperature range, is known as the Krafft point. For some membrane systems, also a (reversible) pre-melting transition is observed [3,10].

Theoretical studies on the gel to liquid phase transition proved that a co-operative gauche to trans transition of the apolar tails is thermodynamically possible [6,11-13]. Until recently, no theory was able to account for both the intercalated and the non-intercalated gel phases, nor does any of them they take the interaction between membranes into account. We will show that the new theory is general enough to account for the observed phenomena and provide detailed information on both of these effects.

Recently, we introduced a self-consistent field theory for which the partition function is worked out with Flory-Huggins type approximations, namely Markov-like chain statistics combined with a local mean field assumption [1]. This theory successfully interpreted the force balance of the lipid membrane. We needed no artificial restrictions on the molecules in the system. The equilibrium membrane thickness is found from a thermodynamic analysis: a free membrane has a vanishing surface tension [14,15]. We were also able to extend our work to study aspects of morphological phenomena of associates of surfactants by also considering lattices with spherical or cylindrical geometry [16]. For small molecules it is very important that the Markov-type statistics is extended to include the so called Rotational Isomeric State scheme. In this approximation any five consecutive segments do not overlap [14].

Although promising a few problems remained. One of them is that the apolar tails in the interior of the membrane showed a melt-like behaviour, so that the membranes found were too thin. Another problem was that the

experimentally observed critical phase behaviour of the membrane system was not reproduced.

A significant improvement of our theory for the lipid membranes can be formulated and is elaborated in this paper. The novel idea is that the statistical weight of each conformations in the membrane is influenced by the orientation of the neighbouring chains. The molecules induce a self-consistent anisotropic molecular field which leads to an orientation dependent packing entropy. We derive the partition function in terms of a set of conformations of the chain molecules. The evaluation of the partition function is facilitated when it is given in terms of segment density profiles. With these segment density profiles a detailed study of a model membrane composed of model lecithin-like molecules is performed.

Self-Consistent Anisotropic Field theory

Even short chain molecules have a huge number of possible spatial arrangements. In order to keep the number of conformations countable, a three-dimensional lattice composed of lattice sites with equal volume is used, to which the molecules in the system are confined. In this paper we will use a lattice with flat lamellar geometry. The lattice layers are numbered $z = 1, \dots, M$ and have L lattice sites each. In each layer inhomogeneities are disregarded, so that a mean field approximation for the interaction energy is appropriate. Each lattice site will be filled with either a solvent (water) molecule or a lipid (apolar or polar) segment. The co-ordination number of the lattice is Z . A fraction λ_0 of these neighbouring sites is in the same layer, a fraction λ_{-1} in a previous layer and a fraction λ_1 in the following layer.

Chain molecules can have various types of composition. Lipid molecules are branched. They have a glycerol backbone on to which there are bound two apolar tails of 12 to 20 CH_2 segments each (actually, one of them is the terminal CH_3 segment) and one head group composed of polar and apolar segments. A complete lipid molecule is assumed to have r segments or, more exactly, the total volume of the lipid molecule is r lattice sites. In the following derivation we will discuss, for the sake of simplicity, linear chains only. Modifications of the molecular structure are easily incorporated in the model, as has been shown in earlier work [14]. In the "Results" section we will discuss membranes composed of lecithin-like molecules.

The partition function

The central issue is how the chain molecules distribute themselves in the system. In reference [17] a conformation is defined by specifying the lattice layers in which the consecutive segments are situated. It is worth realising that each conformation defined in this way is degenerate, for in many cases more than one spatial configuration can be found that obeys this definition. However, in the present derivation of the partition function we decided to treat the various spatial configurations in each conformation individually. The choice is motivated by the fact that it does not effect the final result and that the Rotational Isomeric State scheme is presented more easily in non-degenerate conformations. (We will still use the term conformations.) When the number of segments r_i in chain i is larger than 1 and the first segment is fixed at a given lattice site, the other r_i-1 segments have, in a rotational isomeric state scheme (third order Markov) approximation, $Z \cdot 3^{(r_i-2)}$ viable arrangements, since the first bond of the chain has Z possible directions, whereas all subsequent bonds can choose out of 3 directions, chain backfolding being prohibited.

The total number of molecules of type i in conformation c is denoted by n_i^c . A summation of n_i^c over all conformations gives n_i , the total number of molecules of type i in the system. If the positions of all molecules of type i are known, the partition function can be calculated and our problem is solved. We will work out this procedure for a given but arbitrary set of molecules

The grand canonical partition function can formally be written as:

$$\Xi(M, L, T, \{\mu_i\}) = \Xi^* \frac{\sum_c \Omega \cdot Q^G \exp(-U(\text{int})/kT) \exp(\sum_i n_i \mu_i / kT)}{\sum_c \Omega^* \cdot Q^{G*} \exp(-U^*(\text{int})/kT) \exp(\sum_i n_i \mu_i^* / kT)} \quad (1)$$

and is composed of a combinatorial factor Ω , energetic and entropic contributions from gauche (or trans) configurations Q^G , the interaction energy $U(\text{int})$ and chemical potentials $\{\mu_i\}$. The corresponding quantities of the bulk phase of each pure component (the reference state) are indicated by an asterisk.

Energy

For a given set of conformations, all volume fractions in each layer can be calculated. Each segment has interactions with its surrounding molecules. The energetic effects of these contacts are accounted for by Flory-Huggins energy parameters χ_{xy} . A Flory-Huggins parameter gives the energetic effect in

units of kT of exchanging two types of segments (x and y) from their own environment (pure x , or y , respectively) to the other. Therefore the FH parameters are zero when the segments are the same: $\chi_{xx} = 0$. If molecules i are composed of different segment types, the contact energy of a segment x in the reference state is given by $kT \sum_y \chi_{xy} \phi_{yi}^*$, where ϕ_{yi}^* is the fraction of y segments in molecules i . The total interaction energy of the system is, in a mean field approximation, given by:

$$U(\text{int}) - U^*(\text{int}) = \frac{1}{2} kT \sum_i \sum_z \sum_x \sum_y n_{xi}(z) \chi_{xy} (\langle \phi_y(z) \rangle - \phi_{yi}^*) \quad (2)$$

where both x and y run over all segment types: W (water), A (apolar), B (polar), etc.. The number of x segments in layer z is $n_x(z)$ and their volume fraction $\phi_x(z)$. Here, the angular brackets indicate that an average over three consecutive lattice layers is taken to account for the contacts with segments in these layers:

$$\langle \phi(z) \rangle = \sum_{z'} \lambda_{z'-z} \phi(z') \quad (3)$$

In equation (2) the division by 2 corrects for double counting of the contacts.

In addition to this, one can have energetic contributions originating from local conformations in the chains. In a Rotational Isomeric State (RIS) scheme each sequence of four segments can be in a low energy trans (t) state or in one of the two possible gauche (g^+ or g^-) states having an energy exceeding that of the trans configuration by an amount U^g . Let n_i^{gc} be the number of gauche configurations that molecule that chain i has in conformation c . Then,

$$Q^g = \prod_i \prod_c \exp(-n_i^{gc} U^g / kT) \quad (4)$$

accounts for the energy of the total number of gauche configurations in the system.

Entropy

Next, we will be concerned with the derivation of the, somewhat more involving, combinatory factor for our system. Let us first place the molecules one after the other on the lattice, each having an arbitrary but specified

conformation. This set of conformations has the only restriction that the total number of segments and solvent molecules in each layer equals L . The number of ways to distribute this set of conformations in the lattice contributes to the degeneracy and hence to the entropy of the system. Without excluded volume corrections of other molecules in the system a conformation c is L -fold degenerated, because the first segment has a choice between L starting points. However, the layer is empty only before the first segment is placed in a lattice layer. When subsequent segments are offered, one has to correct for the fact that not all lattice sites in this layer are vacant any longer. If at a certain moment in each lattice layer $v(z)$ sites are filled with segments, only $L-v(z)$ sites are unoccupied. The vacancy probability $P^V(z)$ determines whether a following segment can be placed on the lattice given the fractional occupation of this layer:

$$P^V(z) = \frac{L - v(z)}{L} \quad (5)$$

Figure (1) illustrates equation (5) for dimers. After k segments are placed

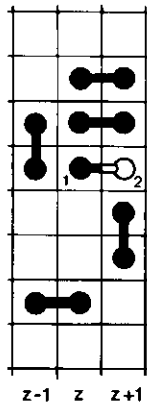


Figure 1.

Dimers on a square lattice. One of the dimers has one of its segments in layer z , while the next segment is to be placed in $z+1$. In a SCF approximation the probability of finding a vacant site in layer $z+1$ in this lattice would be $P^V(z+1) = 4/8$. In a SCAF approximation this probability is $P^V(z+1) = 4/6$, because there are already two bonds in this orientation.

each into a certain layer, k-1 consecutive corrections have been performed. Eventually, the number of ways to place all chain molecules of a given type i in the system is:

$$\omega(n_i) = L^{n_i} \prod_{z, u(z)=0}^{n_i(z)-1} \frac{L - u(z)}{L} \quad (6)$$

The derivation will proceed by filling the remaining sites with other molecules (including the solvent molecules). Along similar lines, the original mean field theory was developed [17].

A serious drawback of this approach is that the excluded volume of neighbouring molecules is only roughly accounted for. Already in 1956 Flory showed that the Flory-Huggins theory could be generalised to treat rigid rod liquid crystals [18]. Di Marzio worked out the partition function of rigid rods on a lattice [19,20], and recently, Van der Schoot showed that the work of Di Marzio can in principle be adapted for the present type of theories [21]. For this improvement not only the position of the segments must be known, but also the segment-segment bond orientations are to be traced. For this purpose, we introduce a notation for bond orientations. In general, the bond orientations follow the possible orientations in the lattice, denoted by $\alpha'' = e'', f'', g'', h'', \dots$. Each orientation α'' can be divided into two opposite directions, denoted by α and α' . The number of bonds α'' between layers z and z' are given by: $n^{\alpha''}(z|z') = n^{\alpha}(z) + n^{\alpha'}(z')$ (the value of z' depends on the direction α). Thus a bond h from layer z to z+1 and the bond h' from layer z+1 to z are added in $n^h(z|z+1) = n^h(z) + n^{h'}(z+1)$. When a chain is added to the lattice, the first segment is put on a vacant lattice site with probability $(L - u(z))/L$. Then, simultaneously with the addition of each subsequent segment of the chain, also an extra segment-segment bond appears in the system.

The insight for the improved statistics is based on the fact that the $n^{\alpha''}(z|z')$ bonds already present in orientation $\alpha(z|z')$ cannot block any next bond to be placed in directions $\alpha(z)$ or $\alpha'(z')$. The correction accounting for this is given by a factor $L/(L - u^{\alpha''}(z|z'))$, because not L, but fewer sites are a priori accessible and hence the factor normalises the probability for the excluded volume correction of equation (6). So in this case the vacancy probability $P^V(z) = (L - u(z))/(L - u^{\alpha''}(z|z'))$. See also figure (1). An alternative argument when $z' = z$ for this correction is as follows. Of all pairs in the same orientation as the direction of the bond to be placed, only

one segment is visible and the other segment is hidden behind this one. The hidden segment cannot prevent the present bond from being placed into the indicated direction.

For each bond of a molecule a correction factor is introduced unless this bond is the first of its kind in the lattice. After all n_i molecules are placed, the number of bonds in orientation $\alpha''(z||z')$ is $n_i^{\alpha''}(z||z')$ and thus there are $n_i^{\alpha''}(z||z') - 1$ correction factors. Equation (6) is replaced by:

$$\omega(n_i) = L^{n_i} \prod_z \frac{n_i(z)-1}{v(z)=0} \frac{L - v(z)}{L} \prod_{z'} \prod_{\alpha''} \frac{n_i^{\alpha''}(z||z')-1}{v_i^{\alpha''}(z||z')=0} \frac{L}{(L - v_i^{\alpha''}(z||z'))} \quad (6a)$$

For a dense highly oriented system, the corrections are very large indeed. In this case our previous SCF theory underestimates the entropy.

After adding the other molecules, including the solvent, and accounting for indistinguishability of the n_i^c molecules, the following expression for the combinatorial factor Ω is found:

$$\Omega = L!^M \prod_i \prod_c \frac{1}{n_i^c!} \prod_z \prod_{\alpha''} \frac{(L - n_i^{\alpha''}(z||z'))!}{L!} \quad (7)$$

It is easy to verify that, for the case of rigid rods (e.g., dimers), this result is identical to equation (A1) of reference [20]. To recover the original equation for Ω [17], just assume that all $\sum_i n_i(r_i^{-1})$ bonds are oriented in different orientations so that $n_i^{\alpha''}(z||z') = 1$ and the last factor in equation (7) reduces to $\prod_i L^{-n_i}(r_i^{-1})$. (Remember that equation (7) is in terms of spatial configurations rather than degenerate conformations.)

As reference states, systems composed of pure molecules i are used. The combinatorial factor Ω_i^* for each state i is analogous to the one derived by Flory [22], extended with orientation effects as in equation (7):

$$\Omega_i^* = \frac{(n_i r_i)!}{n_i!} \prod_{\alpha''} \frac{(n_i r_i - n_i^{\alpha''*})!}{(n_i r_i)!} \quad (8)$$

where $n_i^{\alpha''*}$ is the number of bonds in the reference state in the indicated orientation.

As above the contributions of the gauche and trans configurations are incorporated in a canonical type of partition function:

$$Q_i^{g*} = Z^{n_i} 3^{n_i} (2 \exp(-n_i^{g*} U^g/kT) + 1)^{n_i} (r_i^{-3}) \quad (9)$$

The first bond of each molecule has a choice of Z directions, the subsequent bonds have each a choice of 3 directions, of which 2 are weighted according to the gauche-trans energy difference U^g except for the second bond.

Using Sterling's approximation for the factorials, the entropy $\ln(\Omega/\Omega^*)$ can be written in terms of the set $\{n_i^c\}$:

$$\ln(\Omega(M,L, \{n_i^c\})/\Omega^*) = - \sum_i \sum_c n_i^c \ln \frac{n_i^c r_i}{L} + \sum_z \sum_{\alpha''} [L - n^{\alpha''}(z|z')] \ln(1 - \phi^{\alpha''}(z|z')) - \sum_i \sum_{\alpha''} (r_i n_i - n_i^{\alpha''*}) \ln(1 - \phi_i^{\alpha''*}) \quad (10)$$

where $\phi^{\alpha''}(z|z') = \phi^{\alpha''}(z) + \phi^{\alpha''}(z')$ is the volume fraction of bonds in the indicated orientation. The chemical potentials are derived in appendix A and read:

$$(\mu_i - \mu_i^*)/kT = \ln \phi_i^b - \sum_{\alpha''} (r_i - r_i^{\alpha''b}) \ln(1 - \phi^{\alpha''b}) + \sum_{\alpha''} (r_i - r_i^{\alpha''*}) \ln(1 - \phi_i^{\alpha''*}) + \frac{1}{2} r_i \sum_x \sum_y \chi_{xy} (\phi_{xi}^* - \phi_x^b) (\phi_y^b - \phi_{yi}^*) \quad (11)$$

The subscript xi refers to segment type x in molecule type i (if molecule type i has no segments x the corresponding values are zero). In equation (11) $\phi^{\alpha''b} = \sum_i \phi_i^{\alpha''b}$, $r_i^{\alpha''}$ is the number of bonds molecule i has in orientation α'' and the superscript b refers to the bulk solution.

In order to find the equilibrium distribution of conformations, we differentiate the free energy with respect to n_i^c , given the boundary condition that each lattice layer is filled: $\sum_i \phi_i(z) = 1$ for all z. Introducing Lagrange multipliers $u''(z)$, the unconstrained function

$$f = kT \ln(\Omega/\Omega^*) + kT \ln(Q^g/Q^{g*}) - (U(\text{int}) - U^*(\text{int})) + \sum_i n_i (\mu_i - \mu_i^*) + \sum_z u''(z) (\sum_i \sum_c n_i^c r_i^c(z) - L) \quad (12)$$

is differentiated with respect to n_i^c . In equilibrium the derivative

$\partial f / \partial n_i^c = 0$ for all conformations. The result of the differentiation is for the combinatorial factor:

$$\frac{\partial \ln \Omega / \Omega^*}{\partial n_i^c} = - \ln \frac{n_i^c r_i}{L} - r_i - \sum_z \sum_{\alpha''} r_i^{\alpha''}(z|z') \ln(1 - \phi^{\alpha''}(z|z')) + \sum_i \sum_{\alpha''} (r_i - r_i^{*\alpha''}) \ln(1 - \phi_i^{*\alpha''}) \quad (13)$$

and for the gauche-trans configurations part of the canonical partition function:

$$\begin{aligned} \frac{\partial \ln Q^g / Q^{g*}}{\partial n_i^c} &= -n_i^{gc} U^g / kT - \ln \left(Z \cdot 3 \left(2 \exp(-U^g / kT) + 1 \right)^{r_i - 3} \right) \\ &= \ln \lambda_i^c = \ln \left\{ \frac{1}{2} \frac{1}{3} (\lambda_i^g)^{n_i^{gc}} (\lambda_i^t)^{n_i^{tc}} \right\} \end{aligned} \quad (14)$$

where $\lambda^g = 1 / (2 + \exp(U^g / kT))$ and $\lambda^t = 1 - 2 \lambda^g$ are the probabilities for a gauche and trans configuration, respectively. The differentiation of the interaction energy gives:

$$\frac{-\partial (U(\text{int}) - U^*(\text{int})) / kT}{\partial n_i^c} = - \sum_z \sum_x \sum_y r_{xi}^c(z) \chi_{xy} \langle \phi_y(z) \rangle + \frac{1}{2} \sum_x \sum_y r_{xi} \chi_{xy} \phi_{yi}^* \quad (15)$$

Further,

$$\frac{\partial \sum_i n_i (\mu_i - \mu_i^*)}{\partial n_i^c} = \mu_i - \mu_i^* \quad (16)$$

and finally,

$$\frac{\partial u''(z) (\sum_i \sum_c n_i^c r_i^c(z) - L)}{\partial n_i^c} = u''(z) r_i^c(z). \quad (17)$$

The equilibrium number of molecules i in conformation c in the system can conveniently be written in the form

$$n_i^c = L C_i \lambda_i^c \prod_{s=1}^r G_i^c(z, s) \prod_{s=2}^r G^{\alpha''c}(z(s)|z'(s-1)) \quad (18)$$

where $G_i(z, s)$ is a segment weighting factor which, if segment s of molecule i

is of type x, is given by:

$$G_x(z) = \exp(u'(z) - \sum_y \lambda_{yx} (\langle \phi_y(z) \rangle - \phi_y^b)) \quad (19)$$

where $u'(z) = u''(z) - u''^b$ so that G_x^b is 1 in the bulk solution, and the weighting factors are properly normalised. In the bulk solution the lagrange parameter is:

$$u''^b = -1 + \sum_{\alpha''} \ln(1 - \phi^{\alpha''b}) + \frac{1}{2} \sum_x \sum_y \lambda_{xy} \phi_x^b \phi_y^b \quad (20)$$

In equation (18) $G^{\alpha''}((z(s) \| z'(s-1)))$ is the anisotropic weighting factor according to the orientation α'' of the bond between segment s and s-1:

$$G^{\alpha''}(z \| z') = \frac{1 - \phi^{\alpha''b}}{1 - \phi^{\alpha''}(z \| z')} \quad (21)$$

For each orientation α'' in the bulk $\phi^{\alpha''b} = (2/Z) \sum_i \phi_i^b (1 - 1/r_i)$.

Next, in equation (18) the normalisation constant C_i is for the grand canonical environment

$$C_i = \frac{\phi_i^b}{r_i} \quad (22)$$

and in the case that the number of molecules in the system is given, i.e., in a canonical environment, the normalisation is given by:

$$C_i = \frac{\theta_i}{r_i G_i(r_i)} \quad (23)$$

where $G_i(r_i) = \sum_c \lambda_i^c \prod_{s=1}^{r_i} G^c(z, s) \prod_{s=2}^{r_i} G^{\alpha''c}(z(s) \| z'(s-1))$ is the total weighting factor of molecules i in the system and $\theta_i = \sum_z \phi_i(z) = \sum_c n_i^c r_i / L$ is the amount of molecules i in the system. As we will see below, $G_i(r_i)$ can be found without the explicit summation over all conformations.

Series expansion of equation (21) shows that the leading term is 1. When all other terms are neglected, which is acceptable for low values of $\phi^{\alpha''}(z \| z')$, equation (18) reduces to the SCF one (equation (23) in reference [17]) except that the present equation (18) applies for RIS instead of first order Markov statistics.

With the help of equation (18) the excess free energy $A^G = -kT \ln \Xi$ can now be written in terms of volume fractions. Substituting equation (18) into

equation (10), and taking the maximum term of equation (1) after some rearrangements we find:

$$A^{\sigma}/kTL = \sum_z \left\{ \ln \frac{\phi_w(z)}{b} + \sum_{\alpha''} \ln G^{\alpha''}(z|z') \right. \\ \left. + \frac{1}{2} \sum_x \sum_y (\chi_{xw} + \chi_{yw} - \chi_{xy}) [\phi_x(z) \langle \phi_y(z) \rangle - \phi_x^b \phi_y^b] \right\} \quad (24)$$

Again by series expansion of $\sum_{\alpha''} \ln G^{\alpha''}(z|z')$ and collecting only the leading terms, the isotropic SCF equation $-\sum_i \theta_i^{\sigma} / r_i$ remains, where $\theta_i^{\sigma} = \sum_z (\phi_i(z) - \phi_i^b)$ is the excess amount of segments of molecule type i in the system.

Segment density profiles

In order to obtain segment density profiles from the weighting factor profiles, without the evaluation of equation (18) for each conformation, a recurrence procedure will now be discussed. The rotational isomeric state scheme is performed in a tetrahedral lattice for which $Z = 4$. Each lattice site has four bonds with neighbouring sites, in spatial orientations e'' , f'' , g'' , and h'' , respectively. If a site has bonds in directions e , f , g , and h , then the neighbouring sites must have neighbours in directions e' , f' , g' , and h' , respectively. Consequently, a walk through the lattice, consisting of steps from one lattice site to the other, alternates between directions indicated with and without primes. We define e and h' as directions from z to $z-1$, h and e' as directions from z to $z+1$ and f'' and g'' as orientations in a layer. The symbols α'' , β'' and γ'' are used to indicate arbitrary orientations in the lattice. We assign an orientation to each segment in the chain; it is determined by its bond directions: bond number 1 (pointing to lower ranking number) and bond number 2 (pointing to higher ranking number). As there are 12 bond combinations $\alpha\beta$ and 12 combinations $\alpha'\beta'$, there are in total 24 different segment orientations in the lattice. The RIS scheme is a three-choice propagation scheme. A bond in orientation e'' is succeeded by a bond in either f'' , g'' , or h'' orientation. If a third bond is again in the e'' orientation the sequence of three bonds is a trans configuration and the other two possible orientations of the third bond to the two gauche configurations. The RIS scheme is conveniently written in terms of a recurrence relation which mathematically expresses the physical process of adding extra segments to a string which is already $s-1$ segments long. Let us define a chain end

distribution function $G(z, s_1^{\alpha\beta})$ which gives the statistical weight of finding segment s in layer z with bond 1 of segment s in direction α connected to segment s' of the other $s-1$ segments, while bond 2 will be connected in direction β to the next segment. As free (disconnected) segments have no preferential orientations, $G(z, s^{\alpha\beta}) = G(z, s)$ for all of the 24 possible orientations $\alpha\beta$. The chain end distribution function is given by:

$$G(z, s_1^{\alpha\beta}) = G(z, s^{\alpha\beta}) G^{\alpha''}(z||z') \sum_{\gamma'} \lambda^{\gamma''-\alpha''-\beta''} G(z', s_1^{\gamma'\alpha'}) \quad (25)$$

Note that, because the very first segment has a free bond 1 so that $G(z, 1_1^{\alpha\beta}) = G(z, 1^{\alpha\beta})$, all chain end distribution functions are found after $r-1$ operations as given by equation (25), provided that the free segment distribution functions $G(z, s)$ and $G^{\alpha''}(z||z')$ are known. In equation (25) $\gamma''-\alpha''-\beta''$ is a sequence of bond orientations, which forms either a trans or a gauche configuration. Thus, $\lambda^{\alpha''-\beta''-\gamma''} = \lambda^t$ if $\alpha'' = \gamma''$ and $= \lambda^g$ otherwise. Alternatively, the procedure of generating chain end distribution functions can be started at the other chain end, in which case the equivalent of equation (25) reads:

$$G(z, s_2^{\alpha\beta}) = G(z, s^{\alpha\beta}) G^{\beta''}(z||z') \sum_{\gamma'} \lambda^{\alpha''-\beta''-\gamma''} G(z', s_2^{\beta'\gamma'})$$

As usual, the segment density profiles follow from the chain end distribution functions by a composition formula:

$$\phi(z, s_{12}^{\alpha\beta}) = C \lambda^{\alpha\beta} G(z, s_1^{\alpha\beta}) G(z, s_2^{\alpha\beta}) / G(z, s^{\alpha\beta}) \quad (26)$$

where C is a normalisation constant which is discussed above, see equations (22) and (23), and $\lambda^{\alpha\beta}$ ($= 1/24$) is the a priori fraction of segments in orientation $\alpha\beta$. The weighting factor for a chain of r segments in the system, as necessary in equation (20), is $G(r_1) = \sum_z \sum_{\alpha} \sum_{\beta} \lambda^{\alpha\beta} G(z, r_1^{\alpha\beta})$. When a summation over both α and β are performed in equation (26) the segment density profiles are found. From equation (26) we can select all segments which have bond 1 in orientation α'' :

$$\phi^{\alpha''}(z||z') = \sum_{s=2}^r \left\{ \sum_{\beta} \phi(z, s_{12}^{\alpha\beta}) + \phi(z', s_{12}^{\alpha'\beta'}) \right\} \quad (27)$$

Order parameters

Segment order parameters are defined as

$$S(s) = \left\langle \frac{3}{2} \cos^2(\phi(s)) - \frac{1}{2} \right\rangle \quad (28)$$

In equation (28) the angular brackets indicate an ensemble average and $\phi(s)$ is the angle between the orientation of segment s and the normal of the membrane. In our tetrahedral lattice $\cos^2(\phi(s))$ has only three possible values. Segment orientations e" h" and h" e" are parallel to the bilayer normal so that $\cos^2(\phi^{e" h"})$ and $\cos^2(\phi^{h" e"})$ are unity. Segments in orientations f" g" and g" f" are perpendicular to the bilayer normal and thus $\cos^2(\phi^{f" g"}) = \cos^2(\phi^{g" f"}) = 0$, while segment orientations e" f", f" e", e" g", g" e", h" f", f" h", h" g", and g" h" have an angle of 60 degrees with respect to the normal with $\cos^2(\phi^{\delta" \gamma"}) = \frac{1}{4}$. The order parameter is conveniently calculated as

$$S(s) = \frac{\frac{3}{2} \sum_z \sum_{\alpha'' \beta''} \phi(z, s_{12}^{\alpha'' \beta''}) \cos^2(\phi^{\alpha'' \beta''})}{\sum_z \phi(z, s_{12})} - \frac{1}{2} \quad (29)$$

Thus, if the probability of finding all segments in orientation e" h" or h" e" is 1, the order parameter is 1. On the other hand, when all bonds are parallel to the bilayer, the order parameter is -0.5. A random bond distribution will result in an order parameter $S(s) = 0$.

End segments do not have two bonds, and therefore their orientation is fully determined by the direction of the last bond. Equation (29) can be used for these segments when we assume that the free bond is randomly distributed over the three optional directions. As a consequence the order parameter of an end segment is between -0.25 (last bond in f" or g" orientation) and 0.25 (last bond in e" or h" orientation).

Computational aspects

From an initial guess for the $G_x(z)$ and $G^{\alpha''}(z||z')$ weighting factors, segment densities $\phi_x(z)$ and bond orientation profiles $\phi^{\alpha''}(z||z')$ can be calculated. With these profiles and an initial guess for the M variables $u^i(z)$ the values of the weighting factors and the boundary conditions $\sum_x \phi_x(z) = 1$ can be checked. An implicit set of simultaneous equations results, which can be solved by standard numerical techniques [14].

Near $z = 1$ and $z = M$ reflecting boundaries are introduced, so that weighting factors and segment densities in layer $z = 0$ are exactly identical the same quantities in layer $z = 1$. At one of the boundary layers ($z = 1$) we initiate the bilayer (by an appropriate guess of the weighting factor profile), so that with a proper choice of interaction parameters, an equilibrium membrane is formed with the boundary layer as its centre. This has the effect that the membranes are symmetrical. Together with a reflecting boundary between layers $z = M$ and $z = M+1$ the centre to centre membrane-membrane distance is $2M$. For details of the reflecting boundaries we refer to reference [14].

As we showed before, free membranes have a vanishing excess free energy per surface area, or equivalently, a vanishing surface tension. For a given number of molecules per unit of surface area the excess free energy of the membrane is evaluated with equation (24). An extra iteration is started to find the number of molecules per unit of surface area for which $A^\sigma = 0$ and $\partial A^\sigma / \partial \theta < 0$. For membranes in a frame this extra iteration is not performed, because these membranes cannot adapt their surface area. In such a case, either the equilibrium concentration or the number of molecules per surface area must be given to determine the normalisation constant C from equations (22) or (23), respectively.

Results and discussion

In the following we will first discuss some additional approximations that we have used to simplify the calculations. Subsequently, we will pay some attention to the choices of our energy parameters. Finally, results will be given for both singular and interacting membranes composed of lecithine-like molecules.

Some simplifications

In order to simplify the calculations, we have assumed that the number of bonds in orientations f'' and g'' are always equal. This is probably not a severe limitation, because in the liquid phase this will be the case anyway and in the gel phase there will be only a very few bonds oriented parallel to the bilayer, so that no preference between f'' and g'' orientations will develop. For the e'' and h'' orientations we applied a slightly different approximation. In the derivation of the partition function we treated each orientation separately. We assumed that two different orientations would only

influence each other randomly. However, this is only the case when these orientations are perpendicular. Here we will treat the e" and h" orientations as parallel. This has the consequence that they stimulate each other strongly and that the number of bonds in these orientations are equal.

Mathematically, these approximations are summarised as follows. Instead of equation (26) we use for orientations g":

$$\phi(z, s_{12}^{g''\alpha''}) = \phi(z, s_{12}^{f''\alpha''}) \quad \text{and} \quad \phi(z, s_{12}^{\alpha''g''}) = \phi(z, s_{12}^{\alpha''f''}) \quad (26a)$$

and instead of equation (27) we use for orientations e" and h":

$$\phi^{e''}(z|z') = \phi^{h''}(z|z') = \sum_{s=2}^r \sum_{\alpha=e,h} \sum_{\beta} \{ \phi(z, s_{12}^{\alpha\beta}) + \phi(z', s_{12}^{\alpha'\beta'}) \} \quad (27a)$$

The result is that we need only orientations e" and f" in our calculations, because orientations g" and h" are numerically equivalent with f" and e", respectively.

Energy parameters

The present paper will focus on lecithin-like molecules (denoted by $i = 2$) with the following architecture:



where p is the number of apolar segments in the two tails, q the number of polar segments in the head group. The glycerol backbone is mimicked by a branched structure with two polar (B) segments and three apolar (A) segments. In the present analysis, we only distinguish between polar and apolar groups. The volume of a CH₃ is set equal to the volume of a CH₂. The statistics of branched chains has been reported elsewhere [14]. The solvent ($i = 1$) is modelled as a monomer without structure and is referred to as water (W). The three types of segments in the system give rise to three FH interaction energy parameters. At T = 300 K we choose $\chi_{AW} = 1.6$, $\chi_{BW} = -0.3$, and $\chi_{AB} = 1.5$. For the gauche-trans energy the value of $U^g = 1$ kT at T = 275 K is used. All energy parameters are expected to be inversely proportional to the absolute temperature. The present set of energy parameters was found by comparison of

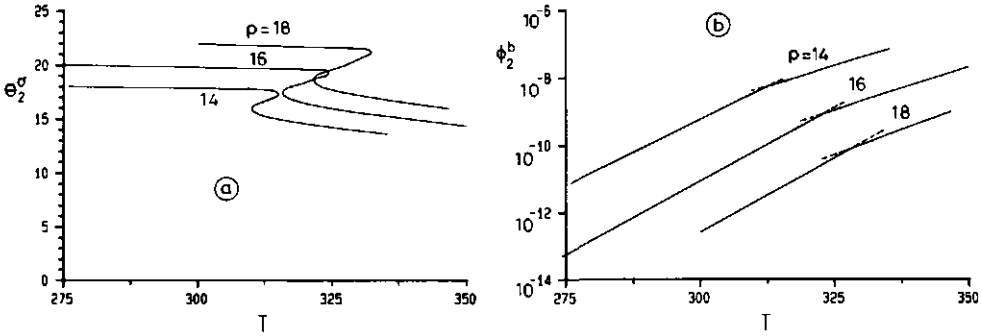


Figure 2.

(a) Excess amount of lipids aggregated, $\theta_2^\sigma = \int_z (\phi_2(z) - \phi_2^b)$, and (b) equilibrium lipid concentration, as a function of the absolute temperature for membranes composed of lecithin-like molecules with a head group of $q = 3$ polar segments and $p = 14$, $p = 16$, and $p = 18$ apolar segments per tail, respectively. The interaction parameters (at 300 K) are: $U^g = 275/300$ kT, $\chi_{AW} = 1.6$, $\chi_{BW} = -0.3$, $\chi_{AB} = 1.5$.

known CMC data of surfactants with calculated ones [16]. This set was also shown to give a satisfactory membrane behaviour [14]. The χ_{AB} parameter promotes the separation between polar and apolar segments and thus contributes to the stability of the membrane system. It can be argued, that the present SCAF theory needs a slightly different choice of these parameters because of the difference with respect to the SCF theory.

Unless stated otherwise, all membrane structures shown below, even the membranes interacting with each other, are equilibrium membranes without any surface tension (vanishing excess free energy A^σ per unit surface area).

Non-interacting membranes

Figure (2) gives information excess amount of lipids per unit of area which is a measure of the membrane thickness and the equilibrium lipid concentration in the bulk solution as a function of the temperature for three homologous lecithins, i.e., $p = 14$, $p = 16$, and $p = 18$ segments per tail. The "loop" in figure (2a), which is more pronounced for longer tails is characteristic for a first order phase transition. The longer the tails, the more pronounced the co-operativity of the transition is. Above the phase transition temperature the membrane thickness increases gradually with

decreasing temperature, but below the transition the system is frozen and does not permit significant structural changes. In figure (2b) we see that at the phase transition the slope of $\log \phi_2^b$ with temperature changes abruptly. This is also found experimentally [23]. As to the tail length dependence we observe an increase in the phase transition temperature of about 4 degrees per segment. In practical systems often a stronger temperature dependence is found. One of the reasons for the difference may be that our energy parameters actually represent free energy parameters and thus should be less dependent on $1/T$ than assumed.

The "loops" shown in figure (2a) are asymmetric. The lower bend is wider than the upper one. This is due to the higher density, hence lower compressibility, in the gel phase compared to that in the liquid phase.

We will study this transition in more detail, taking the $p = 16$ $q = 3$ lecithin molecule as a characteristic example. Figure (3a) gives a liquid membrane at $T = 325$ K, and figure (3b) a gel membrane at $T = 315$ K. There are several differences between the two membranes. With respect to the liquid membrane, the density of the tails in the gel phase is about 7% higher. The centre of the gel membrane is completely filled with tails. Water molecules penetrate the membrane only as far as the glycerol backbones, whereas in the liquid membrane also some water is present in the tail region. We believe that, in the present calculations, the amount of solvent in the liquid

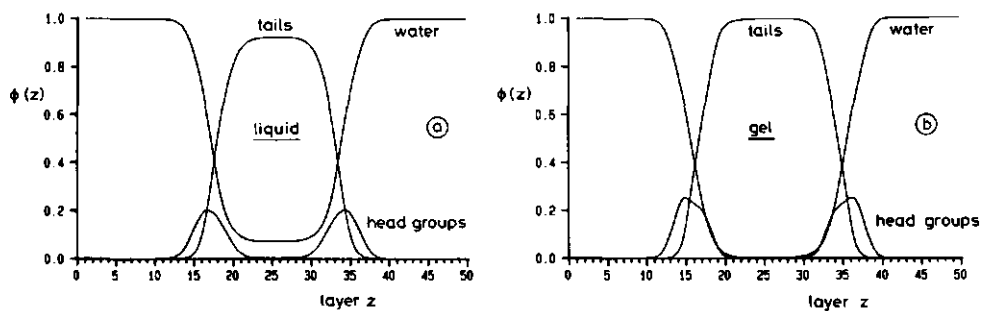


Figure 3.

Segment density profiles through a cross section of a membrane composed of lecithin-like molecules $p = 16$, $q = 3$ in the liquid state (a) at $T = 325$ K and in the gel state (b) at $T = 315$ K. Layers are arbitrarily numbered. Interaction parameters as in figure (2).

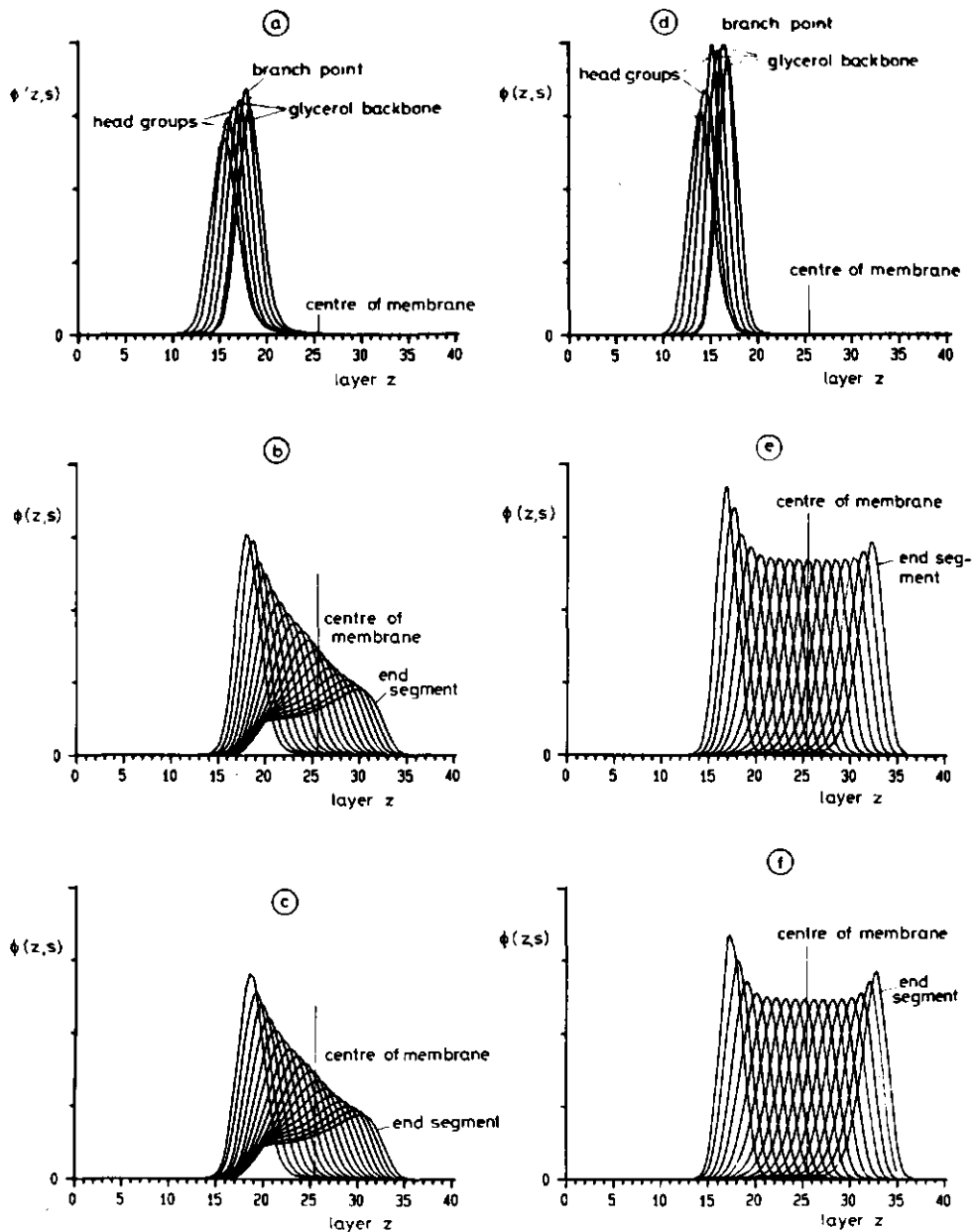


Figure 4.

Individual segment density profiles of molecules with their branch point at the left hand side of the membrane of figure (3), i.e., between layer $z = 1$ and $z = 25$. Left hand side: liquid state, right hand side: gel state. a) and d): head groups and glycerol backbone. b) and e): first tail, next to head group. c) and f): second tail at end of glycerol backbone. The centre of the membrane is indicated.

membranes is somewhat overestimated. This is due to the rather crude modelling of the water molecules (unpolarisable monomers not able to form H-bonds). In addition to this, more realistic calculations would require accounting of free volume in the system. The tendency of the system to have a low chain density in the liquid phase is presently only feasible by allowing water molecules in the membrane. Both the incorporation of free volume and the development of a more advanced theory for the water phase, are left for future work.

We now examine the gel and the liquid membranes of figure (3) in more detail. In figure (4) the individual segment density profiles are given of molecules which have their branch point somewhere in the layers $z = 1, \dots, 25$, hence on the left hand side of the membrane. See reference [1] for more details on the computational aspects of calculating special segment distributions. The density profiles of all those molecules which have their branch point on the other side of the membrane are just mirror images of the given profiles. (The centre of the membrane is between layers 25 and 26.) The graphs on the left hand side (a, b, c) represent the liquid state, whereas in the graphs on the right hand side (d, e, f) the gel state is illustrated. As can be seen in figure (4), the closer to the branch point the more narrow and dense the segment distribution is. This is not very surprising, as the branch points connect tails and head groups which hardly mix. Closer inspection of figures (4b) and (4c) reveals that the tail closest to the head group (4b) is lifted out by about half a layer with respect to the other tail. This is also found in experimental NMR work [24,25]. The average difference in position of the two tail ends is less, but still 0.2 layers. In the gel phase (see graphs d, e, f) near the glycerol backbone this difference in position is about the same (0.54 layers) as in the liquid membrane, but the difference remains so all along the tails. The two end segments are still 0.5 layers apart. This is caused by the fact that in the gel phase the two tails are in all-trans conformations. Both in the gel and in the liquid membrane the tail ends cross the centre of the membrane considerably. In the gel phase the tail ends reach as far as near the glycerol backbone at the opposite side. This enables the tail ends to have a little more space to occasionally form a gauche bond which is entropically favourable. Therefore, for the very end of the tails again some disorder is found (see also figure (5)).

In the liquid phase, at $T = 325$ K, the lipid molecules have on average 20 trans bonds, whereas in the gel phase 28.2 trans bonds are observed. The energy gain upon solidification is 7.5 kT per lipid molecule. As the packing

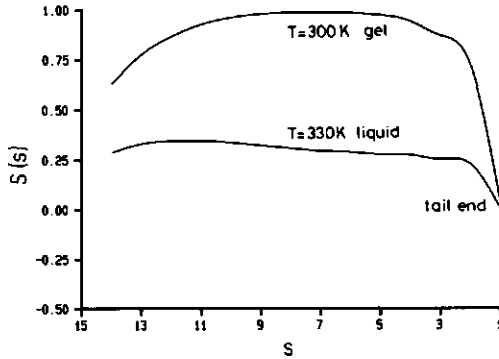


Figure 5.

Segment order parameters of the tail at the end of the glycerol backbone for lecithin-like molecules with $p = 14$ and $q = 3$, for a liquid membrane at $T = 330$ K and a gel membrane at $T = 300$ K. Segment 1 is the end segment of the tail, segment number 14 is the segment attached to the glycerol backbone.

of the tails is more condensed in the gel phase, also a change in contact energy can be expected. Not only the density of the tail region, but also the head group density is higher. As a consequence, the total contact energy changes from 41 kT per molecule (with respect to the reference state) for the liquid membrane to a more unfavourable 46.6 kT in the gel membrane. Thus we find a net gain in energy of about 2 kT per molecule. In calorimetric experiments often 6-10 kT are reported for the main gel to liquid phase transition [3]. This agreement is a very promising, considering the many mutually compensating effects, the crude modelling of water molecules, and the neglect of free volume in the system.

The main emphasis of this paper is to study the apolar region of the bilayer rather than the polar head group region. We show order parameters for the apolar tails only. In figure (5) we give the order parameter profile of the segments in the tail most remote from the head group, for a lecithin-like molecule with $p = 14$. The order parameters of the other tail are not significantly different from the ones given in figure (5). Both for the gel (at $T = 300$ K) and the liquid membrane (at $T = 330$ K) the segment order parameters are fairly constant. In the gel phase the order parameter is almost 1.0, the maximum value, whereas in the liquid membrane the maximum of the order parameter is about 0.34. Near the tail ends the order is slightly less

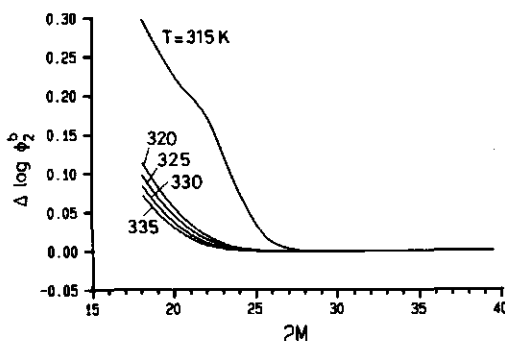


Figure 6.

Interaction between two bilayers below ($T = 315$ K), and above the phase transition temperature ($T = 320$ K, $T = 325$ K, $T = 330$ K, and $T = 335$ K). The relative change in equilibrium volume fraction of the lipids is given as a function of the distance between the two bilayers.

($S(2) = 0.23$). Even in the gel phase the tails are not fully in all trans states. Especially the tail ends may assume gauche configurations. The order parameter of the last segment of the tail ($s = 1$) is very low because the free bond has a random orientation.

Interacting membranes

To investigate whether the present phase transition represents thermodynamically stable membrane systems, it is checked whether membranes are attractive or repulsive. Figure (6) gives $\Delta \log (\phi_2^b)$ which is the difference $(\log \phi_2^b)_{2M} - (\log \phi_2^b)_{2M \rightarrow \infty}$, as a function of the distance between the two centres of the membranes ($2M$). Again the lecithin-like molecules with $p = 16$ are considered. When the membranes approach each other, they are allowed to modify their surface area and equilibrium concentration to relax any induced surface tension. Therefore, the free energy of the system is $\sum_i \mu_i n_i$ and $\Delta \log \phi_2^b$ is a qualitative measure of the interaction energy per lipid molecule. As can be seen, the equilibrium volume fraction increases when the membranes come closer to each other, indicating a repulsion between them. Liquid membranes are thinner than gel membranes, so that their interaction starts at shorter distances. As expected, the more rigid gel membranes are more repulsive than the liquid membranes.

The interaction between bilayers as given in figure (6) originates from the free energy of mixing only. Long range forces, which are expected to be different for the gel and the liquid membranes are not included in the present model. The gel membrane has a higher density of lipids than the liquid membrane and therefore the Van der Waals attraction must be stronger for the gel than the liquid membranes. This can give rise to a local energy minimum in the interaction curves especially for the gel phase. In addition, we expect for the gel membranes less steric repulsion from undulations. Both arguments suggest that, with decreasing temperature, at the phase transition a change from a repulsive to a more attractive system is likely. A full analysis of the membrane-membrane interaction is beyond the scope of the present work.

In concentrated membrane systems membrane-membrane interaction is one of the most important physical factors which must be taken into account. For the gel phase this interaction is illustrated in figure (7). In figure (7a) the excess free energy is given as a function of θ_2^σ , the excess number of segments per surface site for various membrane-membrane distances ($2M$). Note that the value for θ_2^σ cannot exceed $2M$. The excess free energy is found to be zero for at least two values of θ_2^σ . The one at $\theta_2^\sigma \approx 20$ is a thermodynamically stable solution. The second point is unstable because at this point $\partial A^\sigma / \partial \theta_2^\sigma > 0$ and

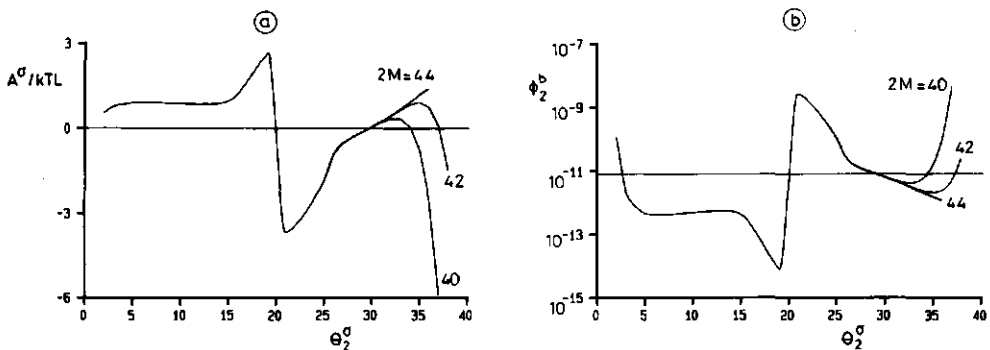


Figure 7.

The excess free energy per surface site (a) and the equilibrium volume fraction (b) as a function of the excess amount of lecithin molecules per surface site for three membrane-membrane distances ($2M = 40, 42,$ and 44 lattice layers). The lecithin molecules identical to those in figure (3) at a temperature of $T = 300$ K (gel state).

the total free energy of the system is at a (local) maximum. For larger θ_2^σ too many molecules are accommodated in the membrane and, as a consequence, it splits up into two separate membranes so that the membrane distance is arbitrary (thus the curve ends). Decreasing the distance between two membranes ($2M$) has no effect when the membranes are thin, i.e., at small θ_2^σ values. Only for very thick membranes the division into two thin ones is blocked, due to the membrane-membrane interaction. In this situation there appears a new point for which the excess free energy is zero, i.e., where the membrane system is again thermodynamically stable. We call these (interacting) membranes stacked or, referring to their structure, spliced bilayers in contrast to the (non-interacting) intercalated bilayers.

Figure (7b) shows how the logarithm of the equilibrium lipid concentration depends on θ_2^σ for the same systems. In agreement with Gibbs' law, variations in chemical potential and excess free energy have opposite signs. The equilibrium concentration for the stacked gel phase is higher than for the non-interacting gel phase. In figure (6), the (intercalated) gel membranes showed a strong increase in chemical potential when they were forced to interact with each other. At the same overall lipid concentration, the spliced bilayers may be more favourable than the intercalated ones. This can be understood by realising that the (thin) intercalated bilayers create more polar-apolar interfaces in the system than the (thick) spliced bilayers.

In figure (8) the stacked membranes are analysed for a constant overall lipid concentration at three different temperatures $T = 260$ K (8a), $T = 275$ K (8b), and $T = 290$ K (8c). As expected, the membranes are much thicker than the non-interacting gel bilayers. These membranes are characterised by a dip in the tail density in the centre of the membrane. This deficit of tail segments is compensated by an excess of solvent molecules and a few head groups in this region. With decreasing temperatures, the dip becomes less pronounced and eventually vanishes. As a consequence, the membrane thickness decreases with decreasing temperature. Such a decrease in membrane thickness is often reported in literature and is usually explained by a gradual pre-transition where the tails start to tilt into given angles. Since in the present approach we have not allowed for co-operative tilt, the decrease in membrane thickness in figure (8) originates from the increase in chain density in the centre. We cannot exclude that a tilt process would occur if we would not have made the simplifications as mentioned at the beginning of this section, i.e., if we would have treated all bond orientations separately.

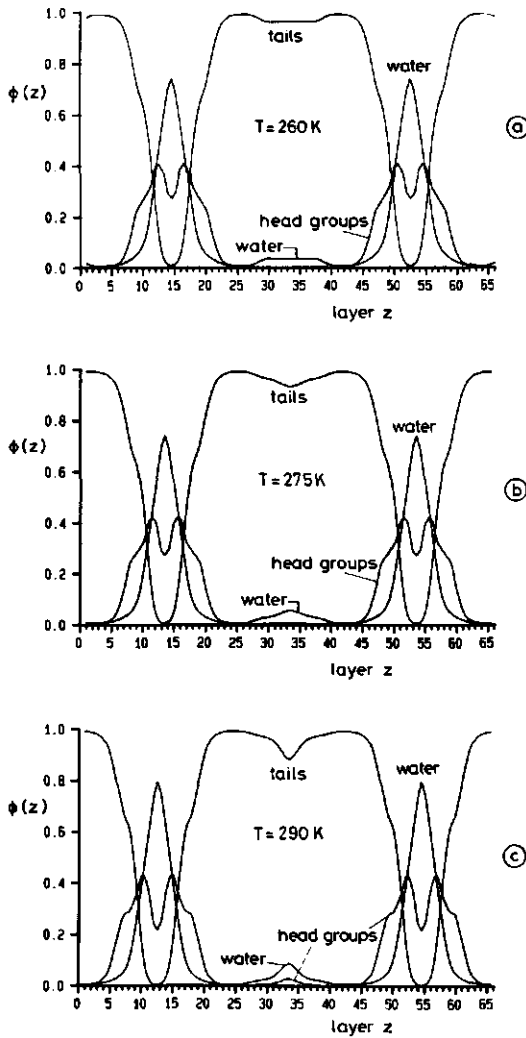


Figure 8.

Segment density profiles of cross sections through stacked membranes composed of the lecithin molecules given in figure (3) at a lipid fraction of $\bar{\phi}_2 = 0.89$ for three different temperatures. a) $T = 260$ K, $2M = 38$; b) $T = 275$ K, $2M = 40$; c) $T = 290$, $2M = 42$. We have plotted one membrane with part of its neighbouring membranes. Layers are numbered arbitrarily.

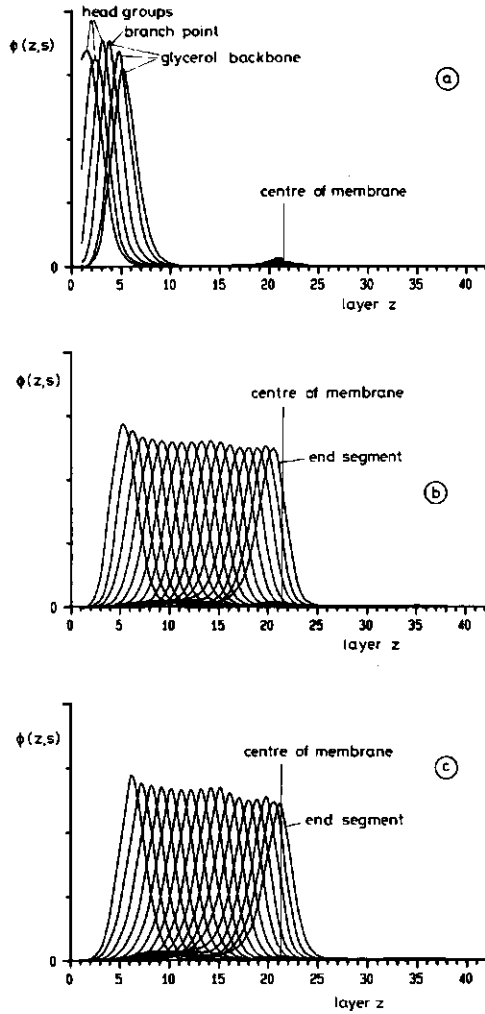


Figure 9.

Individual segment density profiles of lipids with their branch points at the left hand side of the membrane given in figure (8c) (i.e., between layers 1 and 21). a) Head groups and glycerol backbone, b) tail closest to the head group, c) tail at the end of the glycerol backbone.

The individual segment density profiles of the spliced membrane at $T = 290$ K are given in figure (9). In line with expectations, in this case only a few tail segments cross the centre of the membrane occasionally. In the intercalated membrane we found that the positions of the two tails were mutually shifted by half a lattice layer. In figure (9) this shift is one lattice layer.

Conclusions

In this paper we showed that it is possible to obtain much detailed information on lipid membrane systems with the help of an *ab initio* statistical thermodynamical theory. Besides nearest neighbour contact energies, the theory takes into account the anisotropic interaction between the molecules. With this extension co-operative phenomena like order to disorder phase transitions are reproduced. We showed that in a bilayer of model lecithin-like molecules a first order gel to liquid phase transition takes place with increasing temperature. An enthalpy jump of about $2 kT$ per molecule is found. Two types of gel phases are observed: in the dilute regime the bilayer tails are intercalated, whereas in a concentrated regime the membrane is spliced into two almost non-overlapping lipid layers. For both types of gel membranes the tails have a very high degree of order (almost all-trans). The liquid membrane shows a weaker but still significant ordering. This implies that even in the centre of the membrane the segments "feel" that they are attached to the head group. The order parameter profiles show a plateau over the entire tail. Only the tail ends have a lower order. Segment density profiles show that in all cases the tails cross the centre of the membrane, even in spliced membranes. Although the tails are in an all trans conformation, there is a considerable spread in positions for the various segments. The chain density in the gel membranes is found to be about 7% higher than in the liquid membrane.

With respect to the results of our previous theory the present results show much more order in the bilayer. The extremely high segment density in the bilayer is responsible for this order, because at these high densities tails cannot choose their own orientations at random but are "pushed" by neighbouring molecules in a given direction.

We believe that the results of the present theory holds promises for the possibilities to develop an all-round membrane theory based on statistical thermodynamics. The theory can also be used to study crystallisation phenomena in polymer solutions.

Appendix A. Modified Flory-Huggins theory

The Flory-Huggins (FH) theory applies to homogeneous systems where no segment density gradients are present. This corresponds to our bulk solution, and in fact it can be shown that our partition function reduces to that in the FH theory for a homogeneous system. The FH theory can therefore be used to find expressions for the chemical potential. However, consistent expressions for the chemical potential are only found if the FH theory is corrected for the fact that a step in a given direction cannot be blocked by other segment-segment bonds in the same direction.

When no preferential orientation of the system takes place, the population of all bond directions is homogeneous, and the resulting correction factors are the same for every bond direction. Following similar arguments as shown above for the general case where inhomogeneities in the z directions were allowed, the resulting partition function for the case that these inhomogeneities are not present (also with respect to the amorphous reference state) is given by:

$$\begin{aligned}
 -\ln \frac{Q(n_i, V, T)}{Q^*} &= -\ln \frac{\Omega(n_i, V, U)}{\Omega^*} + (U(\text{int}) - U^*(\text{int}))/kT = \sum_i n_i \ln \phi_i \\
 &- \sum_{\alpha''} \{ (V - n\alpha'') \ln (V - n\alpha'') - (V - n\alpha'') - V \ln V + V \} - \sum_i n_i (r_i - 1) \ln V \\
 &+ \sum_i \sum_{\alpha''} \{ (n_i r_i - n_i^{\alpha''*}) \ln (n_i r_i - n_i^{\alpha''*}) - (n_i r_i - n_i^{\alpha''*}) - n_i r_i \ln n_i r_i + n_i r_i \} \\
 &+ \sum_i n_i (r_i - 1) \ln(n_i r_i) + \frac{1}{2} \sum_i \sum_x \sum_y n_{xi} \chi_{xy} (\phi_y - \phi_{yi}^*) \tag{A1}
 \end{aligned}$$

The correspondence with equations (2) and (10) is easily verified, realising that each conformation c is equally probable and that the number of gauche bonds of a chain is the same in the bulk and in the reference phase.

Differentiating equation (A1) with respect to n_i results in the chemical potential of molecule i. As $V = \sum_i n_i r_i$,

$$\begin{aligned}
 (\mu_i - \mu_i^*)/kT &= \ln \phi_i^b - \sum_{\alpha''} \{ (r_i - r_i^{\alpha''}) \ln(1 - \phi^{\alpha''b}) + (r_i - r_i^{\alpha''*}) \ln(1 - \phi_i^{\alpha''*}) \} \\
 &+ \frac{1}{2} r_i \sum_x \sum_y [\chi_{xy} (\phi_{xi}^* - \phi_x^b) (\phi_y^b - \phi_{yi}^*)] \tag{A2}
 \end{aligned}$$

A subindex i refers to a property of molecule type i, whereas if i is not specified a summation over all molecules i is assumed. By series expansion of

the second and third logarithmic terms and leaving out all square and higher order terms, the Flory-Huggins equations are recovered.

Literature

1. F.A.M. Leermakers, J.M.H.M. Scheutjens, and J. Lyklema; *Biophys. Chem.* **19** (1983) 353.
2. J. Seelig, and A. Seelig; *Quarterly Reviews of Biophys.* **13** (1980) 19.
3. C. Gabrielle-Madellmont, and R. Perron; *J. Coll. Int. Sci.* **95** (1983) 471.
4. J.F. Nagle; *Ann. Rev. Phys. Chem.* **31** (1980) 157.
5. G.M. Bell, L.L. Combs, and L.J. Dunne; *Chem. Rev.* **81** (1981) 15.
6. H.L. Scott; *J. Chem. Phys.* **62** (1985) 1347.
7. R.K.R. Blinc, et al.; *Am. Phys. Soc.* **26** (1982) 1816.
8. T.J. McIntosh, R.v. McDaniel, and S.A. Simon; *Biochem. Biophys. Acta* **731** (1983) 109.
9. L.F. Braganza, and D.L. Worcester; *Biochemistry* **25** (1986) 2591.
10. M.J. Janiak, D.M. Small, and G.G. Shipley; *Biochemistry* **15** (1976) 4575.
11. J.F. Nagle; *J. Chem. Phys.* **58** (1973) 253.
12. R.G. Priest; *J. Chem. Phys.* **66** (1977) 722.
13. D. March; *J. Membr. Biol.* **18** (1974) 145.
14. F.A.M. Leermakers; PhD thesis, Wageningen (1988) chapter 2.
15. J.M.H.M. Scheutjens, F.A.M. Leermakers, N.A.M. Besseling, and J. Lyklema; in: "Surfactants in Solution. Modern Applications", (Mittal K.L. Ed.) in press.
16. F.A.M. Leermakers, P.P.A.M. van der Schoot, J.M.H.M. Scheutjens, and J. Lyklema; in: "Surfactants in Solution. Modern Applications", (Mittal K.L. Ed.) in press.
17. J.M.H.M. Scheutjens, and G.J. Fleer; *J. Phys. Chem.* **83** (1979) 1619.
18. P.J. Flory; *Proc. Roy. Soc. (London)* **A234** (1956) 73.
19. E.A. Di Marzio; *J. Chem. Phys.* **35** (1961) 658.
20. E.A. Di Marzio; *J. Chem. Phys.* **66** (1977) 1160.
21. P.P.A.M. v.d. Schoot; NBSIR 86-3466 (1986).
22. P.J. Flory; "Principles of polymer chemistry", Cornell University Press, Ithaca, NY (1953).
23. N.L. Gershfeld, W.F. Stevens Jr., and R.J. Nossal; *J. Chem. Soc., Faraday Disc.* **81** (1986).
24. A.Seelig, and J. Seelig; *Biochem. Biophys. Acta* **407** (1975) 1.
25. J. Seelig, and J.L. Browning; *FEBS Lett.* **92** (1978) 41.
26. M.J. Janiak, B.M. Small, G.G. Shipley; *Biochemistry* **15** (1976) 4575.

CHAPTER 5

INHOMOGENEOUS MEMBRANE SYSTEMS

Abstract

Recently, we introduced a Self-Consistent Field lattice theory to model the lipid bilayer membrane [1,2]. In this theory inhomogeneities in layers parallel to the membrane were neglected. In the present paper we extend our work to account for tangential inhomogeneities along the bilayer. For this, we develop a modified Markov approach for generating the conformations of the chain molecules, which accounts for segment density gradients in two directions. In the remaining dimension a mean field approximation is applied.

The new theory is suitable for studying the interaction between a big copolymer molecule ("protein") with the lipid bilayer. We will give two examples of trans-membrane copolymer interactions. The boundary layer of lipids between the membrane and the polymer molecules is found to depend strongly on the interactions between apolar segments of the copolymer and apolar segments of the lipid molecules.

We also studied lateral phase separation between two nonmixing lipid molecules in the membrane. Water only slightly enriches the boundary between the two lipid regions. The aliphatic chains are very well able to smoothly cover inhomogeneities in the bilayer. No indications of instability of the membrane due to the induced inhomogeneities are found.

Introduction

To understand all properties of biological membranes, knowledge about the membrane-protein interactions is essential. Although these systems are highly complex in nature, we believe that it must be possible to improve our understanding from merely intuitive towards insight based on molecular interactions. Although the present model will not yet take all specific interactions into account, the results give at least some insight into the subtle energy balances which are responsible for the high diversity of membrane systems.

Since Singer and Nicolson proposed their fluid mosaic model of the biological membrane [3], membrane research has been moving towards the study

of the membrane-protein interactions. This generally accepted model explains many of the properties found for biological membranes, but does not give detailed insight on a molecular level.

To the authors' knowledge no full computational analyses of the complex membrane-protein interactions are available. Neither Monte Carlo nor Molecular Dynamic techniques can take the conformational freedom of both the protein and the lipid molecules into account at the same time. This is due to the extremely large computer time needed to solve the problem rigorously. At present only Statistical Mechanical, based on a self-consistent field, techniques must be considered applicable to give information on these matters. In the following part we will discuss a first approach of a theory designed for this goal.

Theory

A well-known theory for the study of polymers in solution is due to Flory and Huggins (FH) [4]. This theory makes use of a lattice on which the polymer chain segments are placed using a first order Markov approximation. This means that a random walk approximation is applied in which the "history" of the chain is only one step (segment) long. Backfolding to previously occupied lattice sites is allowed. Further, a mean field approximation over the whole homogeneous system volume is used. This is illustrated in figure (1a). With these two approximations the partition function of a collection of chains on the lattice can be worked out analytically.

Recently, Scheutjens and Fleer (SF) extended the FH approach, and proposed a statistical mechanical model for homopolymer adsorption [5,6]. This theory has been extended to describe amphiphatic molecules in inhomogeneous systems [1]. The SF approach makes use of a modified Markov statistics in which inhomogeneities in one dimension are accounted for but where the mean field approximation in two dimensions over lattice layers is maintained (see figure (1b)). The partition function for these systems can no longer be solved analytically. Instead, the problem is reduced to a set of implicit equations which can be solved with standard numerical techniques. In this respect the SF-theory may be called "one-dimensional". One of the advantages of this approach is that the computation times are only linearly proportional to the chain length of the polymer. Because of this low dependence of computation time on chain length, there are in this respect no problems to extend the theory to include an arbitrary number of different types of molecules.

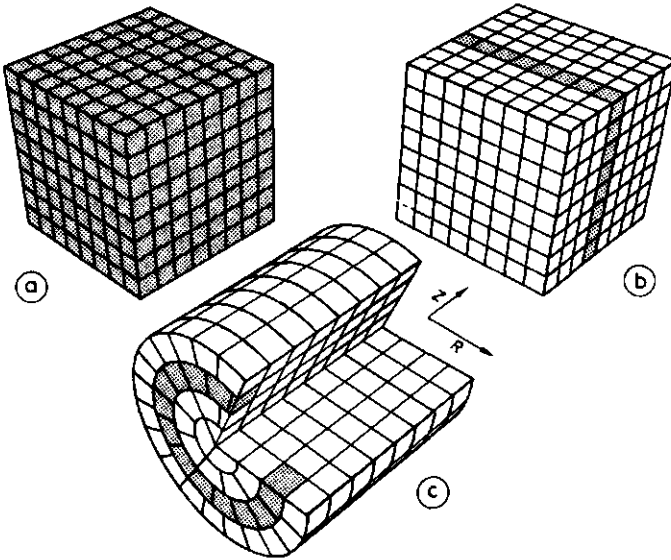


Figure 1.

Lattices used for: a) FH theory, b) SF theory, c) 2D SF theory. The mean field approximation is performed over the whole space, lattice layers, and lattice circles, respectively.

Another advantage of the great computational efficiency is that a two-dimensional extension of the SF theory is possible. Towards this goal the lattice layers are divided up into concentric equidistant rings. The rings in the various layers form a cylinder and cylindrical co-ordinates are introduced. A similar Markov process applies and the mean field approximation is performed in the individual rings. Then segment density gradients in the normal (z) and the radial direction (R) can be followed. In this way, the one-dimensional SF theory becomes two-dimensional. More specifically, in figure (1c) shows a lattice as used in the 2D SF theory. In figure (1c) around a given point in a flat plane concentric rings are drawn. The flat layers are numbered $z = 1, \dots, M_z$ and the cylinders are numbered $R = 1, \dots, M_R$. At the boundary layers $z = 1$, $z = M_z$ and $R = M_R$ reflecting boundary conditions are introduced. We note that M_z and M_R are preferable chosen large enough, so that no significant influence of the boundaries is expected. In this way a virtually infinitely large system is simulated. The number of lattice sites from the centre in a lattice plane up to a layer R' is:

$$A(R') = \pi R'^2 \quad (1)$$

for each layer z . Hence, the number of lattice sites in a given ring is given by:

$$L(R') = A(R') - A(R'-1) \quad (2)$$

The outer circumference of the ring with outer radius R' is found by differentiation of equation (1):

$$S(R') = 2 \pi R' \quad (3)$$

(in lattice units). For the modified Markov-type statistics we need step probabilities for going from one lattice site to a neighbouring one. We allow a step to go up (to lower z), to go down, or to stay in the layer, and simultaneously a step can go inwards, (to lower R), go outwards, or can stay in the same shell. We will make use of a hexagonal lattice with a coordination number $Z = 12$. (Z is assumed constant throughout the lattice.) The fraction of neighbouring sites in a previous layer in the z direction, $\lambda_{-1}(z) = \frac{1}{2}$ and a fraction of the neighbouring sites in a following layer $\lambda_1(z) = \frac{1}{2}$, leaving for the fraction of neighbouring sites in the layer $\lambda_0(z) = \frac{1}{2}$. These fractions can be considered a priori step probabilities to go from a given site to a neighbouring one, as they do not depend on the local potentials. For a step inwards or outwards the probabilities will depend on R . We choose these step probabilities to be proportional to the circumference the step is crossing:

$$\begin{aligned} \lambda_{-1}(R') &= \frac{1}{2} \frac{S(R'-1)}{L(R')} \\ \lambda_0(R') &= 1 - \lambda_{-1}(R') - \lambda_1(R') \\ \lambda_1(R') &= \frac{1}{2} \frac{S(R')}{L(R')} \end{aligned} \quad (4)$$

Now a step simultaneously going up and inwards will have an a priori probability $\lambda_{-1,-1}(z,R') = \lambda_{-1}(z) \lambda_{-1}(R')$. Similar equations hold for all 8 other possible step directions.

Special attention is required to define the boundary conditions in the system. As stated, reflecting boundary conditions both at layer $z = 1$ and $z =$

M_z are introduced. This is realised by assuming the exactly identical behaviour of layers $z = 0$ and $z = 1$ on the one side of the system, and $z = M_z$ and $z = M_z + 1$ on the other side of the system. For each chain which partially steps out of the system, i.e., crosses the boundary, we expect another chain from outside entering the system along the same boundary. This boundary condition induces a symmetry-plane in the system. The boundary conditions in the R direction are more troublesome. At the centre $R = 0$ no lattice sites are available and the boundary condition is already specified with the step probabilities (no chains can leave the lattice at this side). The boundary between the circles M_R and $M_R + 1$ is less trivial. Again a reflecting boundary condition between those two layers is assumed, i.e., $L(M_R) = L(M_R+1)$ and the a priori step probability to step out of the system at this circle is assumed to be the same as the a priori step probability to enter the lattice. We can expect errors caused by this idealised boundary conditions when density gradients in the R direction are present near M_R . To minimise such artefacts, M_R is preferentially chosen so large that these inhomogeneities are absent. Physically, this corresponds with the assumption that the lateral inhomogeneities are spatially remote from each other. In terms of the membrane-protein interaction, the proteins or the protein clusters in the membrane are very dilute and do not interact with each other.

Chain distributions in two dimensions

The chain molecules consist of segments with ranking numbers $s = 1, \dots, r$. The segments do not necessarily have the same physical properties. Although we will present results for branched lecithin-like molecules, we discuss the distribution of linear chains in the present section. When the chain molecules are branched the statistics which account for this are somewhat more involved [2]. To find the distribution of the chain molecules, the statistical weight of each individual conformation must be known. A conformation of a molecule is defined by the sequence of co-ordinates (z, R) where the consecutive segments are situated. In general, each conformation is degenerate: various spatial configurations can belong to the same conformation.

A step-weighted random walk approximation is used for generating systematically all conformations of the chain molecules on the lattice. In this approximation backfolding to previous occupied lattice sites is allowed. The random walk approximation can be expressed in a recurrence relation, which "enlongates" a chain of s segments long to a chain of $s+1$ segments. Each step

in a random walk is weighed by its a priori step probability $\lambda_{z'-z, R'-R}(z, R)$, but we add to the weighting the local potential field, the segments find themselves in. This last weighting factor (also called free segment distribution function) is, for a given segment s , only a function of the position of the segment in the system: $G(z, R, s)$.

When a segment is in a chain it possesses 2 bonds to neighbouring segments. Bond 1 points towards a segment with lower ranking number and bond 2 points to a segment with higher ranking number. End segments have only one bond. The bonds of segment s are indicated by subscripts. For example, s'_1 indicates that segment s' has only a bond 1, implying that it is an end segment. We define the chain end distribution function $G(z, R, s_1)$ as the weighting factor for segment s in position (z, R) subject to the requirement that bond 1 is connected to other segments of the chain. With this chain end distribution function the recurrence equation can be expressed as:

$$G(z, R, s_1) = G(z, R, s) \sum_{z'} \sum_{R'} \lambda_{z'-z, R'-R}(z, R) G(z', R', s'_1) \quad (5)$$

In this equation segment s is connected with bond 1 to bond 2 of segment s' . Segment s is now the end of the chain. The recurrence relation is initiated at the first segment of the chain and as $G(z, R, 1_1) = G(z, R, 1)$ only the free segment distribution functions and the a priori step probabilities need to be known to calculate chain end distribution functions for each segment s at position (z, R) .

Scheutjens and Fler show that by combination with the complementary chain end distribution functions, (the ones started at the other end of the chain $G(z, R, s_2)$, obtained from equation (5) by replacing scripts 1 by script 2), individual segment density profiles are obtained by a composition formula, which couples two chain parts: one with s segments and the other with $(r-s+1)$ segments:

$$\phi(z, R, s) = C G(z, R, s_{12}) = C G(z, R, s_1) G(z, R, s_2) / G(z, R, s) \quad (6)$$

Here the division by $G(z, R, s)$ is introduced to correct for double counting of the overlapping segment and C is a normalisation constant. For given segment density of the molecules in the bulk ϕ^b the normalisation constant C is given by: $C = \phi^b / r$. Alternatively, when the total number of molecules n in the system is known, the normalisation constant is given by: $C = n / G(r_1)$, where

$G(r_1) = \sum_z \sum_R L(R) G(z, R, r_1)$ is the total statistical weight to find the set of chains containing all possible conformations in the system and n follows from the volume fractions: $n = \sum_z \sum_R \sum_s L(R) \phi(z, R, s)$.

The free segment distribution functions have been derived before [2] and can be extended to cover the present 2D analysis. It is a Boltzmann factor that contains a general potential $u'(z, R)$ independent of the segment type and potential contributions, which depend on the local segment densities, specific for a given segment type. When segment s is of type x then $G(z, R, s) = G_x(z, R)$,

$$G_x(z, R) = \exp\left\{-u'(z, R) + \sum_y \chi_{xy} [\langle \phi_y(z, R) \rangle - \phi_y^b]\right\} \quad (7)$$

Here, x and y indicate the nature of the segments (solvent is W , apolar segments A , polar segments B , etc.). The summation y runs over all segment types. χ_{xy} is the well known Flory-Huggins interaction parameter which gives the pair energy difference in excess of those for the pure components. Therefore, only dissimilar contacts ($x \neq y$) have a non-zero χ value. The angular brackets in equation (7) indicate that a local averaging of the segment density profiles with the a priori probabilities is performed:

$$\langle \phi(z, R) \rangle = \sum_{z'} \sum_{R'} \lambda_{z'-z, R'-R}(z, R) \phi(z', R') \quad (8)$$

The set of equations (5,6,7) cannot be solved analytically. For the calculation of the segment density profiles (equation 6) all chain end distribution functions must be calculated (equation 5). This is only possible when the free segment weighting factors (equation (7)) are known, which in turn, depend again on the segment density profiles (equation (6)). The energy $u'(z, R)$ of equation (7) originates from hard core repulsion interactions of all segments in the lattice. Its numerical value is found from the boundary condition that all lattice sites are filled: $\sum_x \phi_x(z, R) = 1$ for all z and R . The number of $u'(z, R)$ variables is equal to the number of boundary conditions. In the bulk solution $u^b = 0$. The set of implicit equations are solved by standard numerical methods [2].

The first order Markov approach as discussed above, is not very accurate for describing small chain molecules [2]. In principle, at least a rotational isomeric state scheme must be followed, which prevents the chain from direct backfolding. On the other hand, when several segments of the chains are grouped in so called statistical chain elements, this problem is also somewhat

relaxed. In this paper, we choose for this last approach. The larger the segment size, the lower the resolution of the calculations. As a compromise, a statistical unit is chosen to be about three CH₂ segments long. Obviously, the energy parameters must be scaled to the segment size.

Boundary conditions

The reflecting boundary conditions are realised by setting: $\phi_x(0,R) = \phi_x(1,R)$, $\phi_x(M_z+1,R) = \phi_x(M_z,R)$ and, for example, $G(0,R,s_1) = G(1,R,s_1)$, $G(M_z+1,R,s_1) = G(M_z,R,s_1)$ for all R. Membranes are generated near one of the boundary layers. As a consequence, the membranes generated with this method are symmetrical with respect of their midplane. In addition to reducing computation time (only half the membrane has to be calculated) this boundary condition is also used to fix the lattice on the membrane. Translational freedom of the membrane in the system is not accounted for. For large membranes, the translational entropy can safely be neglected. Similarly, the inhomogeneities are restricted to the centre of the lattice (near $R = 1$). Consequently, the translational entropy, originating from the distributions of the inhomogeneities along the bilayer is neglected. When necessary, such entropy terms can be included.

Results and discussion

To start the analysis we first describe the segment density profiles of a membrane composed of lecithin molecules. Since a lecithin molecule is a branched chain, the following architecture is chosen:



Here p is the number of statistical units (about 3 CH₂ units long) of tail segments (A), and q is the number of head group units (B). Near the glycerol backbone the statistical units are a little unrealistic. Also, we will neither model any details in the head group itself, nor increase the volume of the CH₃ end groups. Water is modelled as monomers which are as large as the (statistical) units of the chain molecules.

Figure (2) shows the segment density profile of an equilibrium membrane (i.e., with a vanishing surface tension) made of lecithin molecules (p = 6 and q = 2) in a one-dimensional analysis. The Flory-Huggins parameters are chosen

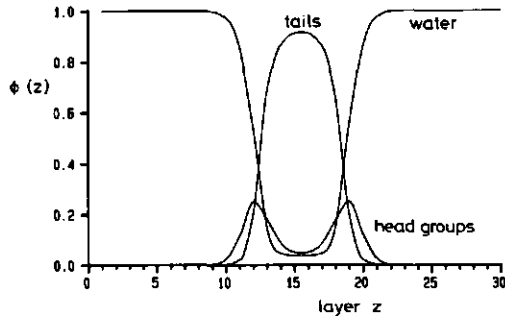


Figure 2.

Segment density profiles through a cross section of a membrane composed of lecithin molecules ($p = 6$, $q = 2$). The equilibrium concentration is $1.6 \cdot 10^{-8}$, and the excess free energy is zero. The energy parameters are: $\chi_{AW} = 3$, $\chi_{BW} = -0.5$, $\chi_{AB} = 2.8$ where A is an apolar, B a polar segment and W represents the water molecules.

in order to mimic a lecithin with 16 CH_2 tail segments, for which the RIS-scheme calculations have been worked out before [2]. The equilibrium volume fractions of lipids in the bulk solution is $1.6 \cdot 10^{-8}$. In the following calculations where additives are put into the system, this equilibrium concentration is established as good as possible.

The very unfavourable tail segment-water contact causes the centre of the membrane to be almost free of water (see figure (2)). Further, the segment density profiles show rather broad distributions indicating that the chains do have a considerable amount of conformational entropy.

Trans-membrane configuration

One copolymer molecule in the bilayer

The copolymer molecule is modelled by a chain with apolar A' and polar B' segments. The prime indicates that the segment belongs to the copolymer. A and A' are chemically different, but of similar polarity. Like B, the polar segments B' are water soluble, but there might be some repulsion between B' and B. We have chosen for a linear copolymer molecule symmetrical with respect to the middle segments. So the two ends will have inverted sequences of polar and apolar segments. Since the present calculations are only meant to be an illustration of a trans-membrane configuration rather than an exhaustive

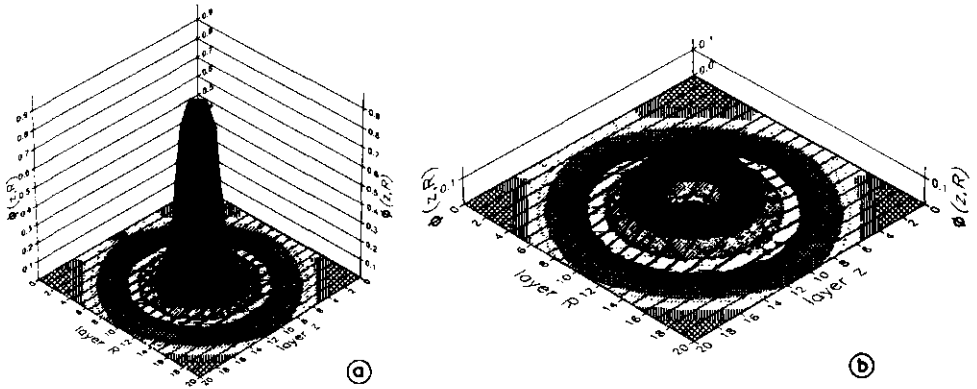


Figure 3.

Segment density profiles through a cross section of the copolymer given in equation (10) left to itself in a homogeneous solution. The energy parameters are $\chi_{A'W} = 2.7$, $\chi_{B'W} = -0.5$, $\chi_{A'B'} = 2.8$.

a) Apolar segments A', b) polar segments B'.

analysis, we choose arbitrarily a specific copolymer. The copolymer (a "model-protein") has 200 units with a fraction of 0.36 polar segment:

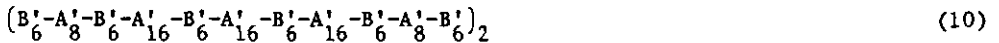


Figure 4.

2D segment density profiles for the interaction between the membrane given in figure (2) and the "protein" given in figure (3). Additional energy parameters: $\chi_{AA'} = 0.8$, $\chi_{BB'} = 0$, $\chi_{AB'} = \chi_{BA'} = 2.8$. The copolymer molecule is put in the centre of the lattice. The lattice layers are numbered arbitrarily. Where expedient, one quarter of the figure is cut out of the profiles to show details of the behaviour in the centre. For this quarter the iso- ϕ -lines are plotted.

a) Upper plane: artist's view. Lower plane: iso- ϕ_W -lines, b) solvent profiles, c) apolar segments of the lipid molecules, d) polar segments of the lipid molecules, e) apolar segments of the copolymer molecule, f) polar segments of the copolymer molecule.

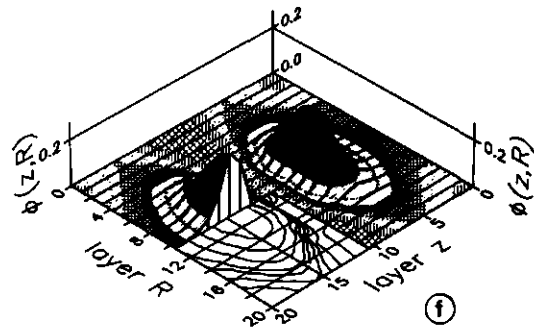
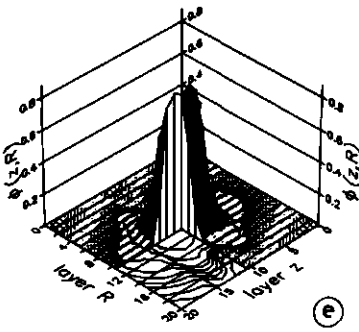
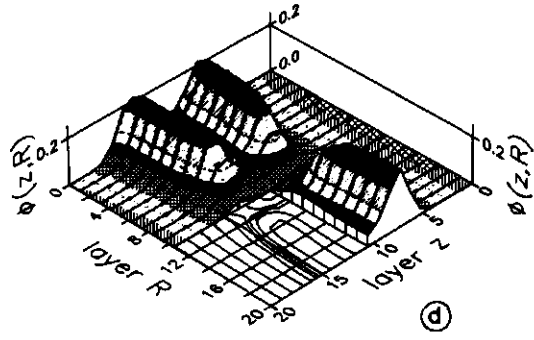
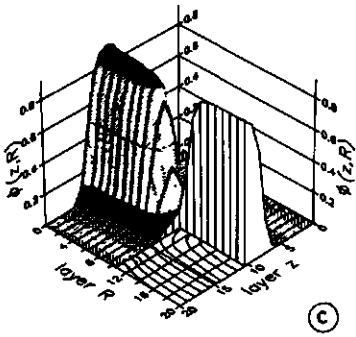
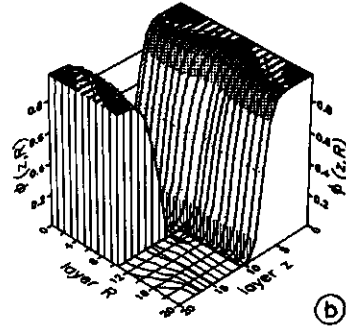
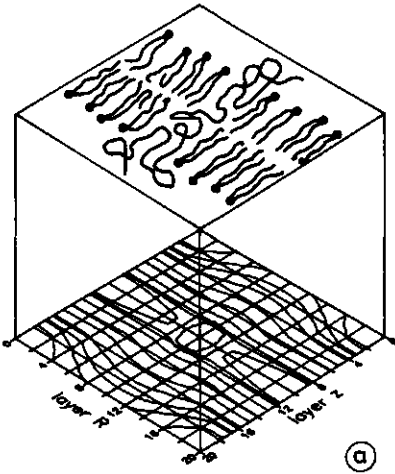


Figure (3) shows the segment density profiles of this polymer molecule in a homogeneous solution. Such segment density profiles are two-dimensional. The layers and rings are renumbered, so the centre of the lattice is not at $(R,M) = (0.5,0.5)$ but at $(10.5,10.5)$. To minimise the number of apolar-water contacts, the molecule assumes a collapsed configuration, as one can see from figure (3) the configuration is globular. Note that the molecule is not forced into that globular structure. It could for example also have chosen for a rod-like configuration and, in fact, molecules of other composition might prefer that.

In figure (4) this copolymer molecule is built into the membrane. Clearly, the chain molecule has rearranged its segments with the polar ones now on both sides of the membrane. At the boundaries of the system, i.e., near $R = 0$ and $R = 20$, the membrane has its unperturbed shape, but near the lattice centre the segment profiles of the membrane are disturbed. Even at the midpoint, where the density of the perturbing molecule is very high, some lipid tails are present. Most energetic interactions of the polar and apolar segments of the two type of molecules are chosen similar. The most sensitive parameter for this distribution is the interaction between the apolar tails of the lipid molecules and the apolar segments of the copolymer. To obtain a compact segment density of the copolymer in the heart of the membrane, this interaction must be repulsive. In the present case $\chi_{AA'} = 0.8$. Since the guest molecule is not of extremely high molecular weight, the profiles of the copolymer and the lipid tails do overlap. A lower value for $\chi_{AA'}$ would increase this overlap and eventually the copolymer would dissolve in the centre of the membrane and form a more or less "random" coil. A much higher value would increase the separation between the two types of apolar segments. We also generated (not shown) this type of membrane-copolymer structures and found that they only existed when the membrane was short of lipids per surface area (i.e., the membrane was not in full equilibrium). When in this case more lipids were offered to the membrane the copolymer was pushed out of the membrane. This indicates that very large deviations in membrane properties cannot exist in the boundary layers as long as the membrane is in equilibrium.

Other parameters can also be relevant for the incorporation of a copolymer in the membrane. The polar-apolar χ_{AB} , $\chi_{A'B}$, $\chi_{AB'}$ and $\chi_{A'B'}$ interactions, inherent in the problem because of the architecture of the amphiphilic molecules, can shift the position of the central molecule when variations in interactions are introduced. Further, it is assumed that the two polar segment mix ideal $\chi_{BB'} = 0$.

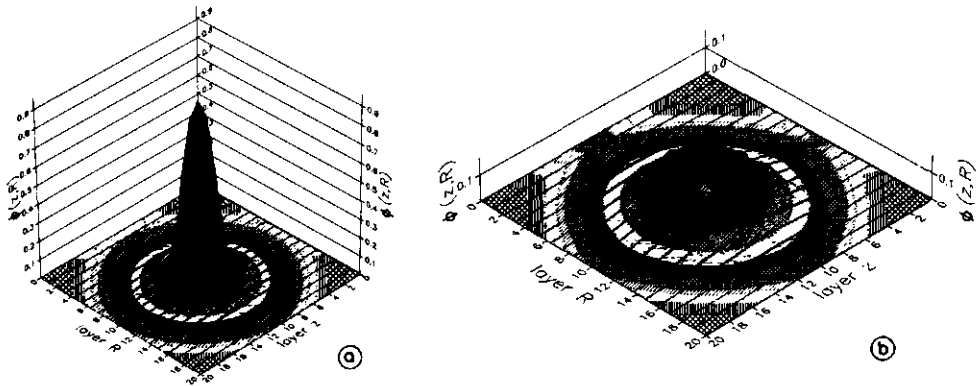


Figure 5.

Segment density profiles through a cross section of the copolymer given in equation (11), left to itself in a homogeneous solution. Energy parameters as in figure (3). a) Apolar segments, b) polar segments.

Cluster of four copolymer molecules in the bilayer

As a second example of membrane-copolymer interaction, we show the incorporation of a more polar chain molecule with a fraction 0.52 of B' segments and the following arbitrary segment sequence:

$$(B'_{10} - A'_4 - B'_6 - A'_{10} - B'_5 - A'_5 - B'_5 - A'_{10} - B'_5 - A'_5 - B'_5 - A'_{10} - B'_6 - A'_4 - B'_{10})_2 \quad (11)$$

In comparison with figure (3) one can see, that this molecule is more hydrophilic: it has more polar parts and it does not have long apolar parts. In figure (5) the segment density profiles of a free molecule are indicated. Also in this case the structure is almost globular. Due to its longer polar parts this copolymer molecule has significantly different segment profiles than the one shown in figure (3).

Since this molecule is much more polar, we cannot expect the copolymer to go into the membrane as easily as in our previous example. Adsorption of the copolymer onto the membrane is more likely. As our membranes are symmetrical, adsorption should only occur at both sides to the same extent. When the chain molecule pushes some head groups of the lipids apart, it is rather difficult, perhaps impossible, for the lipids to fill up the membrane between the

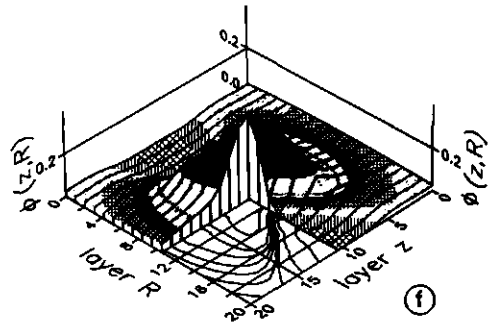
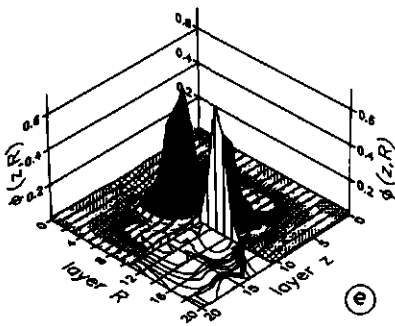
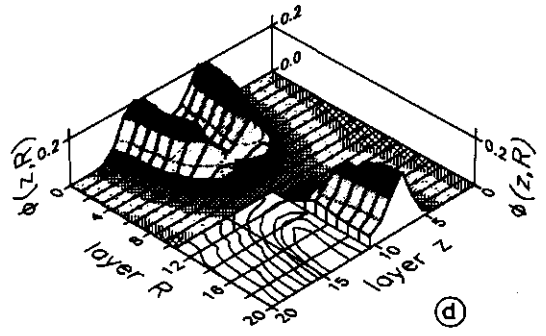
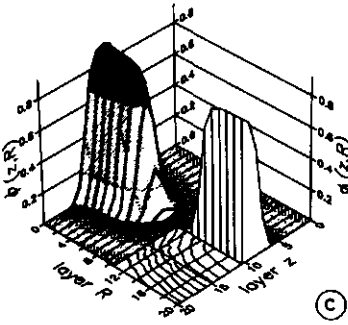
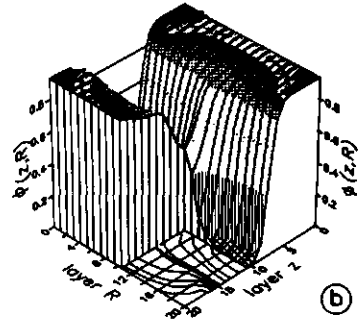
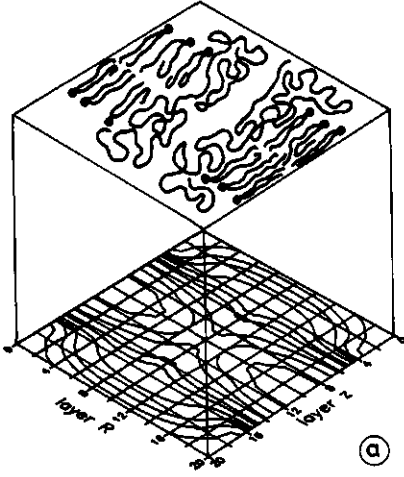


Figure 6.

2D segment density profiles of the interaction between four copolymers given in figure (5) and the membrane given in figure (2). The additional interaction parameters are: $\chi_{AA'} = 0.7$, $\chi_{AB'} = \chi_{A'B} = 2.8$, $\chi_{BB'} = 0.5$. The equilibrium concentration of the lipids is in this case $1.8 \cdot 10^{-8}$.

a. Upper plane: artist's view. Lower plane: iso- ϕ_W -lines, b) solvent profiles, c) apolar segments of the lipid molecules, d) polar segments of the lipid molecules, e) apolar segments of the four copolymer molecules, f) polar segments of the four copolymer molecules.

sandwich formed by the copolymers. This explains why we were unable to find a thermodynamically stable situation when a single copolymer molecule was put in the membrane. Surprisingly, we observed a very remarkable structure when four copolymer molecules were put together in the lipid membrane. Figure (6) gives the segment distributions for this situation. As can be seen, a cluster of four molecules did arrange themselves in the lipid membrane, with a clear pore in the centre. We do not claim that this structure is the only (thermodynamically) stable one, for when the solution would have been more dilute, it might have been possible for the copolymer molecules to leave the lipid bilayer. Alternatively another cluster with three or five copolymer molecules could have been more favourable but we have not investigated this possibility. As in our first example, we have introduced a repulsion between the apolar segments of the copolymer and the lipid tails $\chi_{AA'} = 0.7$. Now, we also have a repulsion between the two types of polar segments $\chi_{BB'} = 0.5$. This repulsion did also contribute to the partitioning between the polar segments of the lipid head groups and the probe as was found in this example. When the apolar segments would mix better, the four copolymers would feel even more at home at their present position. The hydrophilic heart of the aggregate shows that proteins can form hydrophilic pores through which transport of polar molecules may occur.

In many experimental studies on membrane protein interaction, rather high protein/lipid ratios are encountered. Our second example may therefore be relevant for these studies.

Lateral phase separation

Figure (7) shows the segment density profiles of a homogeneous membrane composed of of lecithin molecules of $p' = 7$ apolar and $q' = 3$ polar segments.

For this membrane the excess free energy is zero and the equilibrium lipid volume fraction in the solution is: $8.6 \cdot 10^{-10}$. In comparison with the segment density profiles given in figure (2), this membrane is slightly thicker because the apolar tails of the lipids are one unit longer. Therefore, also the equilibrium bulk volume fraction is lower.

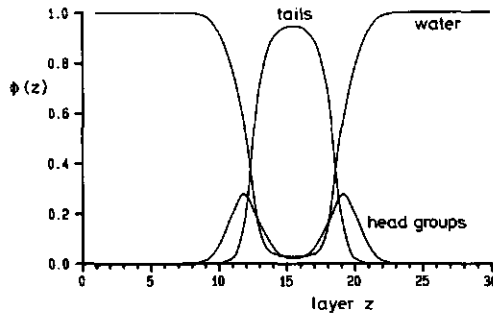


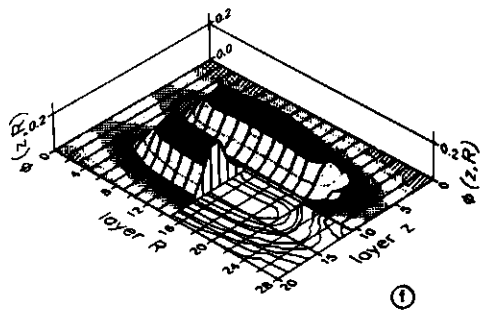
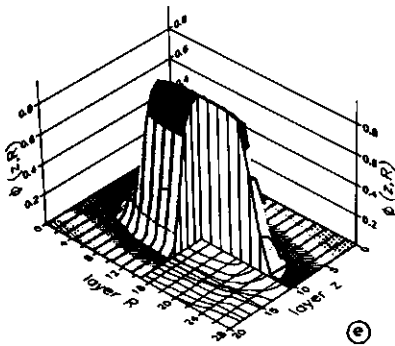
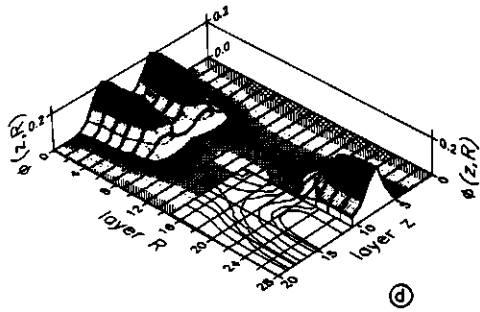
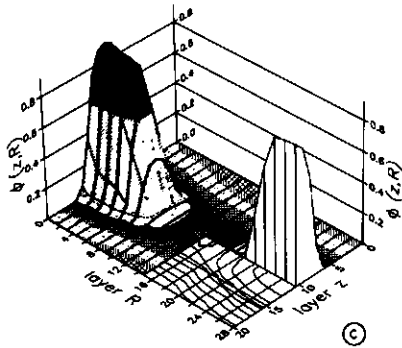
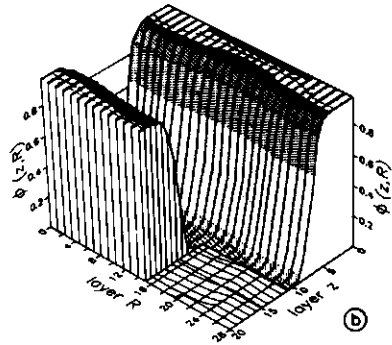
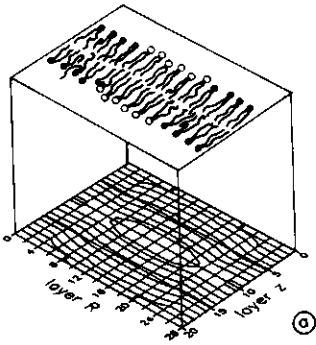
Figure 7.

Segment density profiles of a cross section through a homogeneous membrane composed of lecithin molecules with $p' = 7$ and $q' = 3$. Interaction parameters as in figure (2).

Figure (8) shows the 2D segment density profiles of the two lipid molecules ($p' = 7$, $q' = 3$ mixed with $p = 6$, $q = 2$) in one system. In this case (10.5,14.5) is the centre of the lattice. We assigned a repulsion between the two apolar segments of $\chi_{AA'} = 0.5$ and a stronger repulsion between segments of the two head groups: $\chi_{BB'} = 1$. These repulsions cause a lateral phase separation. Studying the segment density profiles reveals that in the boundary area the concentration of solvent is slightly higher than in either of the two homogeneous membrane phases. This is caused by the fact that the two molecules

Figure 8.

2D segment density profiles of two nonmixing lipid molecules given in figure (2) ($p = 6$, $q = 2$) and figure (7) ($p' = 7$, $q' = 3$). The additional energy parameters are: $\chi_{AA'} = 0.5$, $\chi_{BB'} = 1$. a) Upper plane: artistic view. Lower plane: iso- ϕ_w -lines., b) solvent profiles, c) apolar segments $p = 6$, d) polar segments $q = 2$, e) apolar segments $p' = 7$, f) polar segments $q' = 3$.



avoid each other, and thus the water molecules enter to fill the space. High solvent concentrations are, however, not found in the interfacial region between the two lipids. The energetic effect of exposing tails to water is so unfavourable that the tails do fill up most of the space. There are no indications of membrane rupture, and one has to go to very extreme situations to find an interfacial region in which the water concentration is high.

Conclusions

We have extended the theory for the statistical mechanics of amphiphilic molecules in associates to include inhomogeneities in two directions. Two examples of membrane-copolymer interactions are discussed. In the former example a trans-membrane copolymer was shown. In the second example a cluster of four polymers in the lipid membrane was studied. In the latter case, the four molecules formed a pore, through which transport of hydrophilic molecules is possible. The copolymers dramatically changed their conformation in the membrane with respect to the same in the aqueous solution.

We also studied the lateral phase separation between two different lipids in a membrane. The boundary layer between the two lipid phases was found to be as hydrophobic as in either phase.

The present theory is specifically useful for systems which are characterised by inhomogeneities in interfaces such as: adsorption of chain molecules on heterogeneous surfaces, surfactant adsorption (hemimicelles), reversed micelles in membranes, etc.. Further it is possible to improve the present theory in various respects. One could think of correcting for the backfolding by incorporation of the rotational isomeric state scheme [2] and accounting for an anisotropic orientational molecular field [7] to improve on the correction for the excluded volume of the other chains.

Literature

1. F.A.M. Leermakers, J.M.H.M. Scheutjens, and J. Lyklema; *Biophys. Chem.* **19** (1983) 353.
2. F.A.M. Leermakers; PhD thesis, Wageningen (1988) Chapter 2.
3. S.J. Singer and G.L. Nicolson; *Science* **175** (1872) 720.
4. P.J. Flory; "Principles of Polymer Chemistry", Cornell University Press, Ithaca, NY (1953).
5. J.M.H.M. Scheutjens and G.J. Fleer; *J. Phys. Chem.* **83** (1979) 1619.
6. J.M.H.M. Scheutjens and G.J. Fleer; *J. Phys. Chem.* **84** (1980) 178.
7. F.A.M. Leermakers; PhD thesis, Wageningen (1988) Chapter 4.

List of most important symbols

A	Free energy; Subscript, indicating an apolar segment type.
A_s	Surface area.
A^σ	Excess free energy.
B	Subscript, indicating a polar segment type.
b	Superscript, indicating the bulk solution
C	Normalisation constant.
c	Superscript, indicating a given conformation
CMC	Critical Micelle (Micellisation) Concentration.
e", f", g", h"	Orientations in the tetrahedral lattice. Each orientation has two opposite directions, for example, e" includes e and e'.
$G_x(z)$	Free segment weighting factor for segments of type x in layer z.
$G(z, s)$	Free segment weighting factor for segment s in layer z.
$G(z, s_1)$	Chain end distribution function of the chain part attached to segment s by bond 1.
$G(z, s_{12})$	Distribution function of segment s with chain parts at two of its bonds (1 and 2).
$G(z, s_{12}^{\alpha\beta})$	Segment distribution function with chain parts at two bonds: bond 1 in direction α and bond 2 in direction β .
$G^{\alpha''}(z z')$	Anisotropic weighting factor for a bond in orientation α'' between layers z and z'.
G'	Segment distribution function with curvature corrections.
h	Length of a cylinder in units of lattice sites.
i	Index of molecule type: i = 1 (water), 2 (amphiphile), 3 (additive).
k	Boltzmann's constant.
L(z)	Number of lattice sites in layer z.
M	A layer number in the bulk solution.
n	Number of chain molecules in the system.
n^c	Number of chains in conformation c.
$n(z)$	Number of segments in layer z.
n_g	Number of gauche bonds.

$n^{\alpha''}(z z')$	Number of bonds in orientation α'' between layers z and z' .
$P^V(z)$	Vacancy probability in layer z .
p	Number of apolar segments per tail in the amphiphilic chain.
Q	Canonical partition function.
Q^g	Canonical partition function for gauche configurations.
q	Number of polar head group segments in the amphiphilic chain.
R	Radial direction in the cylindrical co-ordinate system; Index for circle numbers.
R_d	Radius of a disk.
r	Number of monomers in a chain.
r_{y_i}	Number of segments y in molecule i .
$r_i^{\alpha''}(z z')$	Number of bonds molecule i has in orientation α'' between layers z and z' .
$S(s)$	Segment order parameter.
$S(z)$	Contact area between layers z and $z-1$ in units of lattice areas.
s	Index indicating the segment number.
T	Absolute temperature.
U	Energy of the system.
U^g	Energy difference between a gauche and a trans configuration.
$u''(z)$	Hard core potential with respect to the pure reference state.
$u'(z)$	Hard core potential in layer z with respect to the bulk solution.
$u_x(z)$	Potential of segment type x in layer z .
u^c	Potential of a conformation c .
$V(z)$	Volume from layer 1 up to layer z in units of lattice sites.
V_s	Volume of a subsystem, available per association colloid.
W	Subscript indicating water (segment type).
x, y	Subscript, indicating segment type.
Z	Co-ordination number of the lattice.
z	Direction into which inhomogeneities are present; Index for layer numbers.
$\alpha'', \beta'', \gamma'', \delta''$	Index for bond orientations in the lattice. Each orientation can be divided into two opposite directions indicated by, for example, α and α' .
γ	Interfacial tension.
θ	Amount of molecules in the system in equivalent monolayers.

λ^g	Probability of finding three successive bonds in a gauche configuration.
λ^t	Probability of finding three successive bonds in a trans configuration.
$\lambda_{z',-z}(z)$	Fraction of neighbours a site in layer z has in layer z' .
$\lambda^{\alpha\beta}$	Fraction of segment orientations in $\alpha\beta$ direction.
λ_i^c	Weighting factor for a chain i in conformation c .
$\lambda^{\alpha''-\beta''-\gamma''}$	Weighting factor for a $\alpha''-\beta''-\gamma''$ configuration (gauche or trans).
λ^g, λ^t	A priori probability for a gauche and trans configuration respectively.
σ	Superscript, indicating excess with respect of bulk solution.
μ	Chemical potential.
Ξ	Grand canonical partition function.
$\phi(s)$	Angle between the normal of the bilayer and the orientation of segment s .
ϕ_x	Volume fraction of segments of type x .
$\phi(z, s)$	Volume fraction of segment s in layer z .
$\bar{\phi}$	Overall volume fraction in the system.
$\langle\phi(z)\rangle$	Weighted average of the volume fraction ϕ over three layers $z-1$, z , and $z+1$.
χ	Flory-Huggins interaction parameter.
Ω	Combinatory factor.
ω^c	Degeneracy of a conformation c .
*	Superscript, indicating a reference state of a pure, one component, system.

Summary

The aim of the present study was to unravel the general equilibrium physical properties of lipid bilayer membranes. We consider four major questions:

1. What determines the morphology of the association colloids (micelles, membranes, vesicles) in general?
2. Do the apolar tails of the lipids in the bilayer organise themselves more like matches in a box or rather like hot spaghetti in a pan?
3. How does this membrane organisation depend on temperature?
4. How do additives like surfactants or polymers interact with the bilayer?

These four questions cover a wide range of topics currently subject to intensive research. Each one of them calls for a rigorous answer. We believed that it would be possible to design one single theory covering the whole field. The development of such a theory is undertaken in the present thesis.

Recently, the statistical thermodynamics of homopolymers at interfaces has been worked out by Scheutjens and Fleer (SF). This theory is an extension of the Flory Huggins (FH) theory for polymers in solution in the sense that it allows for inhomogeneities in one dimension. In the other two dimensions a mean field, i.e., an average segment density, assumption is applied. One of the strong points of this theory is that, by using a Markov-type approximation, all possible conformations of the chains are considered with a minimum of computational effort. The SF theory can be extended to describe copolymers at interfaces.

For well-chosen amphipolar molecules the theory is able to deal with local phase separation phenomena. Preliminary calculations on surfactant bilayers showed that the SF theory needed some modifications in order to be relevant to the four topics given above. The main reason for this is that for the very small surfactant molecules the Markov-type approximation is not very accurate. Five extensions of the theory are presented in this thesis:

1. For the chain statistics the Markov-type approximation is extended to the so called rotational isomeric state scheme. This scheme prevents backfolding in chain sections of five consecutive segments. The

improvement allowed us to adjust the stiffness of the chain as a function of temperature.

2. The theory is generalised for arbitrary geometries. With this extension the polymorphism of association colloids could be studied.
3. The theory is extended to account for branched chain molecules. This has been used to simulate lipid molecules with two apolar tails and one polar head group.
4. In the SF theory the statistical weight of each conformation is found by Boltzmann statistics. The potential of each conformation depends on segment-segment interactions, hard core contact potentials, and the number of gauche bonds in the chain. A new weighting factor is introduced which accounts for the average orientation of the molecules. The statistical weight of a conformation is increased when its bond directions match with those of the surrounding molecules. With this molecular orientational field co-operative phenomena like crystallisation can be studied.
5. Allowing for inhomogeneities in two dimensions enables us to study membrane-"protein" interactions.

The properties of the theory with these new features are thoroughly examined in five chapters. A short summary of the results and main conclusions of each chapter is given below.

Chapter 1 dealt with the morphology of association colloids. In this chapter we prove that the formation of micelles is a first order transition. However, the theoretical critical micelle concentration is not observed very sharply, because it is very low. We showed that, with increasing concentration of bipolar molecules, the micelles first grow and eventually change their shapes. Lecithin-like molecules prefer lamellar aggregates over globular ones.

In chapter 2 the rotational isomeric state scheme is presented and details of the statistics of branched chain molecules is given. We present an overview of the behaviour of the membranes as a function of the four energy parameters. There is no need to restrict the molecules to pre-assigned positions in the system. The membrane thickness adjusts itself. The equilibrium membrane is free of tension. Its excess free energy per surface area is very small. When fluctuations and long range Van der Waals attractions are neglected the excess free energy is essentially zero.

Vesicle systems are studied in chapter 3. We show that the excess free energy of curvature per vesicle is constant for vesicles composed of one type of lipid, irrespective of the radius of the vesicle. This remains true for bilamellar and hence for multilamellar vesicles. We show that as a rule, the thicker a membrane is the more energy it costs to bend it. Adding surfactants to a system containing vesicle is disastrous for the vesicle structures. Increasing the surfactant/lipid ratio causes the vesicles to break up in micelles. When vesicles are formed by two compatible lipid molecules, the free energy of curvature varies linearly with their composition. If the two bipolar molecules do not mix, they partition themselves over the two membrane sides and the excess free energy of curvature shows, at constant vesicle radius, a minimum as a function of composition. For a given composition the vesicle adopts an optimal vesicle radius.

The membrane structure predicted by the theory significantly improves when the orientational dependent molecular field is applied. We derive the partition function for this SCAF (Self-Consistent Anisotropic Field) theory in chapter 4. Among other things, the order parameter profiles now show the well known plateau along the lipid tails. In agreement with experiments, we find a first order phase transition which transforms the membrane from a high temperature liquid into a low temperature gel state. In the gel phase the lipid tails are virtually in a all trans conformation. Because of this, the density in the gel membrane is higher than in the liquid phase. For the model membrane we observed two possible gel phases. One gel phase was about twice as thick as the other. The thin, intercalated, gel membrane was found in the case that the membranes were isolated, i.e., when they did not interact with each other, while the other gel phase, obviously with non-intercalated membranes, was found in the concentrated regime.

In the final chapter we studied two cases of the interaction of long copolymers ("proteins") with a model membrane. In the first example the molecule is in a trans membrane configuration. In the second example a group of four molecules is clustered together and forms a hydrophilic pore, through which polar molecules can pass the membrane. In this chapter we also study the boundary region between two areas of lipid molecules which do not mix (lateral phase separation). It is characteristic for membrane system, that the lipids in the membrane are very efficient in camouflaging the inhomogeneities in the

boundary layers. No big differences in solvent profiles are observed along the boundary layers. This ability of the lipid molecules to compensate irregularities explains why membranes are not easily disrupted.

It is the first time that a statistical thermodynamical theory is presented that can deal with association phenomena without the requirement to fix the head groups to pre-assigned positions. We showed that this theory does give a very detailed insight into equilibrium membrane properties. The correspondence with experimental data is satisfactory. The theory can be easily extended to incorporate more details in the calculations and better quantitative agreement with experimental data is well feasible.

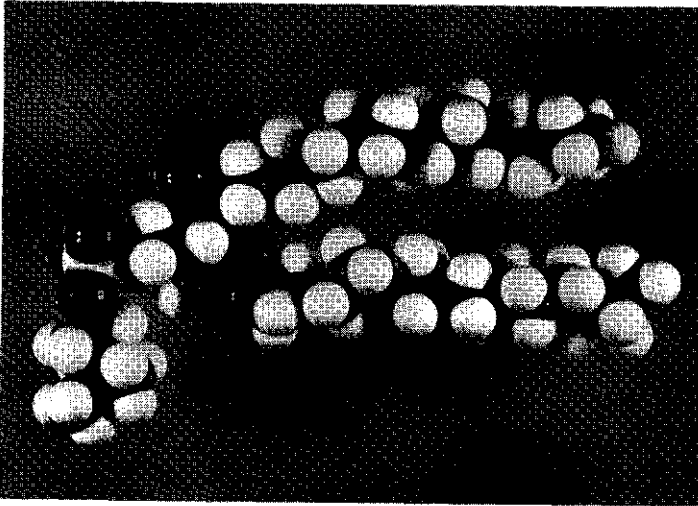
Samenvatting

Niet alle stoffen lossen op in water. Wanneer we olie en water proberen te mengen kunnen we in het beste geval een emulsie maken. Een emulsie is een oplossing van waterdruppeltjes in olie of van oliedruppeltjes in water. Deze oplossing is instabiel en ontmengt in een water- en olielaag. Dit verschijnsel noemen we fasescheiding.

Stoffen die mengen met water, zoals alcohol, noemen we hydrofiel en stoffen die niet in water oplossen worden hydrofoob genoemd. Koolwaterstoffen behoren tot de laatste categorie. Methaan, ethaan en propaan zijn gasvormig onder normale omstandigheden en lossen slecht op in water. Koolwaterstoffen met een hoger moleculair gewicht zoals octaan, nonaan en decaan, zijn vloeistoffen en lossen nauwelijks op in water. Olie bestaat voor een groot gedeelte uit koolwaterstoffen met een vrij hoog moleculair gewicht. (In feite is de term "olie" vaak gebruikt als een verzamelnaam waarmee wateronmengbare vloeistoffen worden aangeduid.) Een alcohol molecuul bestaat uit een ethaan deel waaraan een polaire hydroxyl groep is gehecht. De invloed van de hydroxyl groep is zo groot dat het molecuul in zijn geheel hydrofiel is.

Om een molecuul met een groter koolwaterstofdeel oplosbaar te houden is één klein hydrofiel groepje niet voldoende. Laten we bijvoorbeeld decaan chemisch veranderen door aan een van de einden een polaire groep te hechten. Dan ontstaat er een molecuul met een apolaire "staart" en een polaire "kop". Het molecuul is amfifiel. De ervaring leert dat amfifiele moleculen wel in water oplosbaar zijn, niet als afzonderlijke moleculen, maar in groepjes tegelijk. Deze groepjes worden micellen of associatie-kolloïden genoemd.

Micellen kunnen allerlei vormen aannemen. Onafhankelijk van de micelvorm treffen we de koppen aan in het grensvlak tussen het apolaire staartengebied en de waterfase. De grootte en de vorm van deze associatie-kolloïden, de manier waarop de moleculen in de micellen zitten, en of er al of niet water in een micel zit, wordt bepaald door de energie- en entropiebalans in het systeem. Dit betekent dat de moleculen zoeken naar een evenwicht tussen de drang om zich te organiseren om ongunstige energetische interacties te ontlopen en de drang om zich zo wanordelijk mogelijk te verspreiden. Het is



Figuur 1.

Een model van het lipidemolecuul Dipalmitoylphosphatidylcholine.

goed om nu al vast op te merken dat een relatief kleine variatie in omstandigheden de eigenschappen van de micellen sterk kan veranderen. Zo'n verstoring kan onder andere tot stand gebracht worden door concentratieveranderingen, temperatuursveranderingen en variaties in de verhouding polair/apolair in het amfifiele molecuul. Bolvormige micellen bevatten vaak 50 tot 100 amfifiele moleculen. Een veel groter aggregatiegetal wordt aangetroffen bij vlakke platte micellen, die door hun structuur ook wel bilagen worden genoemd. Ze staan echter beter bekend als membranen. In biologische systemen worden membranen gevormd door lipide moleculen welke over het algemeen twee apolaire staarten en één polaire kop bezitten. Figuur (1) geeft een voorbeeld van een (fosfo)lipide molecuul.

Membranen zijn essentieel voor het leven. Door hun vlakke structuur maken ze de compartimentalisatie mogelijk van levend materiaal. Ze zijn selectief doorlatend (semipermeabel): sommige stoffen mogen het membraan vrij passeren terwijl andere moleculen worden tegengehouden. Op deze manier voorkomen ze dat de inhoud van de cel zich mengt met de omgeving. We komen niet alleen membranen tegen in de wand van de cel maar ook in de cel zelf. Organellen zoals de kern, mitochondriën, liposomen, chloroplasten hebben een membraan omhulsel en bezitten op hun beurt weer membranen. De meeste membranen bevatten naast lipiden ook een groot aantal eiwitten. Het eiwitmolecuul zoekt een

plaats in het membraan zodat het zijn functie goed kan uitoefenen, dit kan variëren van losjes geadsorbeerd aan de buitenkant tot vast verankerd in de lipid-matrix. Verder, en dit maakt membraansystemen nog ingewikkelder, worden niet alleen enkelvoudige membranen, maar ook vaak dubbele membranen en zelfs multilaag membranen waargenomen. We geven enkele voorbeelden: een myeline schede om een axon van een zenuwcel bestaat uit diverse membranen en in chloroplasten zijn grana stapels (geaggregeerde membranen) in evenwicht met stroma lamellen (niet geaggregeerde membranen), in mitochondriën zijn twee membranen op elkaar geadsorbeerd. In al deze voorbeelden speelt de membraan-membraan interactie een belangrijke rol voor het biologisch functioneren.

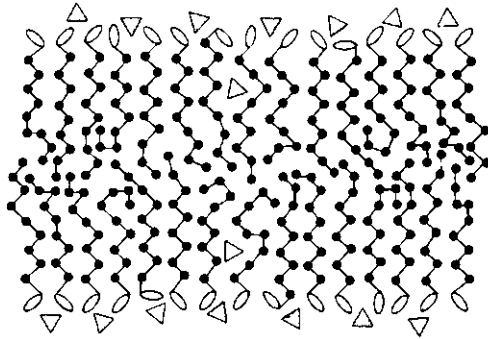
Membranen komen niet alleen voor in cellen. Ook bepaalde virussen, zoals het retrovirus dat AIDS veroorzaakt, bevat een omhullend membraan, waarin viruseiwitten zijn ingebed.

Het is eigen aan de natuur van de mens om zijn inzichten, ontleend aan bestudering van natuurlijke processen, te gebruiken in zijn eigen voordeel. Opnieuw enkele voorbeelden ter illustratie. Kennis van membraaneigenschappen kan helpen bij de ontwikkeling van geneesmiddelen, gewasbeschermingsmiddelen, enzovoorts. Vesikels (gesloten membranen) worden gebruikt om kunstmatige chloroplasten te maken, die inzichten moeten opleveren om de fotosynthese beter te begrijpen. Een interessante ontwikkeling is de toepassing van liposomen om geneesmiddelen in te sluiten. Deze liposomen worden ontwikkeld om gecontroleerde afgifte van het geneesmiddel op een gewenste plek in het menselijk lichaam mogelijk te maken.

Veel van deze toepassingen van membranen staan nog in de kinderschoenen. Een verdere ontwikkeling zou geholpen zijn met een gedetailleerd inzicht in de structuur van het membraan en in de factoren die de membraanstructuur beïnvloeden.

Experimenteel onderzoek aan de lipidematrix heeft al veel eigenschappen aan het licht gebracht:

- het hydrofobe binnenste van het membraan bevat vrijwel geen water.
- de dikte van het membraan is ruwweg twee keer de lengte van de gestrekte lipidestaart.
- de moleculen in het membraan zijn zeer geordend.
- de beweeglijkheid van de lipiden in het vlak van het membraan is groot, terwijl het omtuimelen van de moleculen van de ene naar de andere kant van het membraan zeer traag verloopt. Het membraan heeft dus zowel vloeistof- als vastestof eigenschappen.



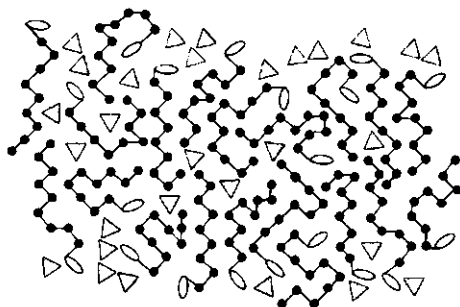
Figuur 2.

Een tweedimensionale doorsnede van een membraanstructuur welke opgebouwd is uit amfifiele moleculen bestaande uit één kopsegment en negen staartsegmenten. De driehoekjes zijn watermoleculen. In deze structuur is een hoge mate van ordening aanwezig.

- membranen bezitten een fasenovergang bij een gegeven temperatuur. Bij hoge temperatuur zijn ze vloeibaar en bij lage temperatuur gel-achtig. De vloeibare fase is biologisch actief.

Men illustreert deze eigenschappen vaak met een plaatje als figuur (2). De staarten zijn zeer geordend en de kopgroepen zitten keurig in hetzelfde vlak. Het is bekend dat deze weergave een versimpeling van de realiteit is, doch vele experimenten suggereren dat het plaatje nog niet zo ver van de realiteit af zit. Begrijpen we waarom een membraan zo'n structuur bezit? Waarom bestaat er zo'n ongunstige organisatiegraad? Is een membraanstructuur zoals geschetst in figuur (3) niet veel gunstiger? Immers, in figuur (3) bestaat duidelijk een lagere organisatiegraad dan in figuur (2) terwijl er maar een beperkt aantal ongunstige staart-water contacten zijn bijgekomen. Het is een van de doelen van dit proefschrift om hier duidelijkheid in te brengen.

De methode die hiervoor gebruikt is staat bekend als de statistische thermodynamica. Op dit gebied zijn de laatste tien jaar grote vorderingen gemaakt, mede omdat de computer ons een flink deel van het rekenwerk uit handen heeft kunnen nemen. De theorie van Scheutjens en FLeer voor de beschrijving van ketenmoleculen in grensvlakken [1] heeft diverse aanknopingspunten gegeven voor het ontwikkelen van een nieuwe theorie waarmee de associatie van lipiden tot membraanachtige structuren bestudeerd kan worden [2]. Deze theorie wordt in dit proefschrift op diverse punten aangepast zodat



Figuur 3.

Zie voor een toelichting figuur 2. Nu is in de membraanstructuur duidelijk meer wanorde aangebracht.

een beter beschrijving van lipidmembranen mogelijk wordt.

In het volgende zullen kort de inhoud en de belangrijkste conclusies van de technische hoofdstukken de revue passeren.

In hoofdstuk 1 zijn de factoren bestudeerd die de micelvorm en -grootte bepalen. Bewezen is dat de vorming van de eerste micellen plaats vindt bij een kritische concentratie en dat de eerste micellen bolvormig zijn. Door verhoging van de concentratie van de amfifiele moleculen neemt de concentratie van micellen toe, de micellen worden groter en veranderen van vorm. Een uitgesproken vormverandering treedt op in een oplossing van lipidemoleculen. Een micel groeit dan uit tot een membraan.

In hoofdstuk 2 wordt de zogenaamde "rotational isomeric state" geïntroduceerd, waarmee de statistiek van de ketenconformaties wordt uitgevoerd. Met deze toevoeging aan de theorie wordt het membraansysteem uitvoerig doorgelicht. De gevoeligheid van een aantal membraaneigenschappen voor aanpasbare parameters wordt bekeken. De evenwichtsstructuur, zo wordt beredeneerd, staat niet onder spanning. Zou dit wel het geval geweest zijn, dan had het membraan zijn oppervlak en dus ook zijn dikte aangepast totdat deze spanning zou zijn verdwenen. Het blijkt echter dat de theoretisch gevonden membraanstructuur nog vrij ver afwijkt van de experimenteel gevonden structuur.

In het derde hoofdstuk zijn vesikels beschreven. Vesikels, gekromde membranen, dus membranen zonder rand, zijn vooral voor experimentele systemen van belang. Om de vesikels te beschrijven is de theorie uitgebreid voor gekromde geometrieën. (In hoofdstuk 1 werd hier ook al gebruik van gemaakt.) Vesikels opgebouwd uit één soort lipiden vertonen de neiging steeds verder te groeien, ze zijn thermodynamisch instabiel. Wanneer vesikels gevormd worden door twee of meer soorten lipiden, en vooral indien deze elkaar niet zo mogen, zal de binnenkant van het vesikelmembraan bevolkt worden door voornamelijk de ene soort lipiden en de buitenkant door de andere soort. Onder deze speciale omstandigheden kunnen vesikels thermodynamisch stabiel zijn. Wordt aan oplossing met vesikel een groot aantal amfifiel moleculen toegevoegd die graag micellen vormen, kan het vesikelsysteem volledig overgaan in een micelsysteem. Verder hebben de berekeningen aangetoond dat het meer energie kost om dikke membranen te krommen tot vesikels dan dunne membranen.

In hoofdstuk 4 is wederom de theorie van een nieuw jasje voorzien. Het doel is om de zogenaamde co-operatieve gel-eigenschappen van de membranen te beschrijven. Met deze toevoeging aan de theorie worden aanmerkelijk betere membraanstructuren verkregen, die veel beter aansluiten bij literatuurgegevens. Nu wordt ook begrepen waarom de orde in de membranen zo hoog is. Dit komt door het grote ruimtegebrek waarin de moleculen hun conformaties moeten zoeken. De verbetering in de theorie wordt aangegrepen om het fasengedrag van membranen te bestuderen. Hier voorspelt de theorie, in overeenstemming met experimentele gegevens, dat het membraan kan overgaan van een vloeibare toestand (bij hoge temperatuur) naar een gel-achtige toestand (bij lage temperatuur). In tegenstelling tot in het vloeibare membraan liggen de lipidestaarten in het gel-membraan in een gestrekte conformatie. Hierdoor pakken de lipiden beter en wordt de dichtheid in het membraan groter. Er worden twee gelfasen gevonden. Het opmerkelijkste verschil tussen deze twee gelfasen is dat de membranen in de ene fase bijna twee maal zo dik zijn dan in de andere. In dit laatste geval blijken de staarten van de lipiden in elkaar te steken zoals je twee kammen in elkaar kunt schuiven.

In het vijfde en laatste hoofdstuk is een eerste stap gemaakt naar de beschrijving van biologisch interessantere systemen. Getracht is om de interactie van grote copolymeren ("eiwitten") met modelmembranen te bestuderen. Om dit te verwezenlijken is de theorie voorzien van de

mogelijkheid om in twee richtingen concentratieveranderingen waar te kunnen nemen. Twee variaties op het thema membraan-copolymeer interacties zijn gegeven. Het eerste voorbeeld illustreert hoe een copolymeer in een transmembraan configuratie plaats kan nemen. In het tweede voorbeeld wordt de associatie van vier copolymeermoleculen in het membraan bestudeerd. Deze vier moleculen laten een porie open waardoor hydrofiele moleculen zich vrij makkelijk een weg kunnen banen. Het laatste onderwerp dat in dit hoofdstuk ter sprake wordt gebracht is de laterale fasescheiding van twee soorten lipiden in een membraan.

In al deze gevallen is gebleken dat inhomogeniteiten in het membraan door de lipidemoleculen in de grenslaag zeer efficiënt worden gecamoufleerd. Dit aanpassingsvermogen verklaart waarom membranen niet zo gemakkelijk "lekgeprikt" kunnen worden.

Als samenvattende conclusie mogen we stellen dat we er in geslaagd zijn een algemene membraantheorie te ontwikkelen. We hebben deze theorie toegepast op diverse membraansystemen. Zo begrijpen we nu waarom lipiden in een membraan zich meer ordenen als lucifers in een doosje dan als gekookte spaghetti in een pan. Over het algemeen is de kwalitatieve overeenkomst met experimentele gegevens goed. Door het verder uitbouwen van de theorie zal naar verwachting een kwantitatieve overeenstemming met experimenten in de toekomst mogelijk zijn.

[1] J.M.H.M. Scheutjens en G.J. Fleer; "Statistical Theory of the Adsorption of Interacting Chain Molecules."

1. "Partition Function, Segment Density Distribution, and Adsorption Isotherms". J.Phys.Chem. **83** (1979) 1619.

2. "Train, Loop, and Tail Size Distribution", J.Phys.Chem. **84** (1980) 178.

[2] F.A.M. Leermakers, J.M.H.M. Scheutjens en J. Lyklema; "On the Statistical Thermodynamics of Membrane Formation", Biophys. Chem. **18** (1983) 353.

Curriculum vitae

Franciscus Adrianus Maria Leermakers werd op 22 februari 1959 geboren te Helvoirt. Na het behalen van het Atheneum-b-diploma op het Mauric college te Vught ging hij in 1977 Moleculaire wetenschappen studeren aan de landbouwhogeschool te Wageningen. In de doctoraalfase werd onderzoek gedaan op de vakgroepen Plantenfysiologisch Onderzoek, Moleculaire Fysica en Fysische en Kolloïdchemie. Hij vervulde een stage op de universiteit van Illinois (VS). In september 1983 studeerde hij cum laude af en ontving de Unilever Research prijs. Van maart 1984 tot maart 1988 werkte hij in tijdelijke dienst als wetenschappelijk assistent op de vakgroep Fysische en Kolloïdchemie van de Landbouwniversiteit te Wageningen. Per september 1988 heeft hij een postdoctorale positie op de Stanford universiteit in San Francisco.

Nawoord

Vier jaar lang heb ik onderzoek mogen doen op een vakgebied waarvoor ik al vroeg in mijn studie interessen kreeg. Deze periode wordt nu afgesloten met dit proefschrift. Ten onrechte staat alleen mijn naam op de kaft van dit boekje. Velen hebben aan de totstandkoming ervan bijgedragen. Enkelen van hen wil ik uit de anonimiteit lichten om hun bijdragen, onder dankzegging, te vermelden.

Er is één persoon die zich bij uitstek heeft ingezet voor het slagen van dit onderzoek. Als leermeester trad hij op de voorgrond en als begeleider liet hij ruim baan voor persoonlijke initiatieven. In vele (langdurige) discussies stonden wij tegenover elkaar en als burens woonden we naast elkaar. Zijn naam, Jan Scheutjens, is onverbrekelijk met dit proefschrift verbonden. Mijn waardering laat zich misschien het best verwoorden door op te merken dat ik tevreden ben met het uiteindelijke resultaat.

Bij het ter schrift stellen van dit werk heeft Hans Lyklema ook een belangrijke rol gespeeld. Efficiënt en nauwgezet heeft hij de soms lastige tekst van opbouwende kritiek voorzien. Ondanks de immer gevulde agenda bleef hij altijd op de hoogte van de vorderingen en als "ambassadeur" heeft hij ons werk menigmaal gepromoot, een promotor waardig.

De goede sfeer zowel op de vakgroep fysische en kolloïdchemie als binnen de polymeergroep heeft ertoe bijgedragen dat ik met plezier terug kijk op de afgelopen jaren. In Boudewijn van Lent en Peter Barneveld had ik enthousiaste collega's waarbij inspanning en ontspanning elkaar op tijd aflosten. Kan ik mijn computerprogramma DUBBEL aan de heren van SIMPOL-SOFT overdragen? Ik ben me er van bewust dat zonder de enorme tijdsinvestering van Olaf Evers om de VAX computer wat gebruikersvriendelijker te maken, het rekenwerk niet op dezelfde manier mogelijk zou zijn geweest.

Tot slot mag het werk van een aantal doctoraalstudenten niet onvermeld blijven. Vooral de hoogst boeiende en gevarieerde samenwerking met Paul van der Schoot zal me nog lang heugen. Relaties met zijn werk zijn in vrijwel ieder hoofdstuk van dit proefschrift aanwezig. Ook van Leon ter Beek, Harmen de Jong en Cas Meijer heb ik veel geleerd. Helaas was er niet voldoende tijd om hun werk in dit proefschrift te kunnen integreren.

Ik hoop dat het membraanonderzoek nog lang een aandachtsveld van de vakgroep mag blijven.